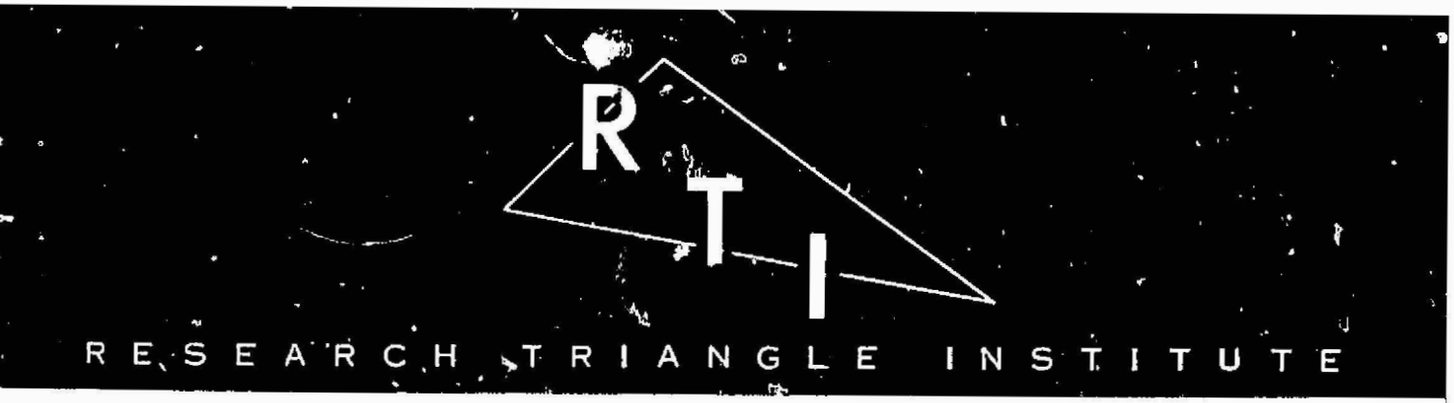

NASA CR-141397

STUDIES OF UNCONTROLLED AIR TRAFFIC PATTERNS

Phase I Report

Contract NAS6-2312

for

National Aeronautics and Space Administration
Wallops Station
Wallops Island, Virginia 23337

by

Systems Engineering Department
Research Triangle Institute
Research Triangle Park, N. C. 27709

RTI No. 43U-840

N75-24703

(NASA-CR-141397) STUDIES OF UNCONTROLLED AIR TRAFFIC PATTERNS, PHASE 1 (Research Triangle Inst., Research Triangle) 136 p HC $5.75 CSCL 17G

Unclas
G3/04 24755

April 1975

Page intentionally left blank

ACKNOWLEDGEMENT

This report was prepared by the Research Triangle Institute, Research Triangle Park, North Carolina, for the National Aeronautics and Space Administration under Contract NAS6-2312. The work is being administered by the Range Safety Office, NASA Wallops Flight Center, Wallops Island, Virginia.

This is a report of work accomplished under Task A of Contract NAS6-2312 and has been coordinated with the contract technical monitor, Loyd C. Parker, at Wallops Flight Center. Dr. C. L. Britt served as RTI Project Manager.

The authors of this report are:

E. G. Baxa, Jr., Senior Engineer

L. L. Scharf, Statistical Consultant*

W. H. Ruedger, Engineer

J. A. Modi, Senior Operations Analyst

S. L. Wheelock, Mathematician

C. M. Davis, Systems Analyst.

*Dr. Scharf, of the Electrical Engineering Department, Colorado State University, Fort Collins, Colorado, participated in this study while on leave at Duke University, Durham, North Carolina.

ABSTRACT

This report describes results of a NASA sponsored study to investigate and analyze the general aviation air traffic flow patterns at uncontrolled airports and to develop traffic pattern concepts which minimize the mid-air collision hazard in uncontrolled airspace. An analytical approach to evaluate mid-air collision hazard probability as a function of traffic densities is developed which is basically independent of path structure. Two methods of generating space-time interrelationships between terminal area aircraft are presented. One is a deterministic model to generate pseudo-random aircraft tracks and this is compared with analyses of results from available real data. Some hazard measures are presented for selected traffic densities. A second model which is a statistical model in preliminary form is discussed. An analytical expression for the statistical description of procedure path deviations is derived.

An analysis of a developed generalized expression for mid-air-collision (MAC) probability results in the conclusion that the probability of encountering a hazard should be minimized independently of any other considerations and that given a certain encounter rate the number of encounters involving visible-avoidable aircraft should be maximized at the expense of encounters in other categories. It is shown that the pilot "look-time" should be proportioned according to the magnitude of the probability of finding a visible-avoidable hazard.

TABLE OF CONTENTS

TABLE OF CONTENTS CONTINUED

LIST OF FIGURES

LIST OF FIGURES CONTINUED

LIST OF FIGURES CONTINUED

LIST OF TABLES

CHAPTER 1

INTRODUCTION

In the growing air traffic environment of today the investigation of mid-air collision hazard is of prime significance to our society. Of particular interest is the relationship between prescribed procedures and the mid-air collision hazard to general aviation aircraft in uncontrolled terminal airspace. With the objective of developing traffic pattern concepts to minimize mid-air collision hazard in uncontrolled airspace, NASA-Wallops personnel have developed a data base consisting of position-time tracking data. The data provide information on terminal area air traffic patterns including those flown by general aviation aircraft at several medium-sized city airports that generally represent uncontrolled airport environments.

The Research Triangle Institute, under contract NAS6-2312, is providing support by developing an analytical concept for the analysis of data obtained by NASA. Various approaches have been investigated to provide realistic measures of mid-air collision risk and reliable methods for mathematical comparison of different air traffic flow situations. These have included the development of preliminary computer mathematical models of the uncontrolled terminal area traffic and methods for validation of these analytical models using the empirical air traffic data collected by NASA-Wallops personnel.

1.1 Problem Statement and Significant Issues

Published procedures for uncontrolled terminal area environments prescribe that an aircraft upon approaching the runway must generally enter a rectangular racetrack-type pattern which involves left turns at relatively high bank angles in a counter-clockwise runway encircling path. Pattern altitudes may vary from runway to runway but generally gradually descending legs are prescribed to allow orderly progression to touchdown. This basic procedure, illustrated in Figure 1-1 (see ref. 1), provides the pilot under VFR conditions with a good continuous view of the runway during the approach and landing phase. In an uncontrolled environment each pilot is dependent basically on the "see-and-avoid" concept to prevent mid-air collisions so that the question of whether or not prescribed terminal

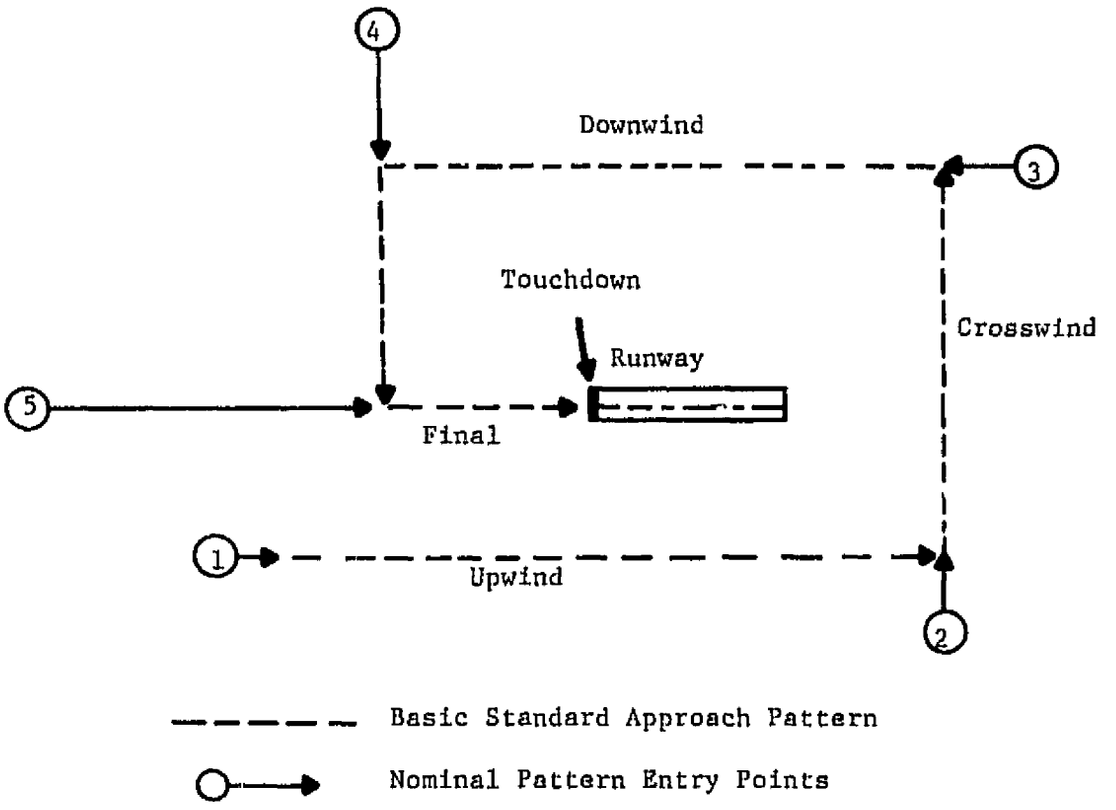

Figure 1-1. Nominal Uncontrolled Runway Approach Pattern.

approach procedures are consistent with minimizing mid-air collision hazard in a see-and-avoid environment is fundamental.

To answer this question it is necessary to evaluate the present uncontrolled patterns flown and to determine improvements in a pilot's ability to see another aircraft (assuming he looks) for various changes in the traffic pattern concept. In refs. 2 and 3 some analysis of approach data has indicated typical adherence to procedure in an uncontrolled environment. Additionally consideration is given to pilot visibility from the cockpit through the use of aircraft vision envelopes to give insight into how approach pattern visibility might be evaluated. No evidence has been found of previous studies which evaluate the approach pattern on the basis of mid-air collision risk in a see-and-avoid environment. However, this type procedure has been proposed as a technique for evaluating the effect of VFR towers on traffic flow and sequencing (ref. 4).

In a controlled environment separation standards (or minimums) are normally enforced so that "natural" course deviations will allow very little collision risk (see refs. 5 and 6). The idea of collision frequency has been developed (ref. 5) as the frequency with which the difference between the actual positions of two aircraft comes within a certain value. A prediction of this frequency can then be termed a probability of collision. The task of relating collision risk to a traffic configuration can be broken into two parts: (1) determining the frequency with which aircraft are exposed to risk by passing close together and (2) determining what chance of collision is inherent in the passing. One approach to evaluate a given path structure is to analyze the flight paths and calculate the relative frequency that these paths are "close" considering total flight time and assuming that aircraft proceed as if no collision occurred when path crossings do occur. In ref. 5 this is called "blind-flying collision risk."

In the uncontrolled region, collision hazard to a particular aircraft has been stated to depend on (1) density of aircraft, (2) heading distribution, and (3) speed distribution (ref. 5). For the situation involving random independent paths a small deviation in flight path will not change the environment and therefore not change the hazard. The statement has been made that the chance of having a collision is then determined by the environment and is unaffected by deviations from the flight path. For the situation of interest here, the assumption of random independent paths is not valid since there is a prescribed procedure even in the uncontrolled

terminal area. Preliminary indications (ref. 2) are that prescribed path deviations are not small enough to be negligible and in fact can contribute to the mid-air collision risk.

In ref. 7 collision hazard is actually divided into two parts. A measure of pilot workload is considered to be related to the percent of time that a given aircraft finds another aircraft in an "encounter" status. An encounter status can be defined in a number of ways and can include relative range, closing velocity, and closing acceleration. A second contributor to collision hazard is encounter rate, which can be related to probability of an encounter during some given time period in which this time period is very small compared to the time basis for measurement of the encounter rate.

In evaluating the inherent risk to be associated with a particular traffic pattern, it seems apparent that the important factors for consideration should include (1) density of aircraft in the terminal area, (2) conflict points inherent in the traffic patterns, (3) speed distribution and type of aircraft, (4) visibility, and (5) pilot workload. These factors are considered in developing an analysis of the uncontrolled terminal area environment in terms of a collision hazard probability.

1.2 Summary of Results

A generalized expression for mid-air-collision (MAC) probability is developed which yields two basic hypotheses about the structuring of patterns for the terminal area. First, the probability of encountering a hazard should be minimized independently of any other considerations. Second, and perhaps not as obvious, if given a certain encounter rate, the number of encounters involving visible-avoidable aircraft should be maximized, thus minimizing the number of encounters in other categories (invisible-avoidable, invisible-unavoidable, or visible-unavoidable). Additionally, an important consideration concerning pilot function is borne out. The pilot "look time" should be proportioned according to the magnitude of the probability of finding a visible-avoidable hazard. Therefore traffic pattern design should (1) minimize encounter rates and (2) maximize visible-avoidable encounters under the constraints of aircraft cockpit binocular design.

Two approaches have been investigated and are described in this report relating to the required analysis of air traffic patterns and their relationship to hazard in the uncontrolled terminal area environment. An analytical occupancy model based on a statistical description of the terminal area airspace is presented. This can serve as a basis for evaluating various approach patterns once the procedure is completely developed and evaluated. Particular pattern characteristics can be defined in terms of input statistics and a measure of hazard probability can be analytically determined. The resulting statistical measure of hazard probability can be evaluated for various pattern characteristics.

Secondly, a trajectory model is described which involves a set of parameters which can be varied to generate approach paths similar to those present in real data. This deterministic approach is demonstrative of a capability to generate realistic traffic paths using a computer algorithm which can readily be altered to conform to essentially any desired approach pattern.

The deterministic model is used in a preliminary form to demonstrate evaluation of encounter probabilities for a path structure designed to represent that currently used in the uncontrolled environment. Paths are time correlated by assignment of touchdown times to entering aircraft according to a Poisson distribution with a rate parameter dependent on the assumed aircraft density. This can provide a baseline measure of the hazard associated with a particular traffic pattern. Flight path deviations are measured and distributions of across-path errors are compared with those obtained from the Wallops Island data analysis to support the premise that this modelling approach can be used to generate realistic flight paths representing the uncontrolled terminal area environment.

Finally, recommendations to improve the deterministic model are given along with suggested extensions to the analytical occupancy model approach.

CHAPTER 2

MID-AIR COLLISION MODELS

The ultimate value of a hazard model for uncontrolled airspaces lies in the utility of the model for predicting and minimizing the mid-air collision probability. In this chapter a general expression for the mid-air collision probability is advanced. The expression shows explicit dependence on aircraft visibility and detectability, pilot function, and hazard probability. The expression illustrates rather straightforward minimization tactics that can be pursued, and dramatizes the dominance of the hazard probability. Models for hazard probability are developed in Chapter 4.

2.1 Mid-Air Collision Probability

An abstract aircraft space is depicted in Figure 2-1. The space dichotomizes aircraft into those that are non-hazardous ($\bar{H}$) to a target aircraft and those that are hazardous (H) and would result in a mid-air collision if no evasive action were taken. The subset of hazardous aircraft has been further refined into disjoint subsets H_i corresponding to generalized geometrical locations (including space and time, for example) of hazardous aircraft. It is convenient to denote the subset of hazardous aircraft by

$$H = \sum_{i=1}^{n} H_i \qquad (2\text{-}1)$$

where n is the number of disjoint subsets H_i. Now let MAC denote the subset of hazardous aircraft that result in mid-air collisions. Since the set MAC is a subset of H, and H is a finite union of disjoint sets, this set can be written as

$$MAC = \sum_{i=1}^{n} MAC \cap H_i \ . \qquad (2\text{-}2)$$

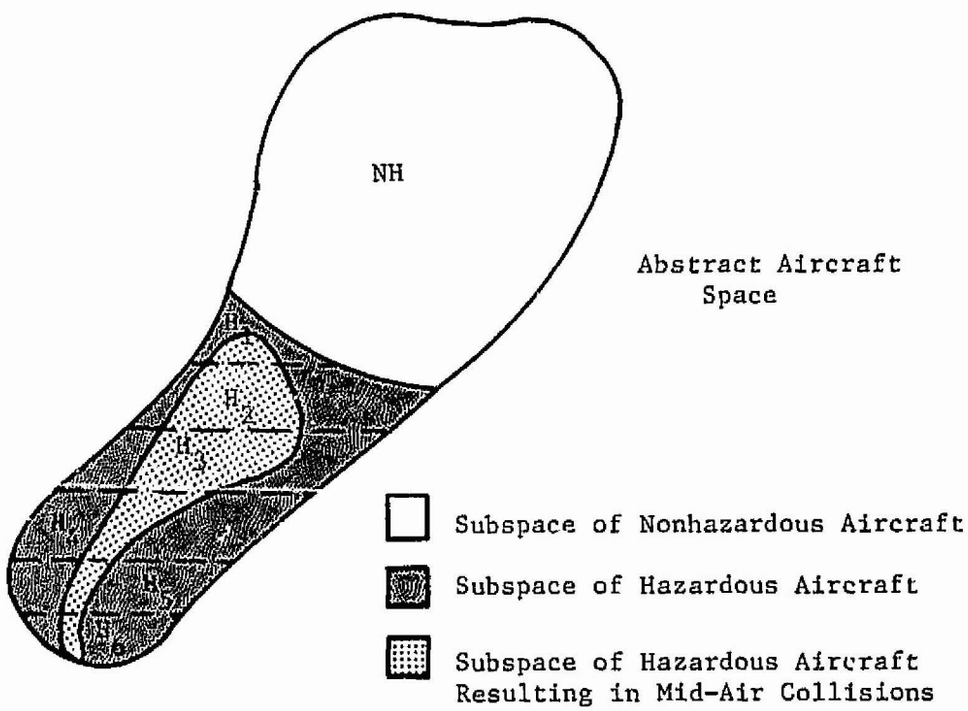

Figure 2-1. Aircraft Space.

The probability of a mid-air collision is

$$P[MAC] = \sum_{i=1}^{n} P[MAC \cap H_i]$$

$$= \sum_{i=1}^{n} P[MAC/H_i]\, P[H_i] \qquad (2\text{-}3)$$

where $P[H_i]$ is a hazard probability. Denoting the complement of MAC by $\overline{MAC}$, note that P[MAC] can be written

$$P[MAC] = \sum_{i=1}^{n} (1 - P[\overline{MAC}/H_i])\, P[H_i]$$

$$= P[H] - \sum_{i=1}^{n} P[\overline{MAC}/H_i]\, P[H_i] \quad . \qquad (2\text{-}4)$$

In words, eq. (2-4) says the probability of a mid-air collision is the probability of encountering a hazard, P[H], minus the probability of encountering and avoiding the hazard. If $P[\overline{MAC}/H_i] = 1$ for all i (i.e., all hazard conditions H_i are avoidable with probability 1) then P[MAC] = 0.

A certain subset of the set H may contain aircraft that are invisible, unavoidable, or both. Such hazardous aircraft result in mid-air collisions with probability one. Thus eq. (2-4) can be rewritten

$$P[MAC] = P[H] - \sum_{i \in I} P[\overline{MAC}/H_i]\, P[H_i] \qquad (2\text{-}5)$$

where $H' = \sum_{i \in I} H_i$ denotes the set of hazardous aircraft that are visible (V) and avoidable (A).

The set (or event) $\overline{MAC}$ is the event that a visible, avoidable, hazardous aircraft is "looked at" (L) by the pilot (but not necessarily seen if the hazard is not perfectly detectable) and detected (D). It is assumed that a visible, avoidable target that is detected will be avoided, thereby ruling out of this analysis the irresponsible pilot who fails to take evasive action. The notation for $\overline{MAC}$ is

$$\overline{MAC} = L \cap D \quad . \tag{2-6}$$

Equation (2-5) can now be written

$$P[MAC] = P[H] - \sum_{i \in I} P[L \cap D \cap H_i]$$

$$= P[H] - \sum_{i \in I} P[D/L \cap H_i] \; P[L/H_i] \; P[H_i]$$

$$= P[H] - \sum_{i \in I} P[D/H_i] \; P[L/H_i] \; P[H_i] \quad . \tag{2-7}$$

The last simplification follows from the observation that the inherent detectability of a hazardous aircraft is independent of whether or not the pilot looks at it. The interpretation of eq. (2-7) is the same as the interpretation following eq. (2-4). However the additional interpretation can be made that the probability of encountering and avoiding a hazard is given by the probability of encountering, looking at, and detecting a visible, avoidable hazard. Several plausible minimization tactics follow.

2.2 Minimization Tactics

It seems plausible that the summation term in eq. (2-7) should be independent of (or weakly dependent upon) the probability of encountering a hazard, P[H]. That is, the nature of the set $H' = \sum_{i \in I} H_i$ of visible and avoidable hazards, and the probability of encountering, looking at, and

detecting this set of hazards, should be independent of P[H]. With this assumption it can be concluded that P[H], the probability of encountering a hazard, should be minimized independently of any other considerations. This is of course a traffic pattern and scheduling issue. Next, the set H' of visible, avoidable, hazardous aircraft should be maximized, subject to the consideration that hazards which are likely to be encountered, looked at, and detected (corresponding to large values of $P[D/H_i]\ P[L/H_i]\ P[H_i]$) are to be included at the expense of others. If $P[D/H_i]\ P[L/H_i]\ P[H_i]$ is independent of H_i, then the cardinality of the set of visible, avoidable targets should be maximized independently of other considerations.

Finally, the following interesting minimization with respect to pilot function is evident. Let $g(i) = P[D/H_i]\ P[H_i]$ denote the probability of encountering and detecting the visible, avoidable hazard H_i. Then to minimize P[MAC], maximize the objective function

$$J = \sum_{i \in I} g(i)\ P[L/H_i] \tag{2-8}$$

where $P[L/H_i]$ is the probability of looking at hazard H_i. This function is maximized by choosing (Schwartz inequality)

$$P[L/H_i] = k\ g(i) \tag{2-9}$$

where $k^{-1} = \sum_{i \in I} g(i)$ (assuming the pilot looks in some generalized hazard location H_i with probability 1). Thus the pilot should spend $[g(i)/\sum_{i \in I} g(i)]\%$ of his time looking in hazard location H_i. Roughly speaking, the percentage of time spent looking in hazard location H_i should be proportional to the probability of detecting a visible, avoidable hazard in that location. The probability of detection of a visible, avoidable hazard is maximized through landing pattern design and aircraft binocular design (ref. 3).

CHAPTER 3

BASIC AIRSPACE MODEL

The critical issue in a model for mid-air collision probability seems to be the determination of hazard probability, $P[H_i]$. Several hazard probability models have been proposed in relation to collision avoidance studies (see, ref. 8 and the references therein). These models are generally geometrical in nature, as they must be, involving complicated kinematic relationships between two or more aircraft. To date, the models have not included the effects of random aircraft entrance times into controlled or uncontrolled airspaces, nor have they accounted for random aircraft trajectories within an airspace. (The suggestions contained in ref. 9 represent a notable exception to this statement.)

In this chapter the issue of random aircraft entrances into uncontrolled airspaces is addressed by developing a basic airspace model. First, consider a simple, but representative, landing pattern and then pose a homogeneous Poisson model for the number of aircraft that land in an arbitrary time interval $[o,t)$. By assigning aircraft entrance probabilities for upwind, downwind, and crosswind legs of the pattern (based on published data, e.g., ref. 8), a basic airspace model for the number of aircraft occupying any region of the pattern at any point in time can be obtained. The airspace model is then generalized to include the nonhomogeneous effects of daily fluctuations in traffic density. Some comments are advanced concerning extensions of the basic airspace model to include random three-dimensional aircraft trajectories.

In Chapter 4 several hazard probability models are derived from this basic airspace model. In Chapters 5 and 6 the airspace model is used to partially specify a trajectory simulation program for generating random aircraft trajectories and obtaining various statistical measures of an uncontrolled airspace.

3.1 Homogeneous Poisson Model for Aircraft Landings

Let the number of aircraft, $N(t)$, landing in the time interval $[o,t)$ be a homogeneous Poisson counting process with intensity ν and rate parameter $\lambda_t = \nu t$; i.e.,

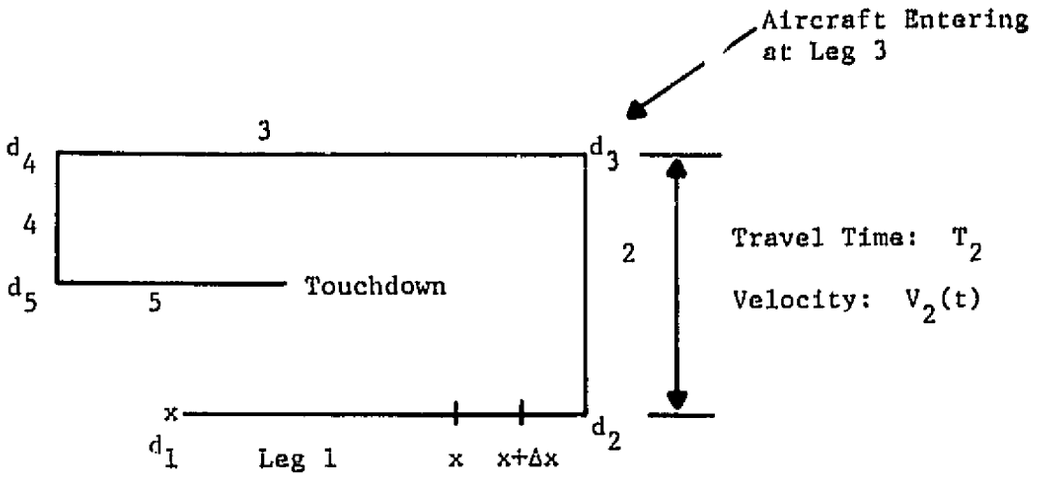

Figure 3-1. Representative Landing Pattern.

$$P[N(t) = n] = \frac{(\nu t)^n}{n!} e^{-\nu t} \tag{3-1}$$

where $P[N(t) = n]$ denotes the probability that $N(t) = n$ and νt is the average number of aircraft landing in $[o,t)$.

Now consider Figure 3-1 depicting a five-leg landing pattern. One might reasonably ask what the probability is that $N_m(t)$ aircraft will enter the landing pattern at leg m in the time interval $[o,t)$. To answer this question, assume the general landing pattern contains M legs, aircraft enter leg m with probability p_m, and $\sum_{m=1}^{M} p_m = 1$. Then the probability that $N_m(t) = n_m$ can be written

$$P[N_m(t) = n_m] = \sum_{n=n_m}^{\infty} P[N_m(t) = n_m / N(t + t_m) - N(t_m) = n] \tag{3-2}$$

$$\cdot P[N(t + t_m) - N(t_m) = n]$$

where T_j is the appropriate "travel time" required for an aircraft to traverse the j^{th} leg, and $t_m = \sum_{j=m}^{M} T_j$ is the total time required for an aircraft to land after entering the landing pattern at leg m. The assumption here is that every aircraft that enters leg m in the interval $[o,t)$ must land in the interval $[t_m, t + t_m)$, where t_m is the time required for an aircraft to travel from the entrance of leg m to the landing point. Then eq. (3-2) follows from the law of total probability.

The first term in eq. (3-2) is the probability of n_m successes (a success defined here as an entrance at leg m) in n trials (a trial defined here as a landing in the time interval $[t_m, t + t_m)$. The distribution is binomial:

$$P[N_m(t) = n_m / N(t + t_m) - N(t_m)] = \binom{n}{n_m} p_m^{n_m} \quad (1 - p_m)^{n-n_m} \quad . \qquad (3\text{-}3)$$

The second probability statement is Poisson with rate parameter $\lambda(t + t_m) - \lambda t_m$, by virtue of the fact that increments of a Poisson process are also Poisson:

$$P[N(t + t_m) - N(t_m)] = \frac{(\lambda t)^n}{n!} \quad e^{-\lambda t} \quad . \qquad (3\text{-}4)$$

Equation (3-2) is now evaluated as follows:

$$P[N_m(t) = n_m] = \sum_{n=n_m}^{\infty} \frac{n!}{(n-n_m)!\,n_m!} \quad p_m^{n_m} \quad (1 - p_m)^{n-n_m} \frac{(\lambda t)^n}{n!} \quad e^{-\lambda t}$$

$$= \frac{p_m^{n_m}}{n_m!} \quad (\lambda t)^{n_m} \quad e^{-\lambda t} \sum_{\ell=0}^{\infty} \frac{(1 - p_m)^{\ell}}{\ell!} \quad (\lambda t)^{\ell}$$

$$= \frac{(p_m \lambda t)^{n_m}}{n_m!} \quad e^{-p_m \lambda t} \quad . \qquad (3\text{-}5)$$

The conclusion is that the number of aircraft entering leg m is Poisson with rate parameter $p_m \lambda t$:

$$N_m(t) : P[p_m \lambda t] \quad . \qquad (3\text{-}6)$$

The parameter p_m can be obtained from experimental observations regarding the relative frequency of aircraft entrances at leg m (ref. 3). The parameter λ is also obtained from experimental observations.

These calculations are based on preservation of the property that the average number of aircraft landing in the interval $[t_1, t + t_1)$ is the average number entering leg 1 in the interval $[o,t)$ plus the average number entering leg 2 in the interval $[t_1 - t_2, t + t_1 - t_2)$ ... plus the average number entering leg M in the interval $[t_1 - t_M, t + t_1 - t_M)$. Since the average number of aircraft entering leg m in the interval $[t_1 - t_m, t + t_1 - t_m)$ is $p_m \lambda t$, it follows that

$$\sum_{m=1}^{M} p_m \lambda t = \lambda t \tag{3-7}$$

and the averages are preserved.

Actually, more can be shown. Consider the individual Poisson processes $N_1, \ldots, N_M$. The number of aircraft landing in $[t_1, t + t_1)$ equals the number of aircraft entering leg 1 in the interval $[o,t)$ plus the number entering leg 2 in the interval $[t_1 - t_2, t + t_1 - t_2)$ ... plus the number entering leg M in the interval $[t_1 - t_M, t + t_1 - t_M)$:

$$N(t + t_1) - N(t_1) = N_1(t) + [N_2(t + t_1 - t_2) - N(t_1 - t_2)]$$

$$+ \ldots + [N_M(t + t_1 - t_M) - N(t_1 - t_M)] . \tag{3-8}$$

The characteristic function of $N(t + t_1) - N(t_1)$ is

$$\Phi(\omega) = E[e^{j\omega N(t + t_1) - N(t_1)}]$$

$$= \sum_{n=0}^{\infty} e^{-\omega t} \frac{(\lambda t)^n}{n!} e^{j\omega n}$$

$$= e^{\lambda t(e^{j\omega} - 1)} , \tag{3-9}$$

But this can be written

$$\Phi(\omega) = e^{\sum_{m=1}^{M} p_m \lambda t(e^{j\omega} - 1)} \cdot$$

$$= \prod_{m=1}^{M} e^{p_m \lambda t(e^{j\omega} - 1)} \tag{3-10}$$

The m^{th} term of the product is the characteristic function of the Poisson random variable $N_m(t + t_1 - t_m) - N_m(t_1 - t_m)$. Thus it follows that the $N_1(t)$, ..., $N_M(t)$ are independent Poisson random processes. These results will be generalized for nonhomogeneous airspaces shortly.

The conclusion is that Poisson models for the independently arriving aircraft at the various landing legs lead to a Poisson model for the number of aircraft landings on an arbitrary time interval (and vice-versa), provided relevant time intervals are carefully chosen. The mathematical model is therefore consistent with the physical constraint that aircraft which enter the pattern must land after an appropriate delay. The appropriate delay has been assumed deterministic, corresponding to the assumption that aircraft trajectories are deterministic. It is very difficult to relax this requirement and still obtain tractable models, but in Chapter 4 some preliminary results are advanced for random aircraft trajectories.

3.2 Interval Occupancy in Homogenous Air Spaces

An important determination to be made for the calculation of hazard probabilities is the number of aircraft, $Q(x;t)$, located in the spatial interval $[x, x + \Delta x)$ along the landing pattern at time t (see Figure 3-1). Consider an interval $[x, x + \Delta x)$ on the first leg (i.e., $d_1 \leq x < x + \Delta x \leq d_2$, with d_1 the beginning of leg 1 and d_2 the beginning of leg 2). It follows that $Q(x;t)$ equals $N_1(t - t_1(x + \Delta x)) - N_1(t - t_1(x))$, the number of aircraft entering the landing pattern at leg 1 in an appropriate interval $[t - t_1(x + \Delta x), t - t_1(x))$. The time $t_1(x)$ is the time required for an aircraft

with velocity $v_1(t)$ to traverse the distance from d_1 to x:

$$\int_0^{t_1(x)} v_1(\tau)\, d\tau = x - d_1 \quad . \tag{3-11}$$

Thus $Q(x;t)$, for $d_1 \leq x \leq x + \Delta x \leq d_2$, is Poisson with rate parameter $p_1 \nu[t_1(x + \Delta x) - t_1(x)]$:

$$Q(x;\, t) : P[p_1\nu(t_1(x + \Delta x) - t_1(x))] \ , \quad d_1 \leq x \leq x + \Delta x \leq d_2 \ . \tag{3-12}$$

When the velocity is a constant v_o, then $t_1(x) = (x - d_1)/v_o$ and the rate parameter becomes $p_1\nu\Delta x/v_o$. The probability that $Q(x;t) = q$ is

$$P[Q(x;t) = q] = \frac{(p_1\nu\Delta x/v_o)^q}{q!}\ e^{-p_1\nu\Delta x/v_o} \ , \quad d_1 \leq x < x + \Delta x \leq d_2 \tag{3-13}$$

For an interval $[x, x + \Delta x)$ on the second leg, $Q(x;t)$ is the number of aircraft entering the landing pattern at leg 2 in an appropriate interval $[t - t_2(x + \Delta x), t - t_2(x))$, plus the number of aircraft that entered leg 1 in an appropriate interval $[t - t_1(x + \Delta x), t - t_1(x))$ and continued in the pattern from leg 1 to leg 2. The time $t_2(x)$ is the time required for an aircraft with velocity $v_2(t)$ to traverse the distance from d_2 to $x \geq d_2$:

$$\int_0^{t_2(x)} v_2(\tau)\, d\tau = x - d_2 \quad . \tag{3-14}$$

The time $t_1(x)$ is simply $t_1(x) = t_2(x) + T_1$, where T_1 is the time required for an aircraft to traverse leg 1. Thus

$$Q(x;t) = [N_2(t - t_2(x)) - N_2(t - t_2(x + \Delta x))]$$

$$+ [N_1(t - t_2(x) - T_1) - N_1(t - t_1(x + \Delta x) - T_1)] . \quad (3\text{-}15)$$

By the independence and homogeneity of N_1 and N_2, it follows that $Q(x;t)$ is Poisson with rate parameter $(p_1 + p_2)\ \nu\ [t_2(x + \Delta x) - t_2(x)]$; i.e.,

$$Q(x;t) : P[(p_1 + p_2)\ \nu\ (t_2(x + \Delta x) - t_2(x))] \quad (3\text{-}16)$$

When $v_1(\tau) = v_2(\tau) = v_o$,

$$Q(x;t) : P\left[(p_1 + p_2)\ \nu\ \Delta x/v_o\right]. \quad (3\text{-}17)$$

Continuing in this manner, it is easy to show that for x contained in the m^{th} leg, $d_m \leq x < x + \Delta x \leq d_m + 1$,

$$Q(x;t) : P\left[\sum_{j=1}^{m} p_j \nu (t_m(x + \Delta x) - t_{m(x)})\right] . \quad (3\text{-}18)$$

For $v_1(\tau) = v_2(\tau) = \ldots = v_m(\tau) = v_o$,

$$Q(x;t) : P\left[\sum_{j=1}^{m} p_j \nu \Delta x/v_o\right] \quad . \tag{3-19}$$

The average number of aircraft in $[x, x + \Delta x)$ is $\nu(\Delta x/v_o) \sum_{j=1}^{m} p_j$. Figure 3-2 is a graph of the average number of aircraft in the interval $[x, x + \Delta x)$ vs. x. It is assumed that the velocity is constant. For the example shown, leg 1 and leg 3 are the most commonly entered legs. Note that the model correctly exhibits increased congestion in the traffic pattern as the touchdown point is approached.

3.3 Nonhomogeneous Poisson Airspace Model

The results of Sections 3.1 and 3.2 can be generalized by allowing the number of aircraft landings in the interval [o,t) to be a nonhomogeneous Poisson process with rate parameter

$$\lambda_t = \int_o^t \nu(\alpha)\, d\alpha \tag{3-20}$$

where $\nu(\alpha) > o$ is a variable intensity parameter that accounts for daily fluctuations in air traffic density. That is,

$$P[N(t) = n] = \frac{\lambda_t^n}{n!} e^{-\lambda_t} \quad . \tag{3-21}$$

Proceeding as before, assign probability p_m to the arrival of an aircraft at leg m and denote by $N_m(t;\tau)$ the number of aircraft entering the landing pattern at leg m in the t-second interval $[\tau, t + \tau)$. Thus, for the distribution of $N_m(t;\tau)$,

$$P[N_m(t;\tau) = n_m] = \sum_{n=n_m}^{\infty} P[N_m(t;\tau) = n_m / N(t + t_m + \tau) - N(t_m + \tau) = n] \tag{3-22}$$

$$P[N(t + t_m + \tau) - N(t_m + \tau) = n] \quad .$$

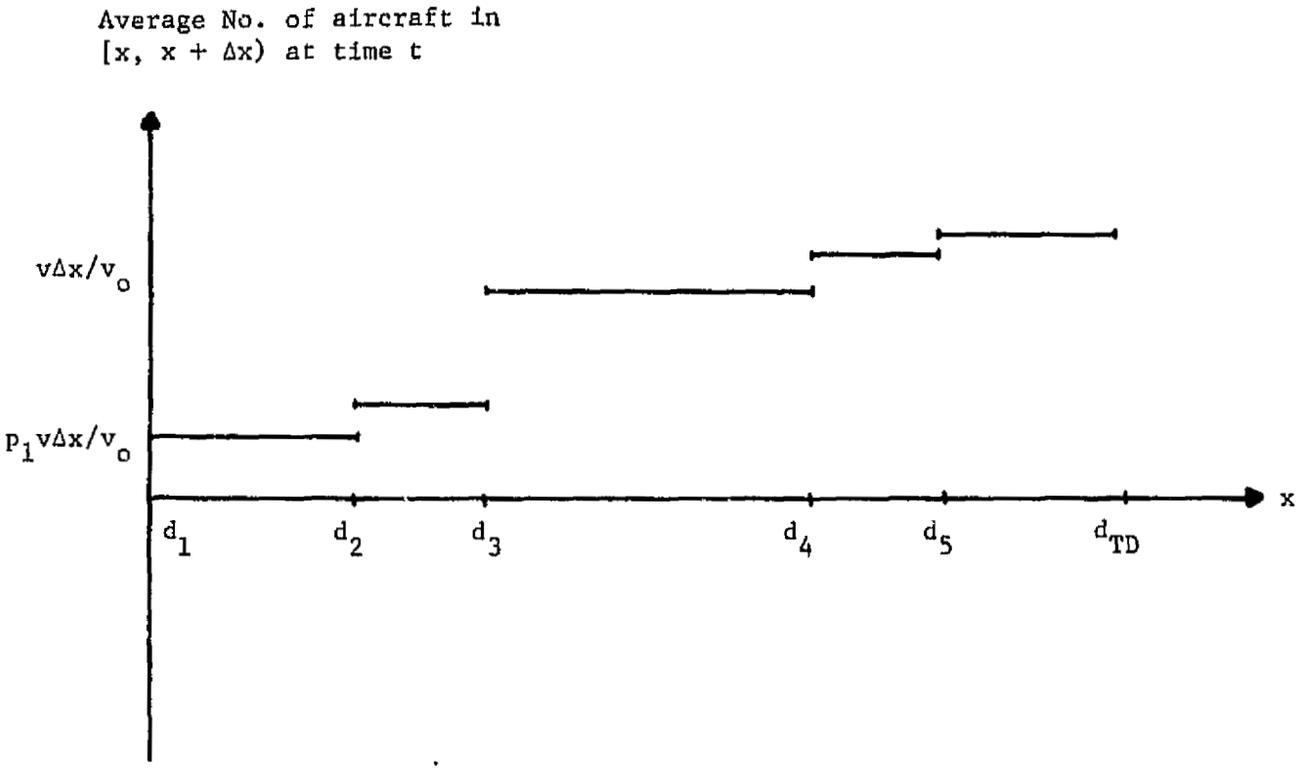

Figure 3-2. Average Number of Aircraft in Interval [x, x + Δx) vs. x.

This uses the law of total probability and exploits the fact that every aircraft entering the landing pattern at leg m must land t_m seconds later. Noting that $N(t + t_m + \tau) - N(t_m + \tau)$ is Poisson with rate parameter $\beta(t;t_m + \tau) = \lambda_{t + t_m + \tau} - \lambda_{t_m + \tau}$, eq. (3-22) can be evaluated as follows

$$P[N_m(t;\tau) = n_m] = \sum_{n=n_m}^{\infty} \binom{n}{n_m} p_m^{n_m} (1 - p_m)^{n-n_m} \frac{\beta^n(t;t_m + \tau)}{n!} e^{-\beta(t;t_m + \tau)}$$

$$= \frac{[p_m (t;t_m + \tau)]^{n_m}}{n_m!} e^{-p_m\beta(t;t_m + \tau)} . \qquad (3\text{-}23)$$

Thus $N_m(t;\tau)$ is Poisson with rate parameter $p_m \beta(t;t_m + \tau)$:

$$N_m(t;\tau) : P[p_m\beta(t;t_m + \tau)]$$

$$\beta(t;t_m + \tau) = \int_{t_m + \tau}^{t + t_m + \tau} \nu(\alpha)\, d\alpha . \qquad (3\text{-}24)$$

Proceeding as in Section 3.1, it can be shown that $N_1(t;\tau)$, $N_2(t;\tau)$, ..., $N_M(t;\tau)$ are independent processes. Note here only that the rate parameters (i.e., average number of aircraft entries) for $N_1(t)$, ..., $N_M(t)$ give the correct rate parameter for $N(t)$. The property is preserved that the average number of aircraft landings in the interval $[t_1, t + t_1)$ equals the average number of aircraft entering the landing pattern at leg 1 in the interval $[o,t)$ plus the average number of aircraft entering at leg 2 in the interval $[t_1 - t_2, t + t_1 - t_2)$ ... plus the average number entering leg M on the interval $[t_1 - t_M, t + t_1 - t_M)$. To show this

$$\int_{t_1}^{t + t_1} \nu(\alpha)\, d\alpha = p_1\beta(t;t_1) + p_2\beta(t;t_2 + t_1 - t_2) + \ldots$$

$$+ p_m\beta(t;t_M + t_1 - t_M)$$

$$= \sum_{j=1}^{M} p_j\beta(t;t_1)$$

$$= \beta(t;t_1) \ , \qquad (3\text{-}25)$$

and therefore the averages are preserved as required.

One can proceed as in Section 3.2 to determine the number of aircraft in the spatial interval $[x,x + \Delta x)$ in a nonhomogeneous airspace. The results are direct extensions of eqs. (3-18) and (3-19).

3.4 Multidimensional Extensions to the Basic Airspace Model

Multidimensional extensions to the basic airspace model are obtained by considering processes of the form $N(\bar{t})$ with $\bar{t}$ a multidimensional t-set. Then for example, one can define $\bar{t} = [o,t) \times [o,x) \times [o,y) \times [o,z)$ to be a cross-product set consisting of temporal and spatial variables. The process $N(\bar{t})$ becomes the number of aircraft contained in the region of space $[o,x) \times [o,y) \times [o,z)$ during the time interval $[o,t)$. If $N(\bar{t})$ is a Poisson process, then the relevant probability statement is

$$P[N(\bar{t}) = n] = \frac{\lambda_{\bar{t}}^{n}}{n!} e^{-\lambda_{\bar{t}}} \qquad (3\text{-}26)$$

where $\lambda_{\bar{t}}$ is now the average number of aircraft in the t-set $\bar{t}$. The rate parameter is related to a multidimensional intensity paramter, $\nu(\bar{t})$,

describing the temporal-spatial intensity of aircraft in the space:

$$\lambda_{\bar{t}} = \int_{0}^{\bar{t}} d\bar{\alpha}\ \nu(\bar{\alpha}) \quad . \tag{3-27}$$

The intensity parameter $\nu(\bar{t})$ is, in turn, chosen to describe the geometric properties of a typical aircraft trajectory in a pre-specified landing pattern.

CHAPTER 4

MODELS FOR HAZARD PROBABILITY

In this chapter a hazard is modelled as the occupancy by two or more aircraft of a common region of airspace. The hazard model is tied to the basic airspace model of Chapter 3 and analytical expressions are derived for hazard probability. When aircraft trajectories are fixed-velocity and deterministic, the hazard probability can be readily evaluated. Numerical results indicate that th parameter $\xi=\frac{\nu\alpha}{v_o}$, with ν the airspace intensity parameter and α/v_o the so-called dwell time of an aircraft in a hazard-free interval, is a reasonable figure of merit for uncontrolled airspaces. Hazard probability is reduced by reducing ξ.

Some discussion is given to a hazard model that is applicable when aircraft trajectories are random. The resulting expressions for hazard probability can be evaluated for arbitrary random trajectories.

4.1 An Occupancy Model for Deterministic Trajectories

Assume all aircraft in the landing pattern of Figure 3-1 are flying deterministic, fixed velocity (v_o) trajectories. In Section 3.1 it was shown that Q(x;t), the number of aircraft occupying the spatial interval $[x,x + \Delta x)$, $d_m \leq x < x + \Delta x \leq d_{m+1}$, is Poisson distributed:

$$Q(x;t) : P[\mu] \quad .$$

$$\mu = \frac{\nu\Delta x}{v_o} \sum_{j=1}^{m} p_j \quad . \tag{4-1}$$

In this model, μ is the average number of aircraft in the region $[x,x + \Delta x)$ at time t.

Now assume that the number of aircraft in $[x, x + \Delta x)$ is $Q(x;t) = q$. It follows from the basic properties of the Poisson process that the unordered occupancy points for the q aircraft are uniformly distributed in $[o,t)$. The ordered occupancy points $x \leq x_1 < x_2 < \ldots x_q \leq x + \Delta x$, where x_i is the location of the i^{th} aircraft, are distributed as the order statistics $U_1, U_2, \ldots, U_q$; that is,

$$f_{\bar{U}}(\bar{u}) = \begin{cases} \dfrac{q!}{\Delta x^q} & , \quad x \le u_1 < u_2 < \ldots < u_q \le x + \Delta x \\ 0 & , \quad \text{otherwise} \end{cases} \tag{4-2}$$

where $f_{\bar{U}}(\bar{u})$ denotes the density function for $\bar{U} = (U_1, U_2, \ldots, U_q)$.

A rather classical result that will be needed for our analysis of hazard probability is the probability that all inter-aircraft distances $u_{i+1} - u_i$ exceed a hazard-free distance α. This is the probability that $x \le u_1 < x + \Delta x - (q-1)\alpha$, $u_1 + \alpha < u_2 < x + \Delta x - (q-2)\alpha$, $\ldots$ $u_{q-1} + \alpha < u_q < x + \Delta x$. Denoting by $P[\bar{H}/Q(x;t) = q]$ the probability that the q-1 inter-aircraft distances all exceed the hazard distance α (the choice of notation will be clear shortly), then

$$P[\bar{H}/Q(x;t) = q] = \frac{q!}{\Delta x^q} \int_x^{x+\Delta x-(q-1)\alpha} du_1 \int_{u_1+\alpha}^{x+\Delta x-(q-2)\alpha} du_2 \quad \ldots \quad \int_{u_{q-1}+\alpha}^{x+\Delta x} du_q \, . \tag{4-3}$$

Letting $\gamma_i = (u_i - x)/\Delta x$,

$$P[\bar{H}/Q(x;t) = q] = q! \int_0^{1-(q-1)\alpha/\Delta x} d\gamma_1 \int_{\gamma_1+\alpha/\Delta x}^{1-(q-2)\alpha/\Delta x} d\gamma_2 \quad \ldots \int_{\gamma_{n-1}+\alpha/\Delta x}^{1} d\gamma_q \, . \tag{4-4}$$

This can be simplified (ref. 10) yielding

$$P[\bar{H}/Q(x;t) = q] = \begin{cases} 1 & , \quad q \le 1 \\ [1 - (q-1)\dfrac{\alpha}{\Delta x}]^q & , \quad 1 < q \le \left[\dfrac{\Delta x}{\alpha} + 1\right] \\ 0 & , \quad \text{otherwise} \end{cases} \tag{4-5}$$

where $[\Delta x/\alpha + 1]$ denotes the largest integer less than or equal to $\Delta x/\alpha + 1$. The parameter $\Delta x/\alpha$ is the number of contiguous hazard-free intervals in the interval $[x, x + \Delta x)$.

This yields a model for hazard probability for uncontrolled airspaces of the form depicted in Figure 3-1. A hazard is defined to exist in the airspace interval $[x, x + \Delta x)$ at time t if two or more aircraft occupy a common region of airspace. If the common region of airspace is taken to be an interval of length α, then the result of eq. (4-5) can be used to model the probability that no hazard ($\bar{H}$) exists in the airspace $[x, x + \Delta x)$ at time t, given that q aircraft occupy the airspace interval $[x, x + \Delta x)$. The law of total probability then yields the following model for the probability that a hazard (H) exists in the airspace region $[x, x + \Delta x)$ at time t:

$$P[H] = 1 - P[\bar{H}]$$

$$= 1 - \sum_{q=1}^{\infty} P[\bar{H}/Q(x;t) = q]\, P[Q(x;t) = q]$$

$$= 1 - e^{-\mu}[1+\mu] - \sum_{q=2}^{\left[\frac{\Delta x}{\alpha} + 1\right]} e^{-\mu} \frac{\mu^q}{q!} \left(1 - (q-1)\frac{\alpha}{\Delta x}\right)^q \qquad (4\text{-}6)$$

Equation (4-6) is a basic expression for the probability of a hazard. In Figures 4-1 and 4-2, P[H] is plotted versus the rate parameter μ and parametrized by $\Delta x/\alpha$, the number of contiguous, non-overlapping, hazard-free regions in $[x, x + \Delta x)$. The parameter $[\Delta x/\alpha + 1]$ is the maximum number of aircraft that could, in principle, be placed on the interval $[x, x + \Delta x)$ without creating a hazard. The results of Figure 4-1 indicate that the hazard probability is small when μ, the average number of aircraft to be found in the airspace interval $[x, x + \Delta x)$, is very much smaller than the number

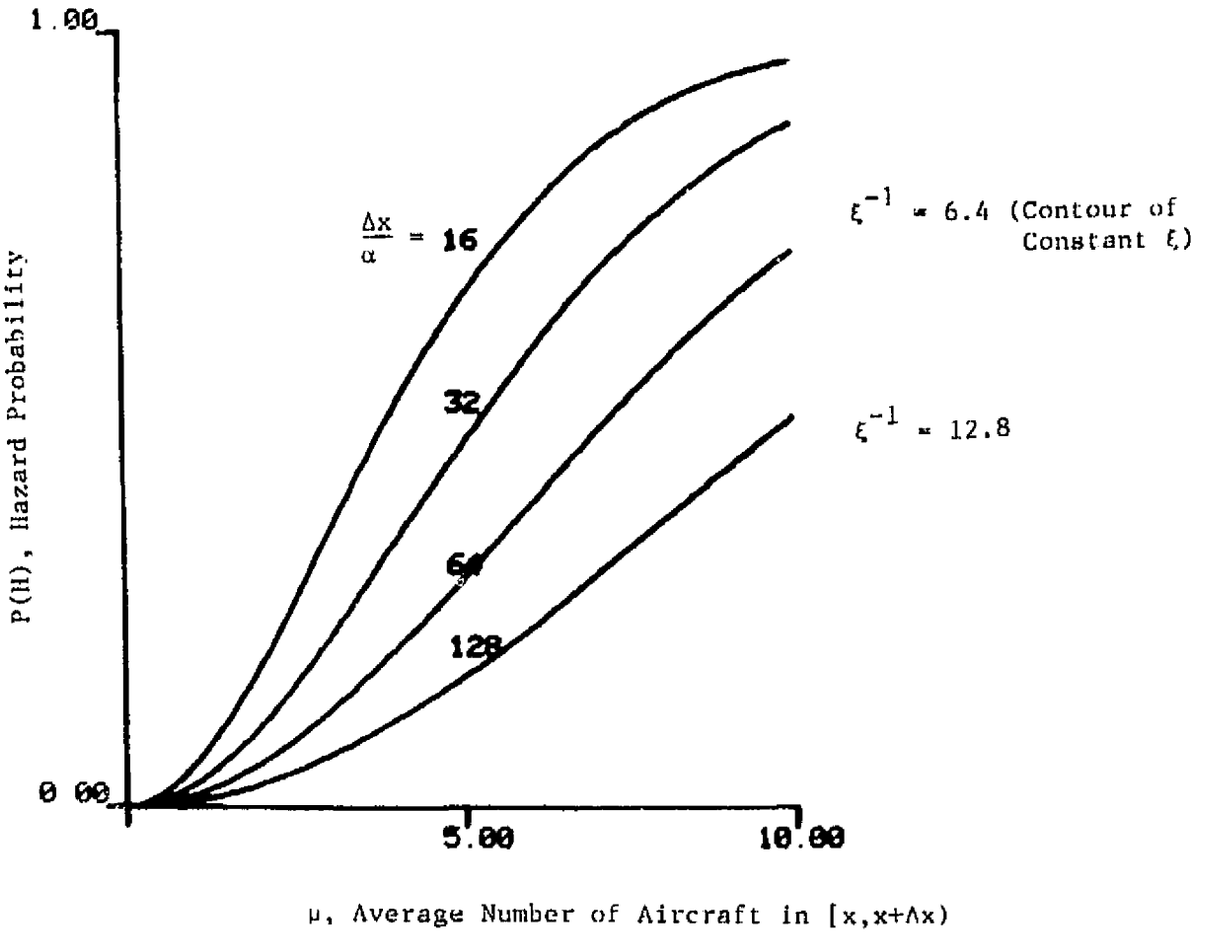

Figure 4-1. Hazard Probability vs. Average Number of Aircraft.

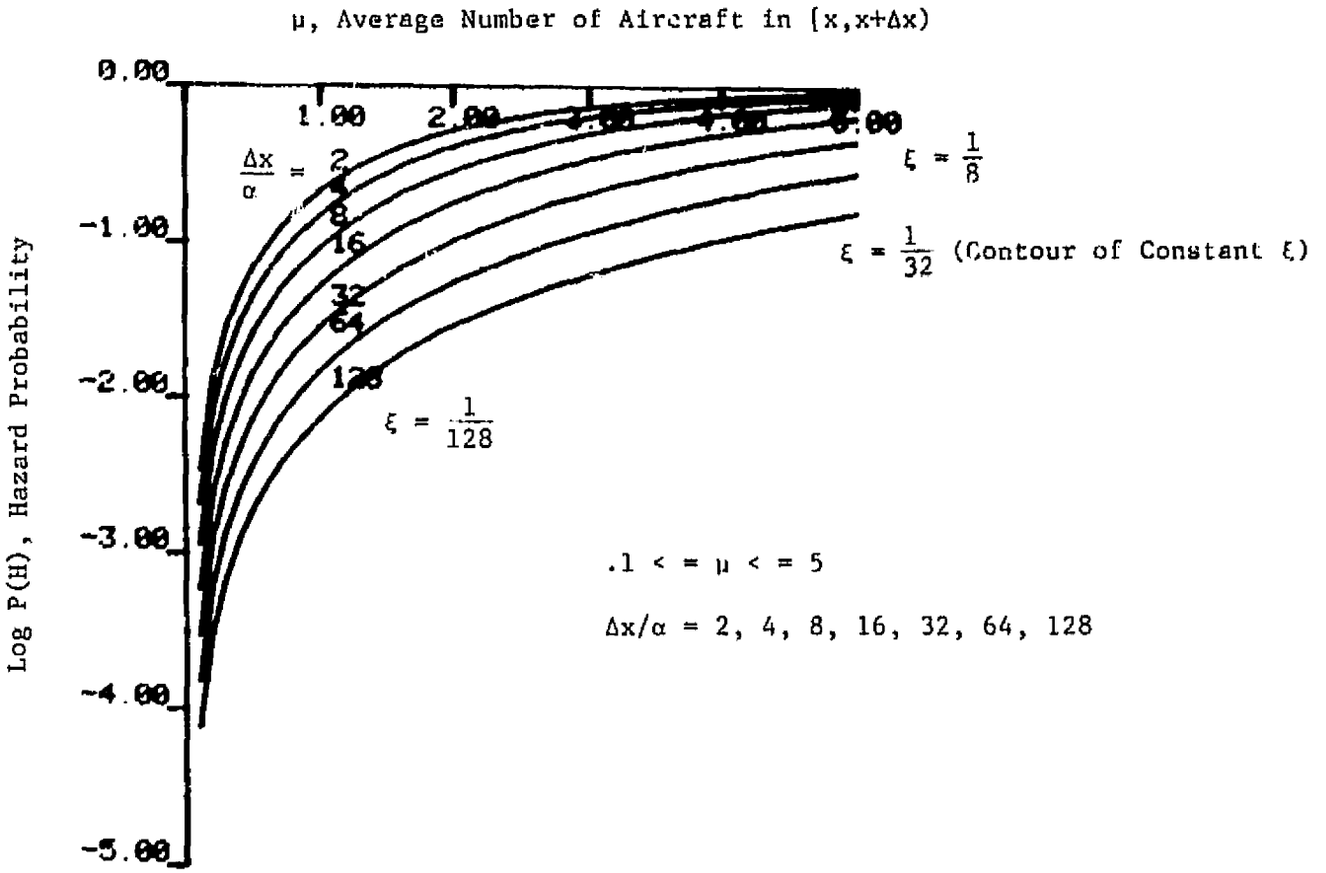

Figure 4-2. Hazard Probability vs. Average Number of Aircraft - Expanded for Small μ.

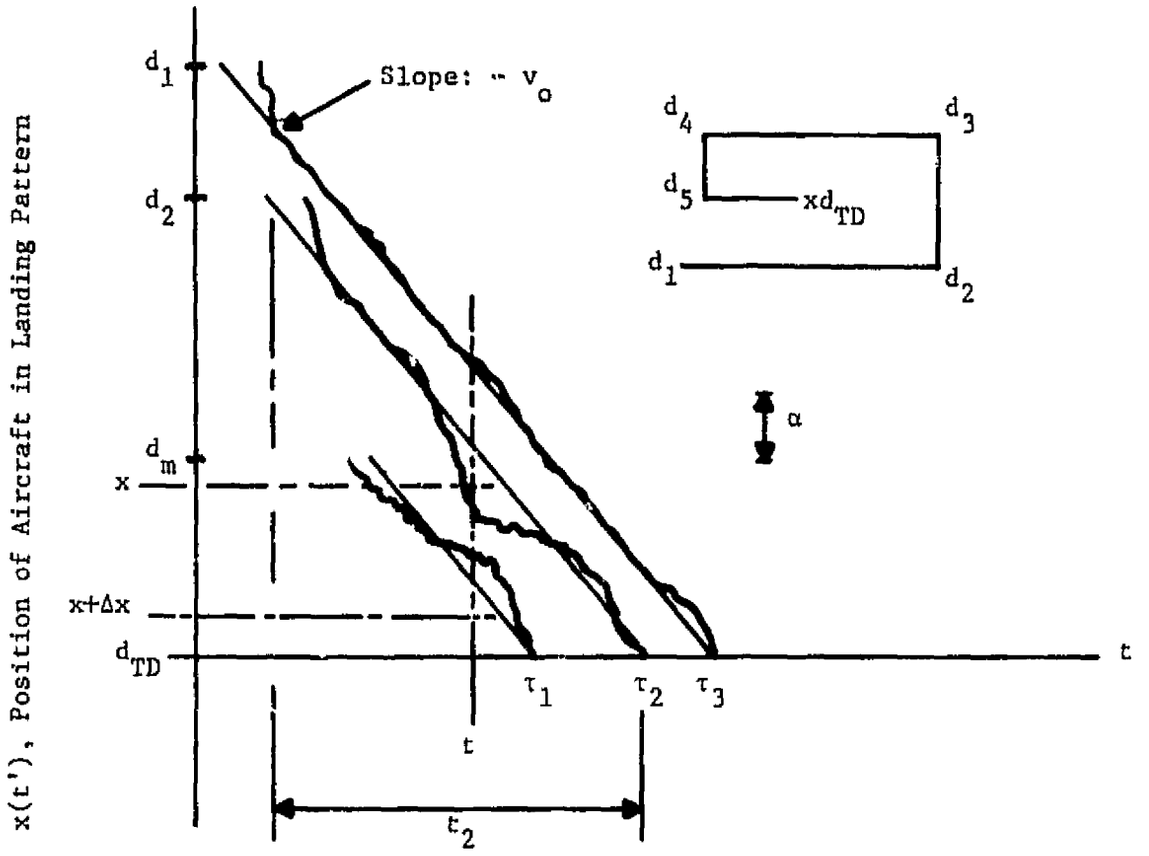

Figure 4-3. Random Aircraft Trajectories.

of contiguous, non-overlapping, hazard-free regions in $[x, x + \Delta x)$. That is, for small P[H],

$$\mu << \Delta x/\alpha \ . \tag{4-7}$$

Equivalently, a figure of merit can be defined as

$$\xi = \mu \, (\Delta x/\alpha)^{-1}$$

$$= \frac{\nu\alpha}{v_o} \sum p_j \tag{4-8}$$

requiring $\xi << 1$ for low hazard probability. The parameter α/v_o is the time it takes a constant velocity aircraft to travel one hazard-free distance. Thus, for $\sum p_j = 1$ (worst-case), the figure of merit ξ is the average number of aircraft that enter the airspace in the time it takes an aircraft to traverse one hazard-free distance. From Figure 4-2 it is found, for example, that ξ on the order of $\xi = 0.01$ ensures P[H] on the order of P[H] = 0.01.

4.2 An Occupancy Model for Random Trajectories

When aircraft trajectories are random rather than deterministic, $Q(x;t)$, the number of aircraft occupying the airspace region $[x, x + \Delta x)$ at time t, is no longer Poisson distributed; and the previously derived results for hazard probability must be modified. To achieve this modification, consider the diagram of Figure 4-3. Several nominal, fixed-velocity, deterministic trajectories are illustrated, along with random trajectories that deviate from these nominals. The trajectories terminate at the Poisson event times $\tau_1, \tau_2, \ldots, \tau_n$ corresponding to the homogeneous process N(t) that characterizes the number of aircraft landings in the time interval [o,t). Note in the figure that the first aircraft to enter the airspace enters at leg 2, whereas the first aircraft to land enters at leg m.

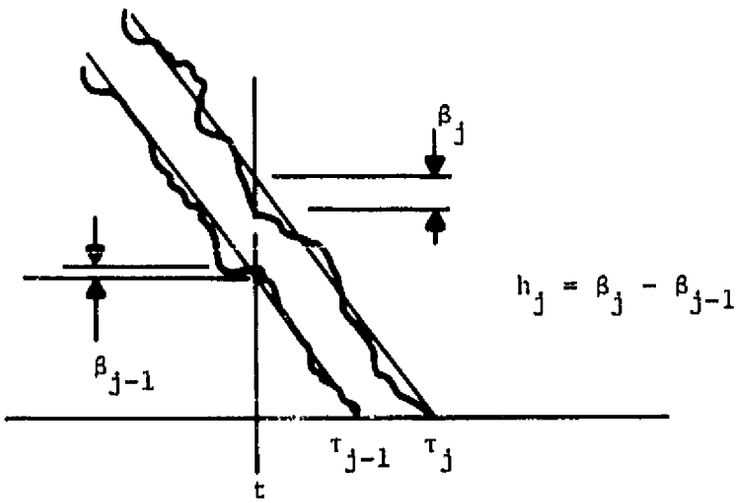

Figure 4-4. Use of Slack Variables.

It would be desirable to evaluate the probability that, given $Q(x;t) = q$, no two aircraft occupy the same region of airspace. Then the procedure of Section 4.1 could be used to evaluate a hazard probability. The difficulty is that even when the nominal, deterministic trajectories are separated by a distance α, the corresponding random trajectories may come well within α of each other. This effect is illustrated in Figure 4-3 where it is shown that two random trajectories in the region $[x, x + \Delta x)$ at time t come within α (and therefore constitute a hazard) even though all nominal trajectories are separated by more than α.

These difficulties imposed by the random trajectories can be overcome by requiring the nominal trajectories to be separated by α plus a random slack variable that guarantees the corresponding random trajectories are also separated by α. This strategy is illustrated in Figure 4-4. Trajectories j and j-1 (with landing times τ_j and τ_{j-1}) are required to be separated by the distance $\alpha + h_j$ where

$$h_j = \beta_j - \beta_{j-1} \tag{4-9}$$

and β_j is the random perturbation of the j^{th} trajectory from its nominal trajectory at time t.

Now consider the ordered occupancy points $x \leq x_1 < x_2 < \ldots x_q \leq x + \Delta x$ for the q nominal-trajectory aircraft located in $[x, x + \Delta x)$. These occupancy points are distributed as the order statistics $U_1, U_2, \ldots, U_q$, as shown in eq. (4-3). The probability that the j-th and (j-1)-st aircraft are separated by $\alpha + h_j$ for $j = 2, 3, \ldots, q$ is the probability that $u_j - u_{j-1} > \alpha + h_j$. Equivalently, this is the probability that all random trajectories are separated by at least α. For given $h_1, h_2, h_3, \ldots, h_q$, the appropriate probability statement is

$$P[\bar{H}/Q(x;t) = q,\ h_1,\ \ldots,\ h_q] = \frac{q!}{\Delta x^q} \int_x^{x + \Delta x - (q-1)\alpha - \sum_{j=2}^{q} h_j} du_1$$

$$\cdot \int_{u_1 + \alpha + h_2}^{x + \Delta x - (q-2)\alpha - \sum_{j=3}^{q} h_j} du_2 \ \cdots \int_{u_{q-1} + \alpha + h_q}^{\Delta x + x} du_q \cdot \tag{4-10}$$

Letting $\gamma_j = (u_j - x)/\Delta x$,

$$P[\bar{H}/Q(x;t) = q,\ h_1,\ \ldots\ h_q] = q! \int_0^{1 - (q-1)\frac{\alpha}{\Delta x} + \frac{1}{\Delta x}\sum_{j=2}^{q} h_j} d\gamma_1$$

$$\int_{\gamma_1 + \frac{\alpha}{\Delta x} + \frac{h_2}{\Delta x}}^{1 - (q-2)\frac{\alpha}{\Delta x} - \frac{1}{\Delta x}\sum_{j=3}^{q} h_j} d\gamma_2 \ \cdots \int_{\gamma_{q-1} + \frac{\alpha}{\Delta x} + \frac{h_q}{\Delta x}}^{1} d\gamma_n \cdot \tag{4-11}$$

After simplification

$$P[\bar{H}/Q(x;t) = q,\ h_1,\ \ldots,\ h_q] = \begin{cases} 1\ , & q \leq 1 \\ [1 - (q-1)\ \frac{\alpha}{\Delta x} - (\beta_q - \beta_1)]^q\ , & 1 < q \leq \left[\frac{\Delta x}{\alpha} + 1\right] \\ 0\ , & \text{otherwise} \end{cases} \tag{4-12}$$

Defining the random variable $\gamma = \beta_q - \beta_1$, and assuming the perturbation β_q is independent of q, for $1 < q \leq [\frac{\Delta x}{\alpha} + 1]$,

$$P[\bar{H}/Q(x;t) = q,\ h_1,\ \ldots,\ h_q] = P[\bar{H}/Q(x;t) = q,\ \gamma] = [1 - (q-1)\ \frac{\alpha}{\Delta x} - \gamma]^q . \tag{4-13}$$

The result here is very similar to the result of eq. (4-5). However, to obtain the unconditional probability of a hazard, P[H], in this model, averaging over the joint distribution of Q(x;t) and h is necessary. Denoting the distribution of γ by F_γ,

$$P[H] = 1 - P[\bar{H}]$$

$$= 1 - \sum_{q=1}^{\infty} \int dF_\gamma\ P[\bar{H}/Q(x;t) = q,\ \gamma]\ P[Q = q] \tag{4-14}$$

$$= 1 - e^{-\mu}\ [1 + \mu] - \sum_{q=2}^{\left[\frac{\Delta x}{\alpha} + 1\right]} e^{-\mu}\ \frac{\mu^q}{q!} \int dF_\gamma \left[1 - (q-1)\ \frac{\alpha}{\Delta x} - \gamma\right]^q .$$

This is the basic result for hazard probability when aircraft trajectories are random. Note that by using the binomial expansion for $(a + b)^q$, eq. (4-14) can be written in terms of the moments of γ:

$$P[H] = 1 - e^{-\mu}\,[1+\mu] - \sum_{q=2}^{\left[\frac{\Delta x}{\alpha}+1\right]} e^{-\mu}\,\frac{\mu^q}{q!}\,\frac{1}{\Delta x^q}\,\sum_{k=1}^{q}\binom{q}{k}\,[\Delta x - (q-1)\alpha]^k \int dF_\gamma\,(-\gamma)^{q-k}$$

$$= 1 - e^{-\mu}\,[1+\mu] - \sum_{q=2}^{\left[\frac{\Delta x}{\alpha}+1\right]} e^{-\mu}\left(\frac{\mu}{\Delta x}\right)^q\,\sum_{k=1}^{q}\frac{[\Delta x - (q-1)\alpha]^k}{(q-k)!\,k!}\,(-1)^{q-k}\,m_{q-k}$$

where (4-15)

$$m_{q-k} = E[\gamma^{q-k}]$$

Thus, by simply knowing the first $\left[\frac{\Delta x}{\alpha}+1\right]$ moments of γ, one can in principle compute the hazard probability. When the slack variable γ is normally distributed, say with mean zero and variance σ^2, then $m_{q-k} = 1\cdot 3 \ldots (q-k-1)\sigma^{(q-k)}$ for q-k even and zero otherwise. Then eq. (4-15) can be easily evaluated.

4.3 Multidimensional Extensions

Multidimensional extensions of the results given in Sections 4.1 and 4.2 are, in principle, straightforward. One simply considers multidimensional Poisson processes $N(\bar{t})$, with $\bar{t}$ the multidimensional t-set discussed in Section 3.3 and examines the probability that aircraft are separated by a suitable function of the multidimensional variable $\bar{t}$. In this way geometrical considerations for hazard regions can be included and more complicated trajectories analyzed. The results for hazard probability will be multidimensional analogs of eqs. (4-6) and (4-14).

CHAPTER 5

SIMULATED AIR SPACES

5.1 General

A preliminary study has been conducted on data previously collected by NASA Wallops personnel at three uncontrolled airports in Maryland. The data consist of single radar tracks of general aviation aircraft in an uncontrolled environment. Consideration is given to ways in which these data can be used to evaluate alternative patterns and procedures in such environments. To evaluate collision risk in an air traffic environment one approach is to analyze an environment which provides representative space-time relationships between aircraft for given patterns and procedures. The real data do provide spatial relationships which are representative of pilot adherence to the current procedure for runway approach.

To evaluate current procedure one obvious method is to assign some time correlation to the real data tracks and then sample this finite set of position-time situations. Sampling could be done on a "with replacement" basis to provide an indefinitely large (but finite) set of "situations." The method is direct and should not be difficult to implement but it precludes tracks other than the specific ones in the data base (tracks which are plausible but did not occur) from being analyzed. This could conceivably introduce a bias in the results. Furthermore, since it is desired to develop the capability to evaluate other patterns and procedures besides those which gave rise to the tracks in the data base, a simulation model to generate tracks for analysis is desirable. Another consideration involves the fact that the real data base is not presently available in a form which is suitable for computer analysis. Thus to even validate, for example, the statistical occupancy model evaluation discussed in Chapters 3 and 4, it is necessary to have some simulation model to provide track data.

The simulation model to be discussed here is a generating approach in the sense that tracks are generated which are plausible in light of the data, but which are not themselves in the data base. This approach would regard those tracks in the data base as a sample from which population distributions would be derived. The tracks to be used in collision risk

analysis would then be generated using some Monte Carlo sampling from such distributions. This approach minimizes the danger of bias, is readily adaptable to different patterns and procedures, and can be implemented very easily once a method is defined to characterize air traffic.

One of the first issues addressed in this study to provide a basis for a simulation model was how traffic flows can be characterized. This issue is important in identifying different traffic flows and in the validation of computer models. The resulting approach presented here as a recommendation of this study is based on the major segments of tracks flown, classified by type of aircraft, and each aircraft entry point into a defined airspace. Each segment is characterized by a few basic flight variables such as headings, segment lengths, turn radii, speed, altitude, etc. This approach seems feasible from the standpoint of the capabilities of the data base and appears adequate for the purposes of the analysis considering precision requirements and cost of analysis.

Sections to follow provide a description of a prototype digital simulation model which has been used to generate traffic for the existing environment. A capability is described to model simultaneous tracks in a multiple aircraft environment designed to represent an uncontrolled terminal area airspace. The model should be applicable in an existing situation as well as in a hypothetical environment which can be reasonably postulated. Central to the development of this capability is a means of generating a virtually unlimited number of tracks in the environment to be modelled. The descriptions are not complete but are intended to convey an idea of how the simulation model would work and how it can be used to analytically evaluate the traffic patterns from a mid-air collision hazard standpoint.

Data requirements for the prototype simulator are discussed. Essentially these are empirical distributions of path lengths, headings, and turn-radii of legs that make up a track. These requirements can be readily met by the data retrieval and analysis programs now being developed by NASA.

5.2 Characterization of Air Traffic Flows

For purposes of this development the uncontrolled airport airspace will not be the entire "Airport Traffic Area" conventionally defined as that airspace within a 5 statute mile (8 km) radius of the center of the airport up to but not including 2000 ft (609.6 m) altitude. The available track data in the NASA Wallops data base drops off rapidly beyond a 3 n.mi. radius (5.6 km) of the radar site. Furthermore the main feature of interest is the prescribed landing approach pattern which is usually flown within this 3 mile radius of the runway. Therefore, a perimeter of 3 n.mi (5.6 km) radius from the runway threshold will be defined to encompass the airport airspace in the pursuing analytical discussion. A coordinate system with origin at the threshold and the y-axis coincident with the runway centerline as shown in Figure 5-1 will be used. This choice of coordinate system should not prejudice the main concepts and results to be presented.

The digital traffic generation model described represents a simple yet plausible characterization of the uncontrolled environment. Aircraft movements are described in terms of a few basic flight variables. Tracks are defined in terms of major component segments and the general environment is defined in terms of traffic types and the prevailing patterns and procedures.

5.2.1 Relevant parameters.— In simulated traffic studies entry of aircraft into the defined airspace is often the fundamental "driving event." Hence, a logical first variable of characterization is the time between entries.* This includes arrivals to the perimeter of aircraft coming in to land, or flying through, as well as aircraft presenting themselves at runways for take-off. Time between entries is a variable that often has diurnal and other longer term variations which can be accounted for as necessary.

---

*Virtually all of the variables described are best thought of as random variables, and when considering a variable for characterization its empirical frequency distribution should be used. The totality of such distributions will be said to characterize the traffic.

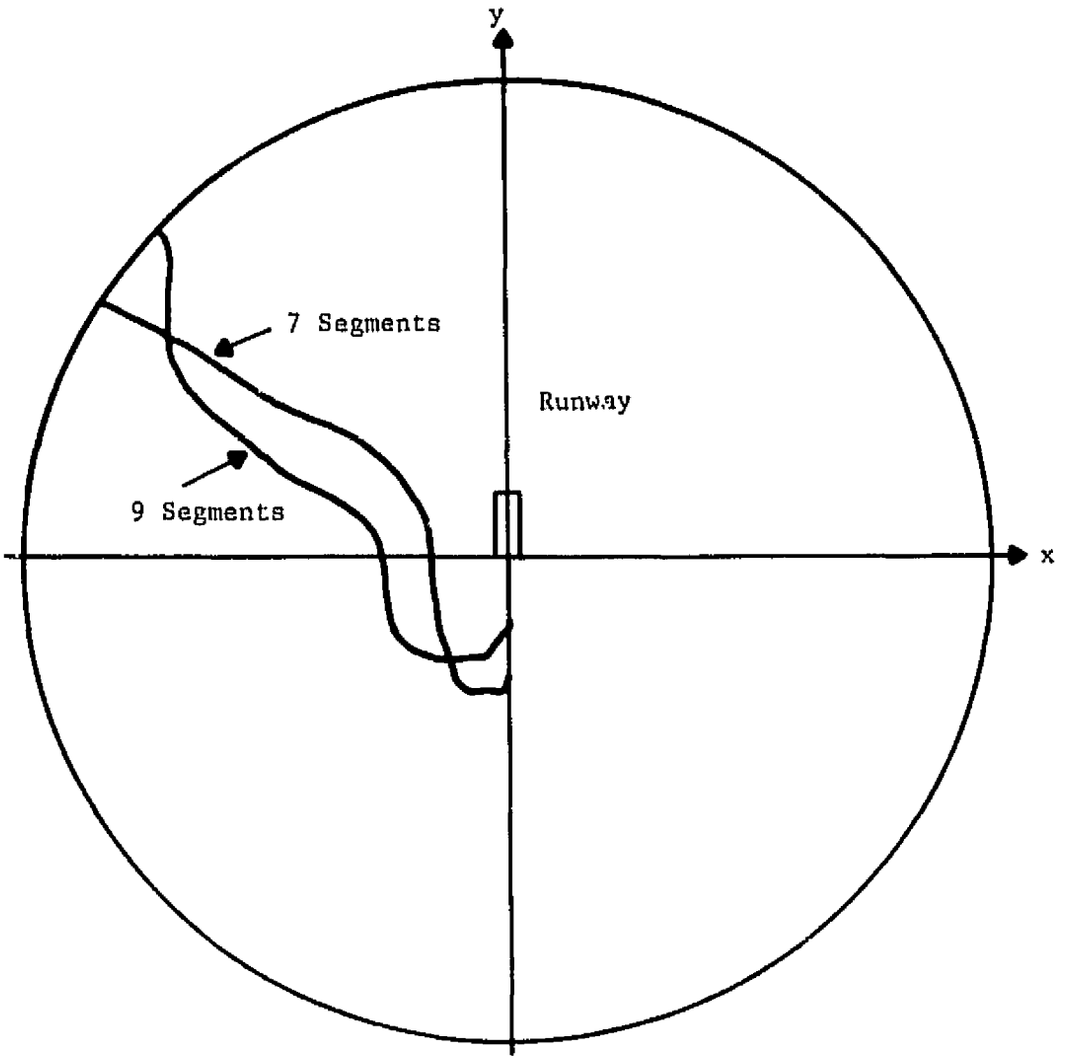

Figure 5-1. Illustrating Airspace, Axes, and Tracks.

Next, a classification of various types of driving events and the frequency with which they occur should be considered. The simplest classification, which should be adequate here, is "arrivals," "departures" and "fly-bys." Arrivals and departures are commonly the greater portion of airport traffic relative to fly-bys and in the long run must be of equal frequency for most analytical purposes. Thus it should be enough to state the fly-bys as a fraction of arrivals, or perhaps airport operations.

Having characterized traffic by its inter-event time and by type of event, further characterization is best done separately for the three types of events. In what follows, only the characterization of arrivals is considered. This operation is somewhat more complex than the others and is perhaps of greater interest for collision hazard studies since proportionally, arrivals spend more time in the airspace than other types. In any case, the basic approach to traffic characterization would be similar for the other types of operations also.

The arrival traffic flow within a given airspace depends greatly on the type of aircraft, the point from which it enters and the runway on which it lands. Therefore, the distribution of arrivals by type along the perimeter and the distribution of runway usage are important items for characterization of traffic.

For a given type of aircraft, entry point, and runway, the flow patterns of traffic are governed by a variety of factors such as rules and procedures, weather conditions, presence of other aircraft, individual characteristics of aircraft and pilots, etc. No attempt will be made to characterize traffic flows by any specific factor in the above group. It will be enough to accept empirically whatever flows do evolve under the influence of all of these factors, and to try to characterize flows on the basis of major segments in the flight path.

In order to define a segment, it is necessary to recognize six modes of flight: straight climb, straight descent, straight-and-level, climbing turn, descending turn, and flat-turn. Then a segment is defined as the portion of flight path over which a particular mode is maintained; the start of a new mode marks the start of a new segment. This essentially simple concept poses two practical problems. One is the difficulty of identifying a sharp changeover point from one mode or segment to another; the other is

the distinction between the "fundamental" mode and the "random" deviations from it. These problems will not be completely and quantitatively resolved here. The model will be designed to recognize no more than (k + 4) segments to any path, where k is a number that depends on the entry point of the arrival and represents some reasonable number of segments necessary to fly the recommended pattern for the airport. For example, in Figure 5-1, for arrivals from the sector shown, k may be taken to be 7: inbound, turn on downwind, downwind, turn on base, base, turn on final, and final. Hence, the assumption can be made that no path through this sector need have more than 11 segments. If more than 11 segments seem to exist in fact, then it will be assumed that some of the apparent segments are indeed "ripples" and will be combined into a total of 11 or fewer segments.

The above scheme is very helpful in characterizing traffic flows because it provides a means of classifying flight paths--by the number and sequence of segment types. The number of different types of flight paths (for a given aircraft type from a given sector) is likely to be quite manageable, because many segment types are in practice incompatible with one another, and it is possible to specify the frequency with which different flight path types are found at a given airport. Thus, the characterization of traffic at an airport should include a specification of empirical distribution of flight path types.

Finally, for each type of flight path, the segments need to be characterized by distributions of a few basic variables: headings, speeds, altitudes, decelerations, descent rates, and turn radii.

The above scheme represents a convenient way of characterizing traffic at an airport. In fact, it leads directly to the method of track regeneration and traffic simulation to be discussed in following subsections.

5.2.2 Track generation.— In the generating approach, the track is developed point by point and segment by segment. The first step is to locate the arrival on the perimeter. This is done by sampling from distributions for entry point, initial speed, initial altitude, and initial heading for the particular segment and type of aircraft involved. It may

be that entry speed, altitude and heading will be dependent upon entry point and this dependence would need to be quantified before defining distributions. This is markedly true for initial headings, as may be seen from the data base, and the dependence can be identified from a plot of initial headings versus entry points.

Having established the arrival on the perimeter, the next step is to generate what will be called the initial leg; this is the segment flown immediately after entering the perimeter. Again, the nature of this segment (with respect to the 6 modes mentioned earlier) depends very much on the entry point. From a brief observation of the data it seems there are some entry points with a large proportion of straight-and-level initial legs, while other entry points exhibit a large proportion of low-bank-angle descending turns directly onto the final course. The proper distribution for the particular entry point needs to be set up and sampled.

Assuming for the sake of further illustration that the initial leg is determined to be straight and level, a distribution of leg lengths for the particular aircraft type and sector is sampled. From the information developed thus far it is then possible to generate the path of the arrival in space and time from the perimeter up to some point within the airspace.

Next, the nature of the second segment needs to be determined by sampling from an appropriate distribution. Assume it is a descending right turn. Then the rate of turn, descent altitude and final heading are determined by sampling, and the generated path is extended to include the turn.

This turn may or may not put the aircraft in the pattern; it depends on the entry point. Assume for the sake of discussion that it puts the aircraft on downwind. Then the next step would be to sample proper distributions for downwind headings and other characteristics of the downwind leg, so that the path can be generated up to the point where the base turn begins.

The number of segments can vary from 1 (for sweeping turns directly onto final) to about 12 (for aircraft beginning with upwind legs and executing a full pattern) depending on point of entry; similarly, the nature of the segments will vary, depending on type of aircraft. All these relationships can be gleaned from the data and programmed into the logic of the track generating routines. The feasibility of this approach has been checked out by some preliminary test programs, and the approach seems quite capable of generating tracks which are a faithful reproduction of reality--the quality of the reproduction being determined by the level of detail employed in the set of sampling distributions used.

To evaluate collision risk in an air traffic environment it will be necessary to create an environment which provides some time-space relationship between aircraft which can be representative of an actual environment. The simulation approach as described thus far provides a means of characterizing flight paths such that a path generator algorithm can recreate single track data.

For the model to adequately represent the air traffic environment it is necessary to provide time correlation between aircraft tracks. The method proposed and used to illustrate how the model can provide baseline evaluation of collision risk involves assignment of entry times to single tracks generated using Monte Carlo sampling. The same procedure could be used to reconstruct a meaningful time correlation between individual tracks in the NASA-Wallops data. Thus each track generated in the airspace will have an entry time assigned (randomly) which then defines a space-time history to that track with an assumed velocity for the aircraft type corresponding to the track.

5.2.3 Model validation.— Once the model is implemented there is a need to provide some means of validation. One method is actually a two-phase approach. A first validation can be done on all of the same variables that are used to characterize the traffic. Distributions would be compiled on these variables from a large number of generated tracks, and compared against corresponding distributions from data base tracks of the same aircraft type and entry point. If the distributions match to some stipulated goodness of fit, the generated tracks may be considered valid. Because of

the close relationships between the distributions generated, the distributions sampled from and the distributions developed from the data, the above test by itself does not provide adequate reassurance as to the validity of the generated tracks. Hence, a second-level validation is proposed which does not involve distributions used in track generation. These could be cross-sectional distributions of the type investigated in previous NASA studies. A number of planes can be selected and cross-sectional distributions developed from the data base as well as the generated tracks. If the distributions match to some stated degree of fit, the generated tracks may be considered further validated; if not, more detail needs to be incorporated in the set of generating distributions. Of course, all this needs to be done with due regard to sample sizes, sampling errors, and all the other requirements of statistical testing.

The following sections describe the path generation simulation model as applied to two of twelve possible entry sectors. The algorithm for assignment of interarrival times is included in this discussion. In Chapter 6 model validation is discussed and illustrated.

5.3 Air Traffic Simulator for the Uncontrolled Environment

In Section 5.2 air traffic path characteristics were discussed in terms of variables which can provide for computer generation of aircraft tracks. The procedure for generating tracks was described in general. Appendix A contains a detailed description of how entries from two of the twelve possible entry sectors are assigned paths within the airport airspace. Path segments are generated by random sampling from parametrized distributions. These parameters are defined so that the distributions can be changed to conform with distributions that could be obtained from real data or might be analytically determined from chosen pattern characteristics and procedures prescribed for a given uncontrolled airport.

Once this ability to generate tracks is developed as described in Appendix A it is possible to design a computer simulation model to study the collision hazard in a given environment. This section describes the model and how it operates.

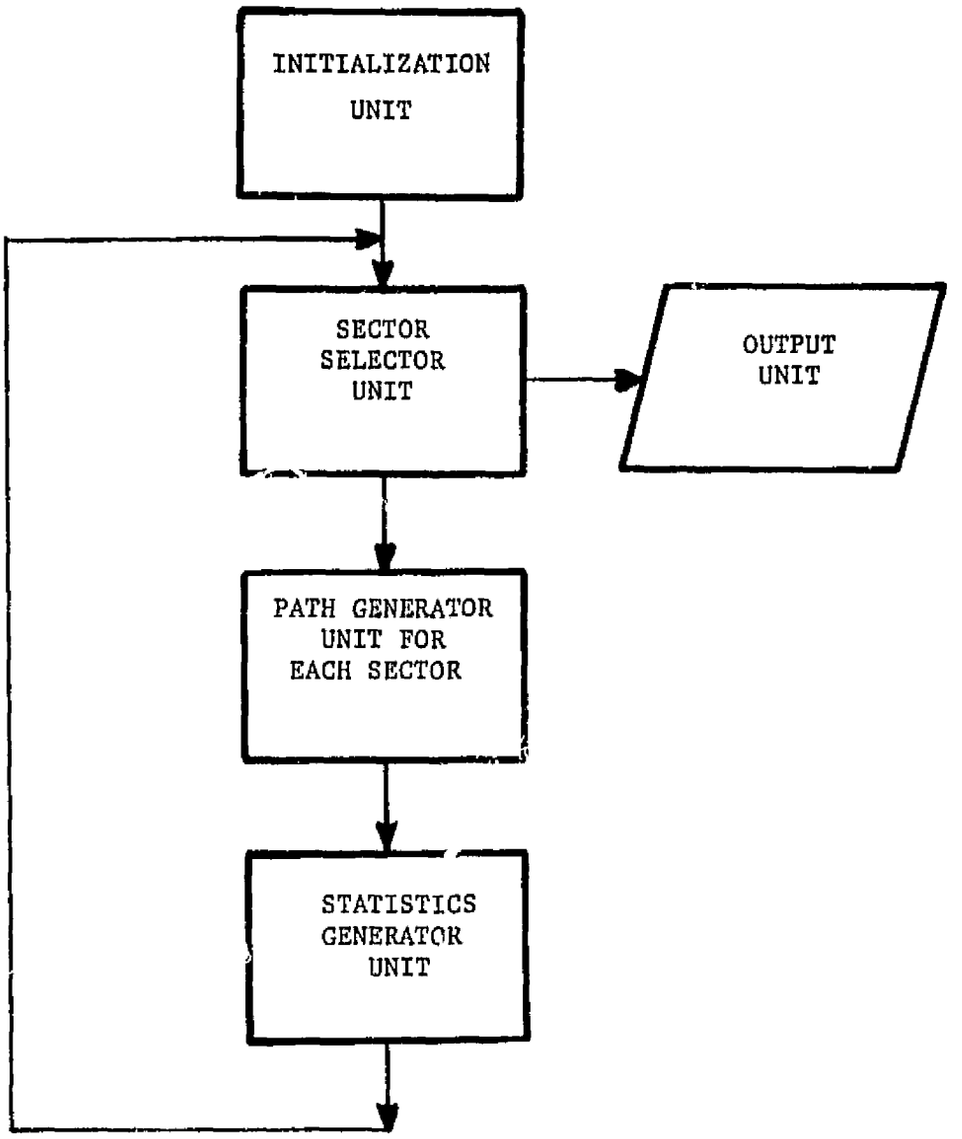

Fig. 5-2. General flowchart of logic.

The computer model has the following characteristics:

(1) It assigns an arrival time for each aircraft (if time is to be a factor in the simulation). The aircraft arrival time is based on the assumption that the inter-arrival times are exponential. The following equation was employed to generate exponential inter-arrival times:

$$TAU = -\frac{1}{\lambda} \ell n(u)$$

where λ = number of aircraft/unit time,

u = uniform random number.

(2) The flight paths are generated as described in Appendix A. Points along the flight path are calculated based on a specific time interval and velocity. Each flight may be defined in both time and space.

(3) The amount of computer storage required to maintain the flight data was kept to a minimum by examining flight paths in sequential pairs. To illustrate, the first flight pair would be AC1 and AC2 where AC1 was the prior flight and AC2 is the current flight. Once data are obtained from the two flights and the statistics updated, another flight is generated and AC2 becomes the prior and AC3 becomes the current. This procedure simplifies the calculation of the time parameter in that the prior flight will always be entering the airspace at time zero and the current flight will be entering at time TAU.

The computer model consists of five logical units as shown in Figure 5-2. The Initialization unit handles variable assignment and sets specific parameters by user input. It initiates the entire air pattern simulation. The Sector Selector handles the selection of the appropriate sector from which an aircraft will be entering the airspace. It also tallies the total number of flight paths simulated. The Path Generators are sets of programs (one for each sector) that operate flight paths based on the sector entry trajectories (see Appendix A). The Statistics Generator maintains desired histograms and updates the recursive mean and sums of squares functions. The Output unit handles the output of the desired histograms and related means and standard deviations.

There are currently five main programs that comprise the Air Pattern simulator. These are outlined in Appendix B along with the logic unit association. Individual flowcharts for each program are also given in Appendix B with a brief description.

For collision risk analysis the simulation model output consisting of prescribed histograms and statistics is used as input to special analysis programs. The types of output available and some of the analysis methods used are discussed in Chapter 6 along with presentation of selected results. The types of output available include that necessary to provide validation of the model. In the computation and interpretation of hazard statistics proper account must be taken of the fact that the tracks generated do not reflect any avoidance maneuvers. This is a basic limitation of the simulator which is really imposed by limitations in the real data. The data do not provide information concerning what parts, if any, are the results of pilot maneuvering to avoid a potential conflict situation. This limitation could be presumably overcome by including decision making algorithms in the simulation model. In doing this it would be desirable to obtain surveillance type data which could give a composite picture of the traffic at all times and the maneuvers performed in conflict situations.

CHAPTER 6

STATISTICAL ANALYSIS OF SIMULATED AIRSPACES

6.1 Histograms of Spatial Trajectory Deviations

6.1.1 Numerical results.— In order to verify that the trajectory model could generate valid flight profiles (in at least two dimensions), 500 aircraft were cycled through the approach pattern and statistics were calculated at downwind 1 (DW1), downwind 2 (DW2), and base plane (BASE) locations (see ref. 2). In addition to histograms of distance deviation, histograms of distance difference and time difference of sequential aircraft pairs were generated. All data presented in this section were generated with the arrival rate parameter selected at 100 aircraft per hour. The results may be generally summarized as follows: the distance histograms appear nearly normal with slight skew at the longer distances, the distance difference histograms appear to resemble a one-sided normal curve, and the time difference histograms appear exponential as would be expected. These data are included in Figures 6-1 through 6-9.

6.1.2. Comparison with published data.— Figure 6-10 shows selected distance deviation data from actual aircraft observations (ref. 2). Only distance data at SW1, DW2 and BASE planes are shown. Notice that in general the histograms are similar to those generated by the trajectory model with the exception of the increased skew at larger deviations. This difference in skew may be attributed in part to the random number generator in the trajectory model and in part to the skewness introduced by single engine high wing aircraft in the observations (see Figure 6-10d). Table 6-1 shows a summary comparison of first and second order statistics between actual and simulated distance deviations. Agreement is good at the DW1 and DW2 planes but tends to appear suspect at the BASE plane. This can perhaps be attributed to trajectory model constraints in the base leg turn and the fact that approaches directly into the base leg are not considered in the current simulation.

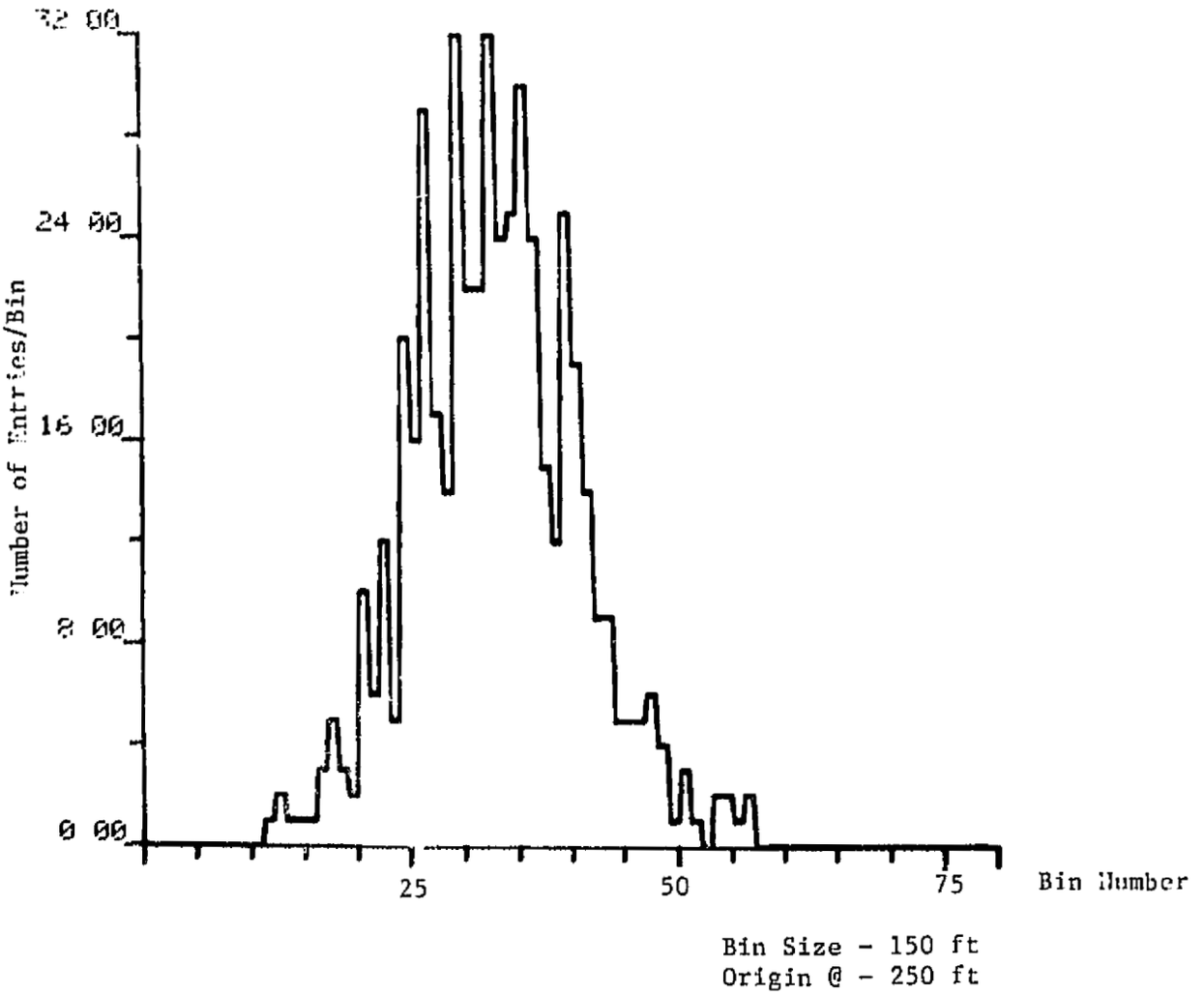

Figure 6-1. Distance Deviation - Downwind 1 Plane.

$\bar{x}$ = -5200 ft

σ = 1162 ft

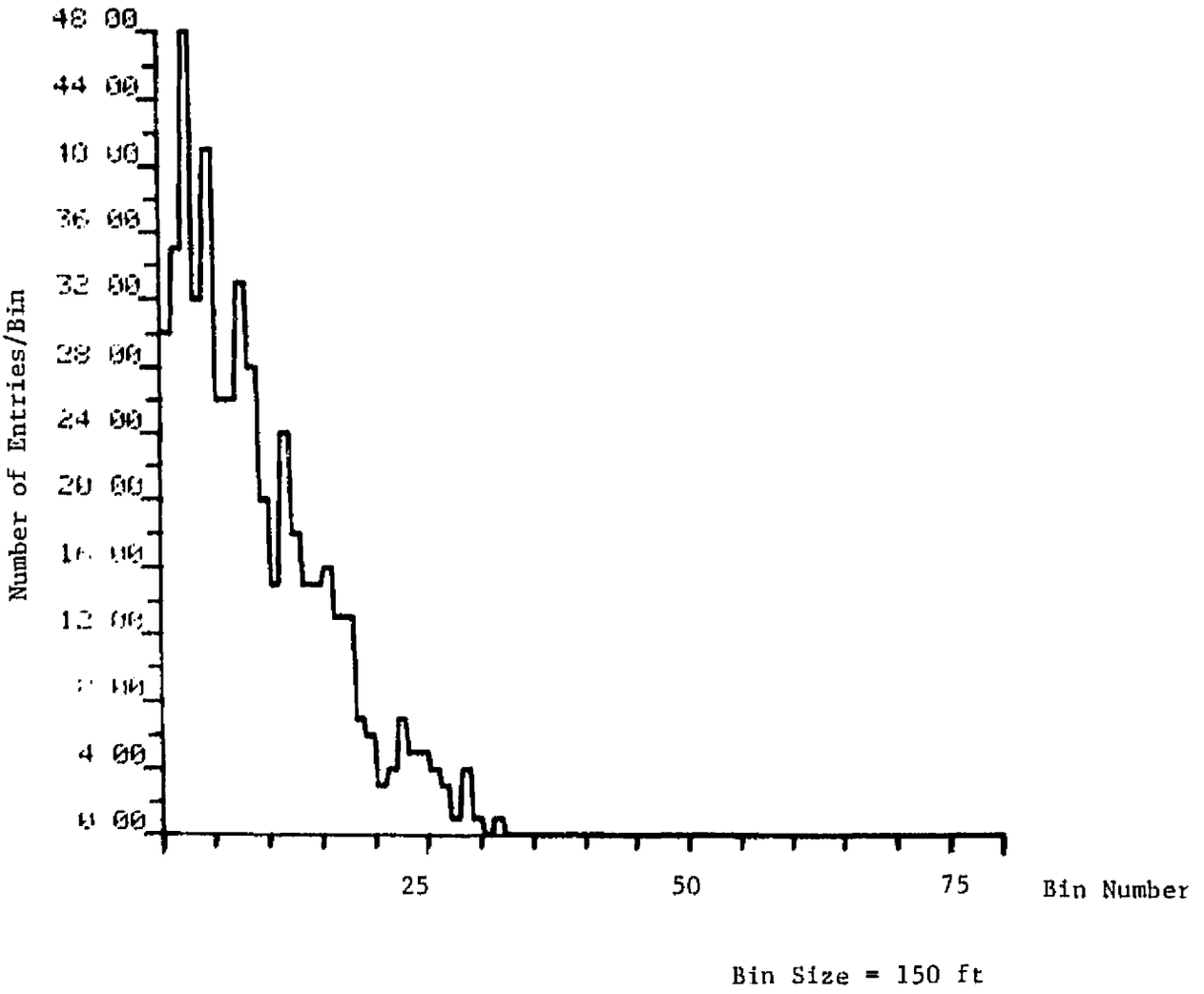

Figure 6-2. Distance Difference for Sequential Aircraft, Downwind 1 Plane.

$\overline{\Delta x}$ = 3126 ft

σ = 1011 ft

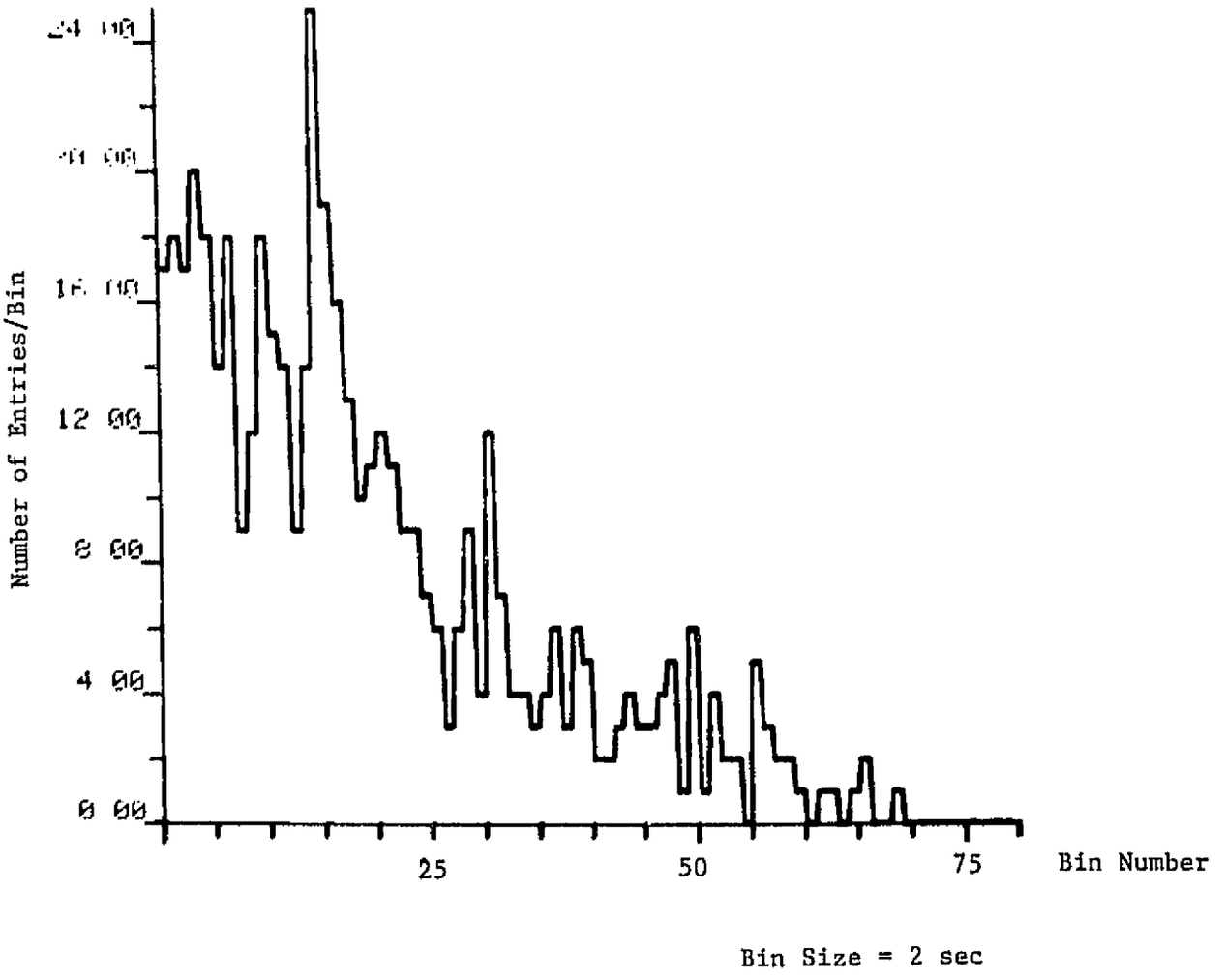

Figure 6-3. Time Difference for Sequential Aircraft Downwind 1 Plane.

$\bar{t}$ = 32 sec

σ = 31 sec

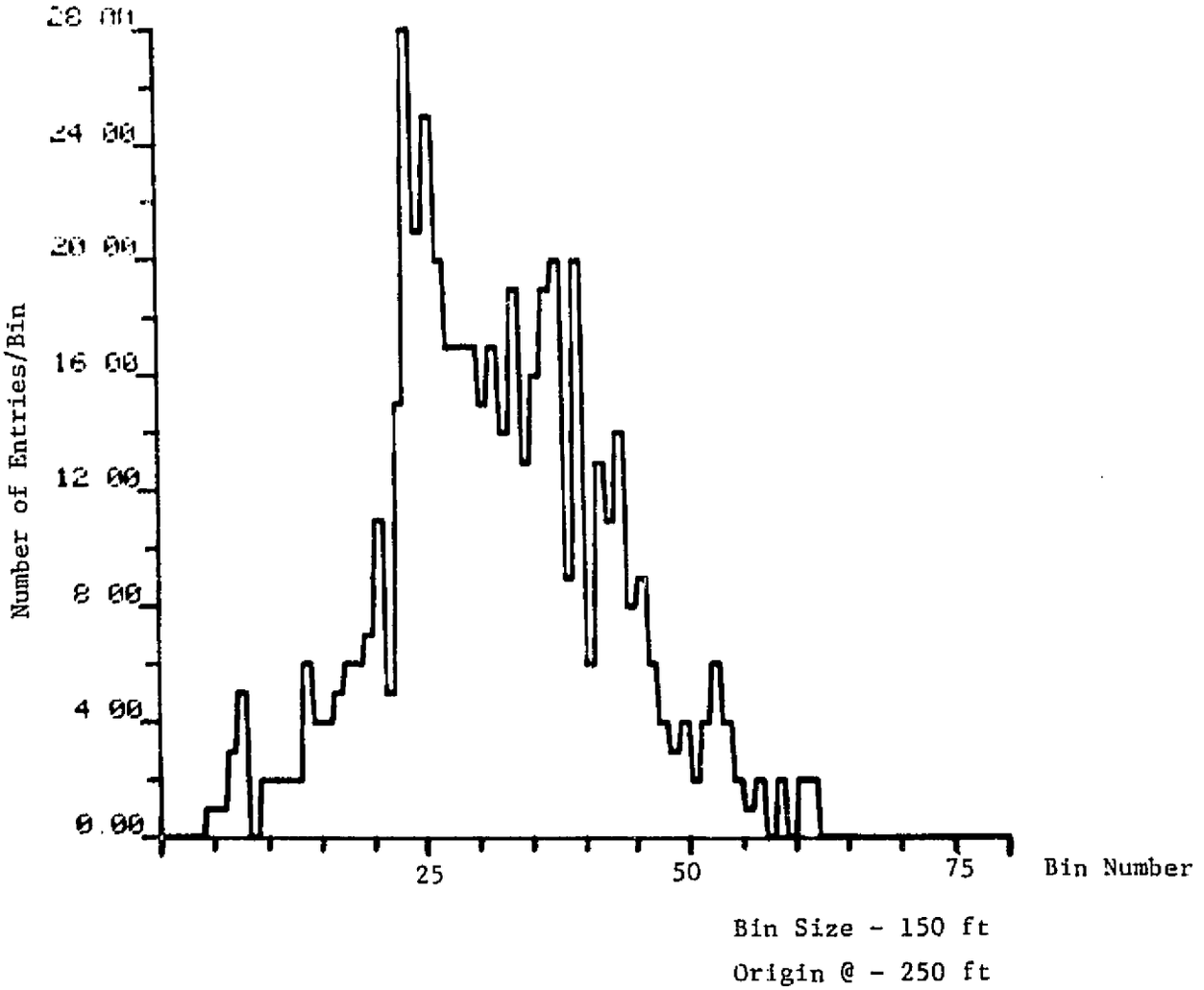

Figure 6-4. Distance Deviation - Downwind 2 Plane.

$\bar{x}$ = -5011 ft

σ = 1596 ft

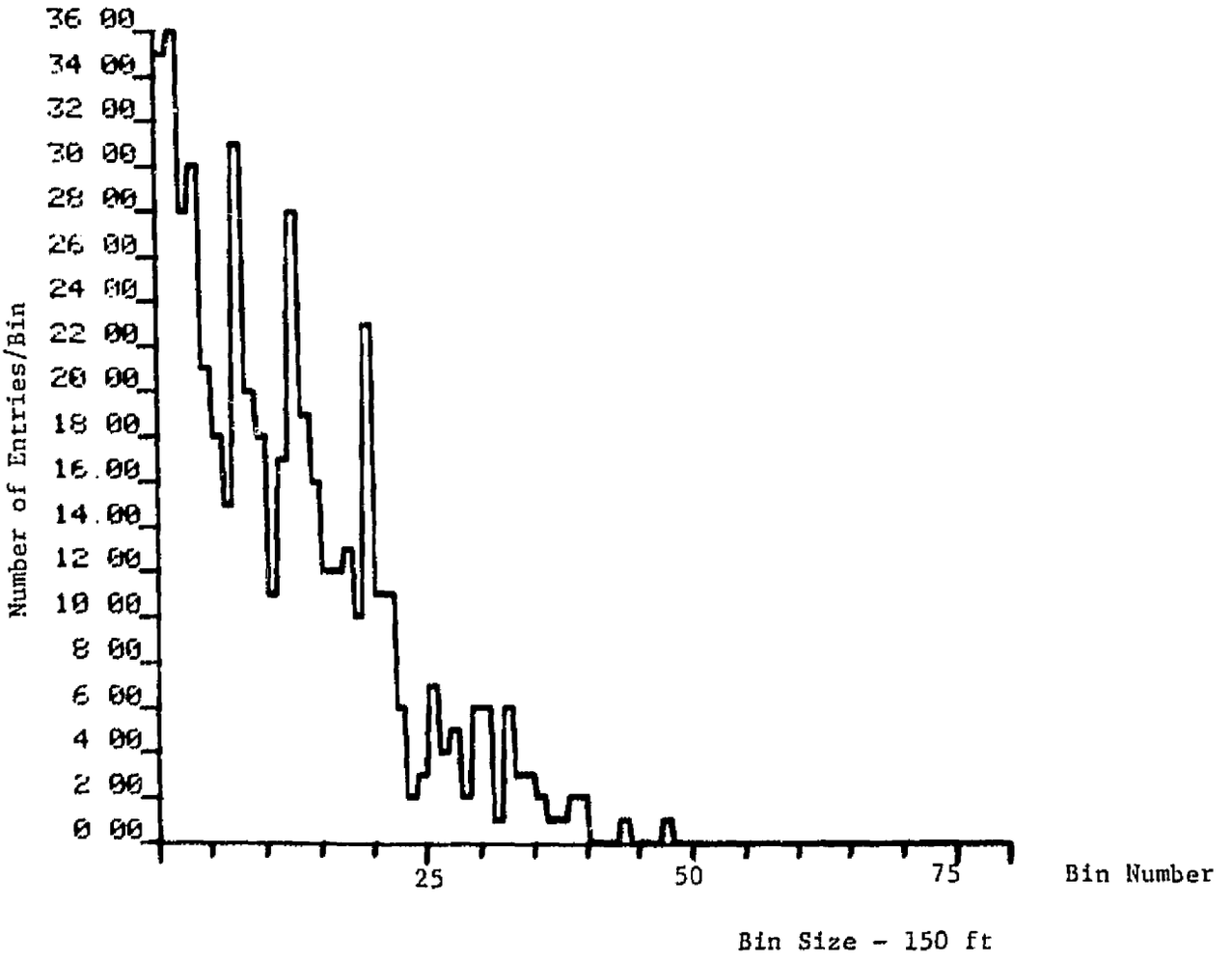

Figure 6-5. Distance Differential for Sequential Aircraft, Downwind 2 Plane.

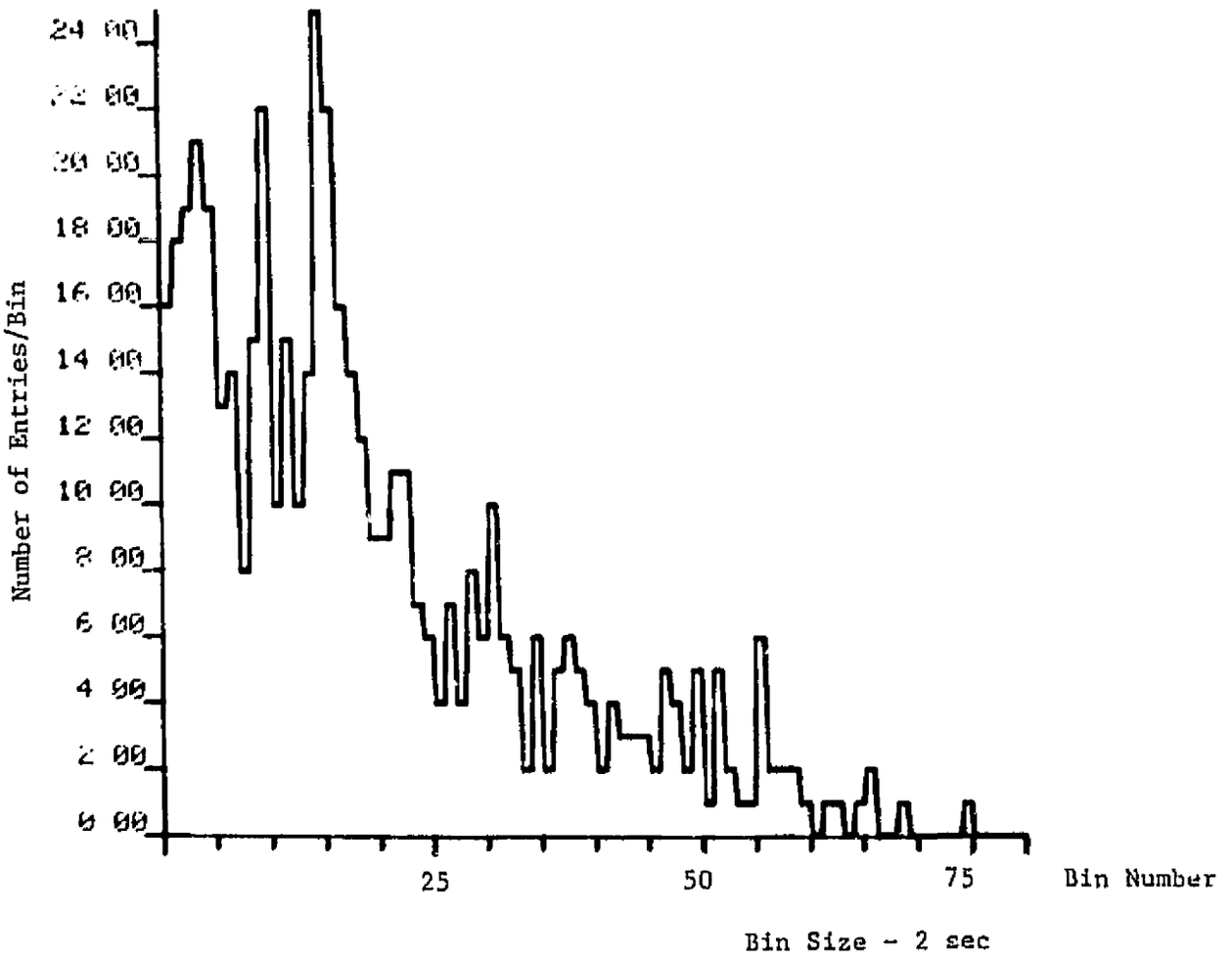

Figure 6-6. Time Difference for Sequential Aircraft, Downwind 2 Plane.

$\bar{t}$ = 39 sec

σ = 31 sec

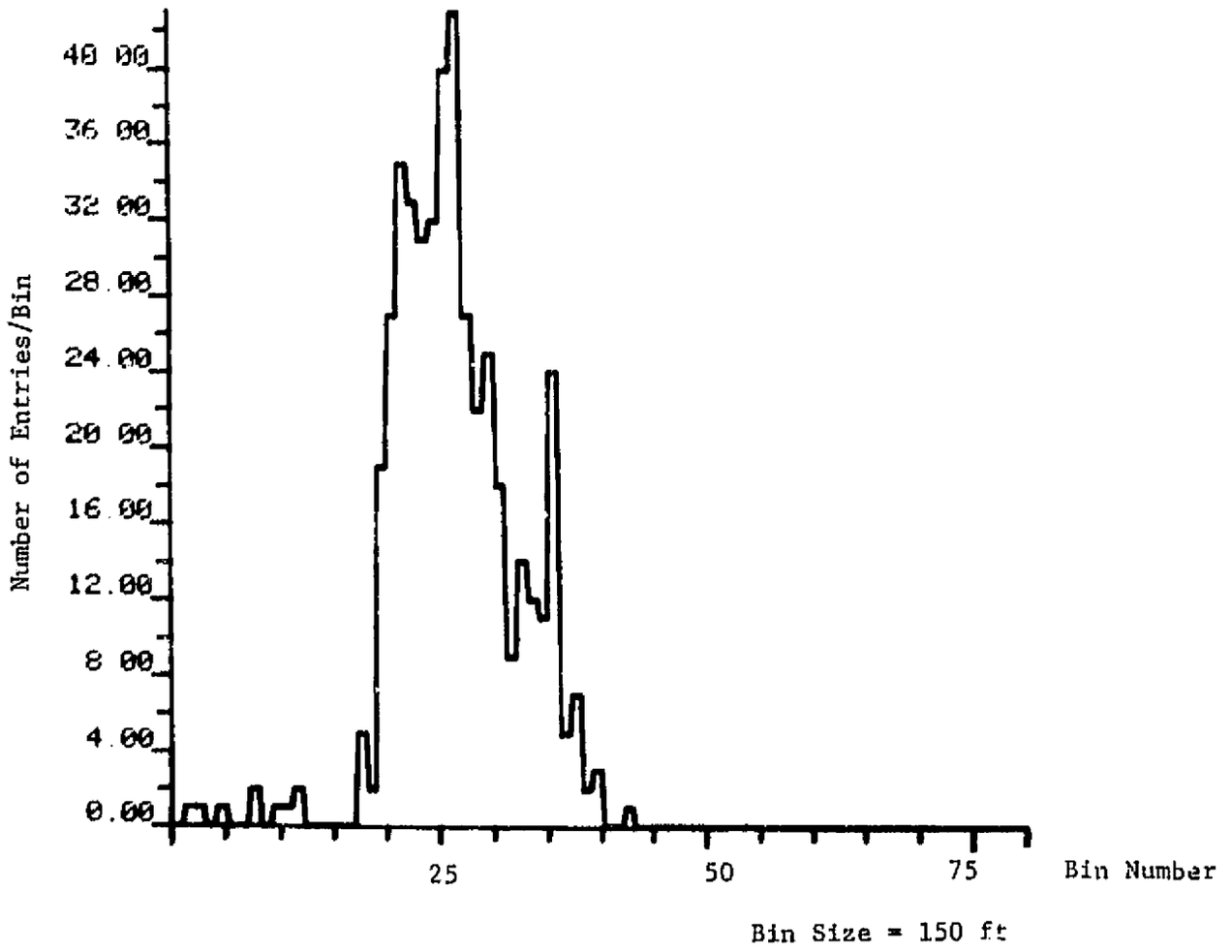

Figure 6-7. Distance Deviation - Base Leg Plane.

$\bar{y}$ = -3414 ft

σ = 1986 ft

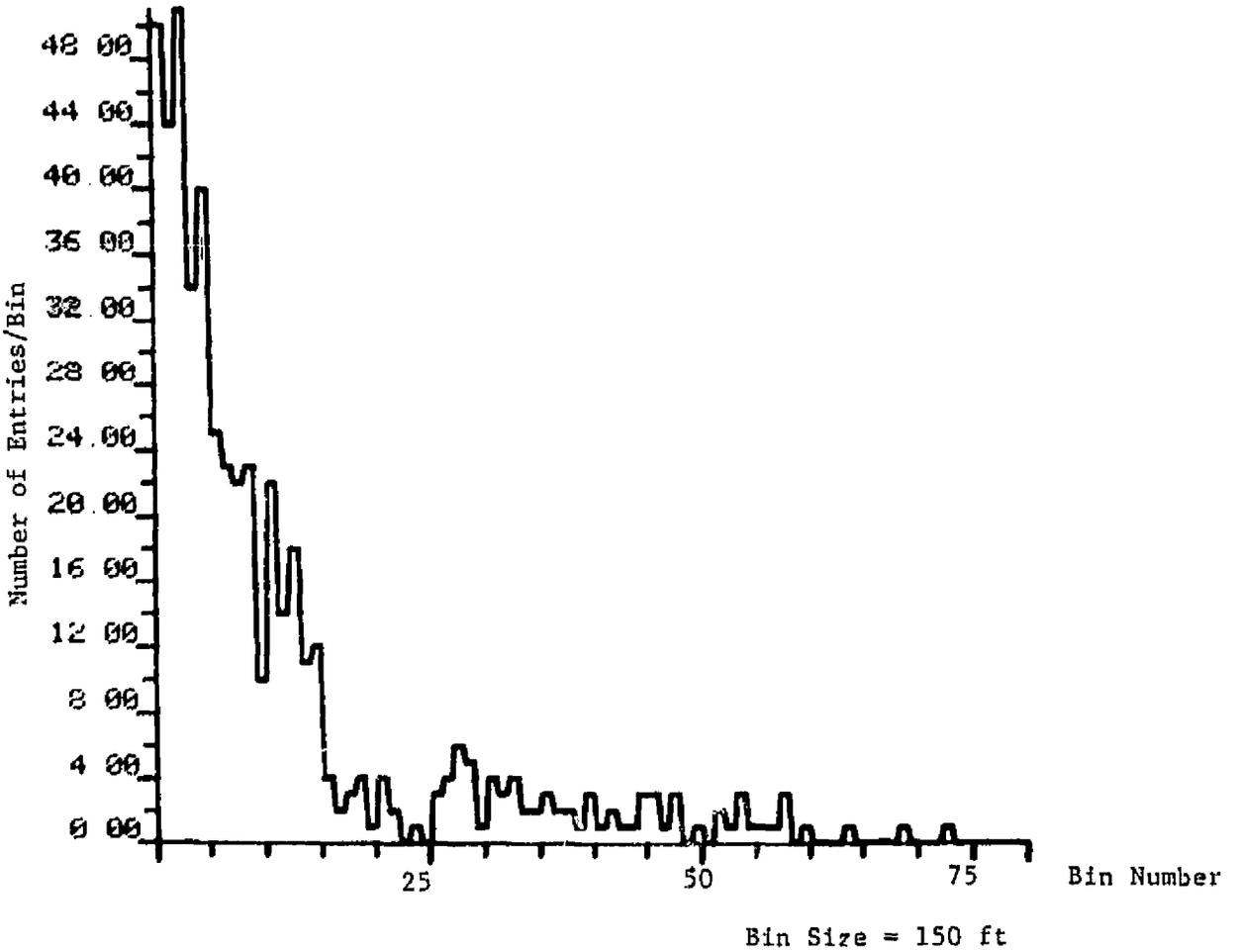

Figure 6-8. Distance Difference for Sequential Aircraft, Base Leg Plane.

$\overline{\Delta y}$ = 1743 ft

σ = 2153 ft

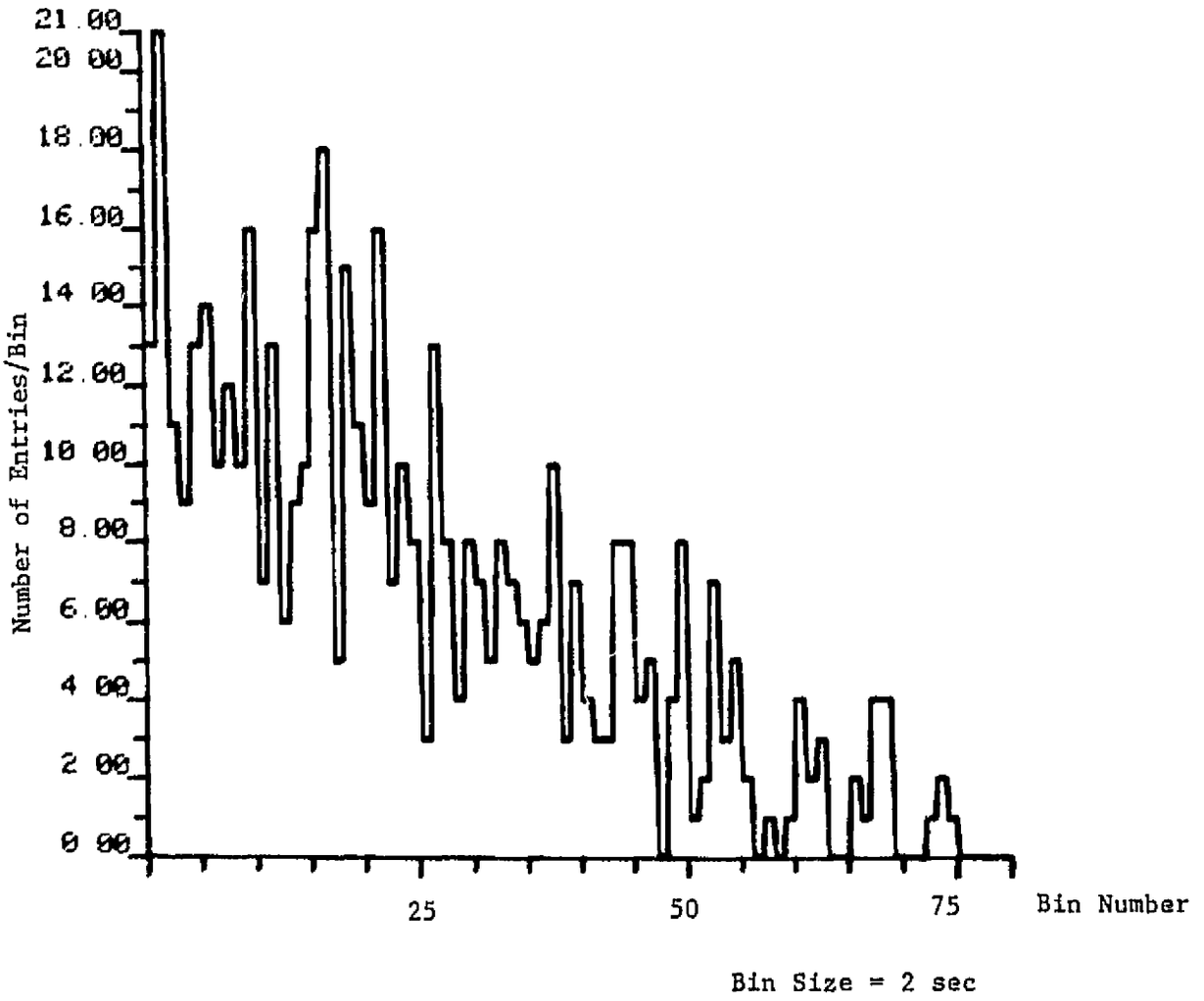

Figure 6-9. Time Difference for Sequential Aircraft, Base Leg Plane.

$\bar{t}$ = 49 sec

σ = 38 sec

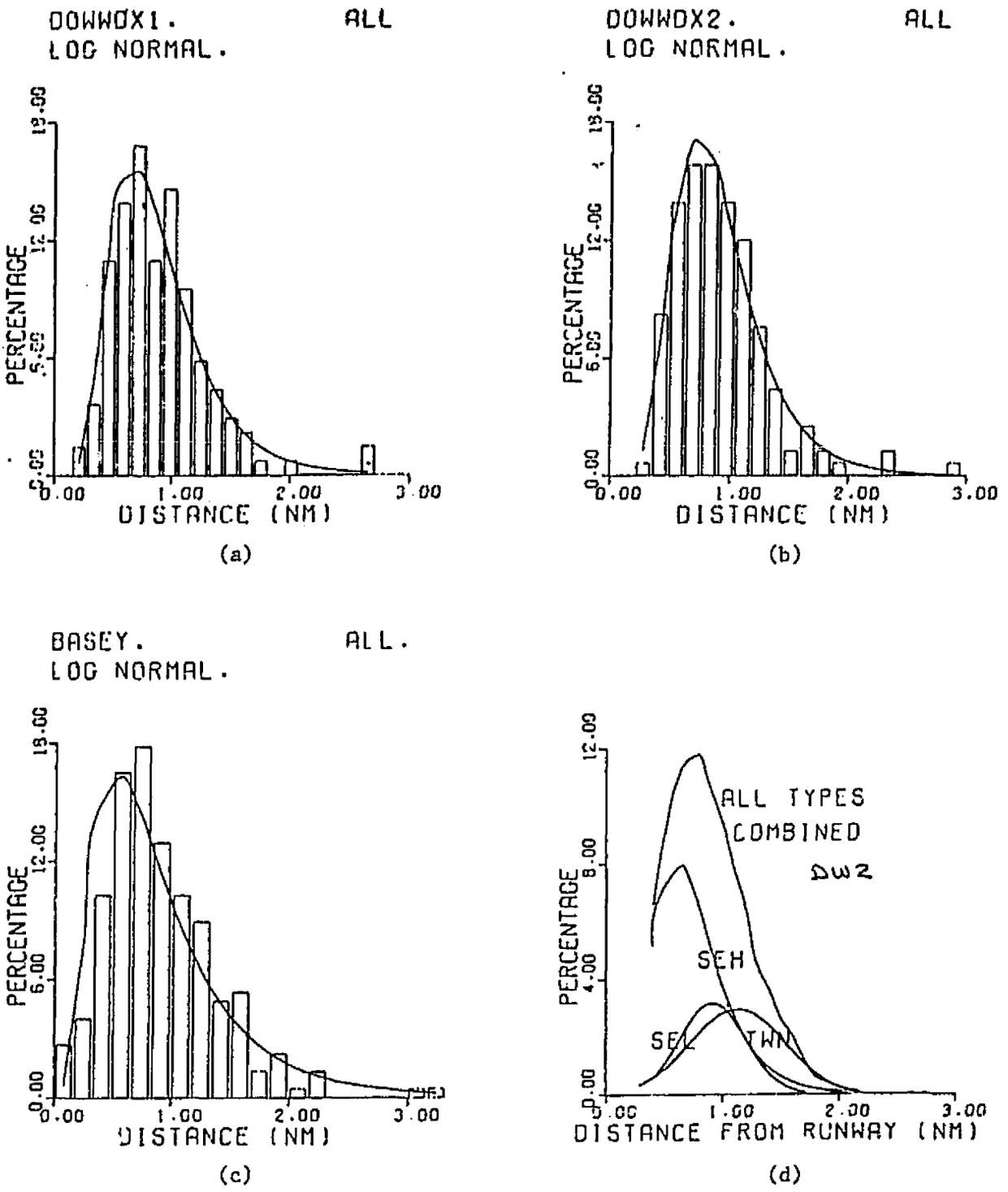

Figure 6-10. Published Data (ref. 2) from Actual Aircraft Observations in Uncontrolled Terminal Area.

Table 6-1. Comparison of Actual and Simulated Statistics at DW1, DW2, and BASE Planes.

	Actual (ref. 2)		Simulated	
	mean	std dev	mean	std dev
DW1	-5440'	2402'	-5200'	1162'
DW2	-5600'	780'	-4869'	1561'
BASE	-5535	552'	-3414	1986'

It is apparent from the preceding discussion that the current simulation can to a limited degree describe an uncontrolled terminal area in terms of the types of data previously published. It is felt that additional flexibility, when incorporated, will allow the trajectory model to be utilized in concert with the theoretical model discussed in previous chapters to assess hazard probabilities.

6.2 Estimated Hazard Probabilities

The trajectory model can be used to generate an estimate of hazard probabilities by observing the simulated airspace on an aircraft pairwise basis. If the simulation is exercised in such a manner that the separation distance of two aircraft occupying the area jointly is indexed versus time, and if this is performed over all aircraft pairs, then several outputs become available.

The least complex of these is a histogram of separation distance over the entire ensemble of aircraft pairs. While being the simplest output, it perhaps is also the least meaningful in predicting or assessing a hazard except to give an intuitive feel for the value of distance to closest approach which would (or should) be used to estimate hazard status from the other available outputs.

Figures 6-11 through 6-13 show histograms of separation distance for intensity parameters of 50, 100 and 200 aircraft/hour. The shape of the histograms for 50 and 100 aircraft/hour are similar in that a predominance is indicated about line number 20 (3000 ft) and that a relatively uniform distribution of distances is observed elsewhere. The histogram for 200 aircraft/hour begins to take on fairly uniform characteristics over its entire range and apparently indicates that a saturation situation exists and intensity parameters in this range should not be expected to generate realistic results. It would appear that minimum separation distances of one to three thousand feet are proper parameters for evaluating hazard probabilities (within the influence imposed by the limited capability simulation). It should also be remarked that distances greater than ten thousand feet were deleted from consideration.

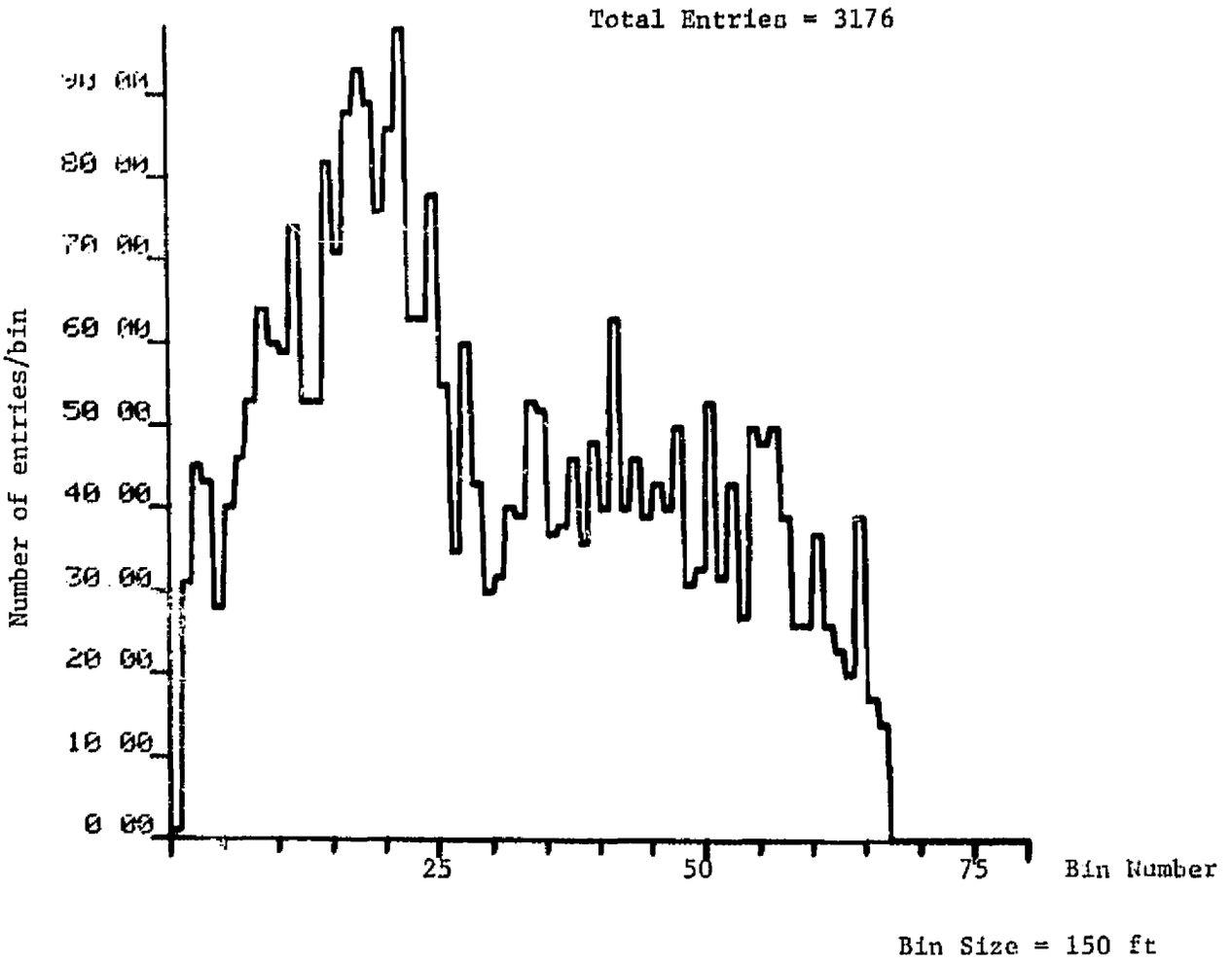

Figure 6-11. Distance Histogram for 50 Aircraft/Hour

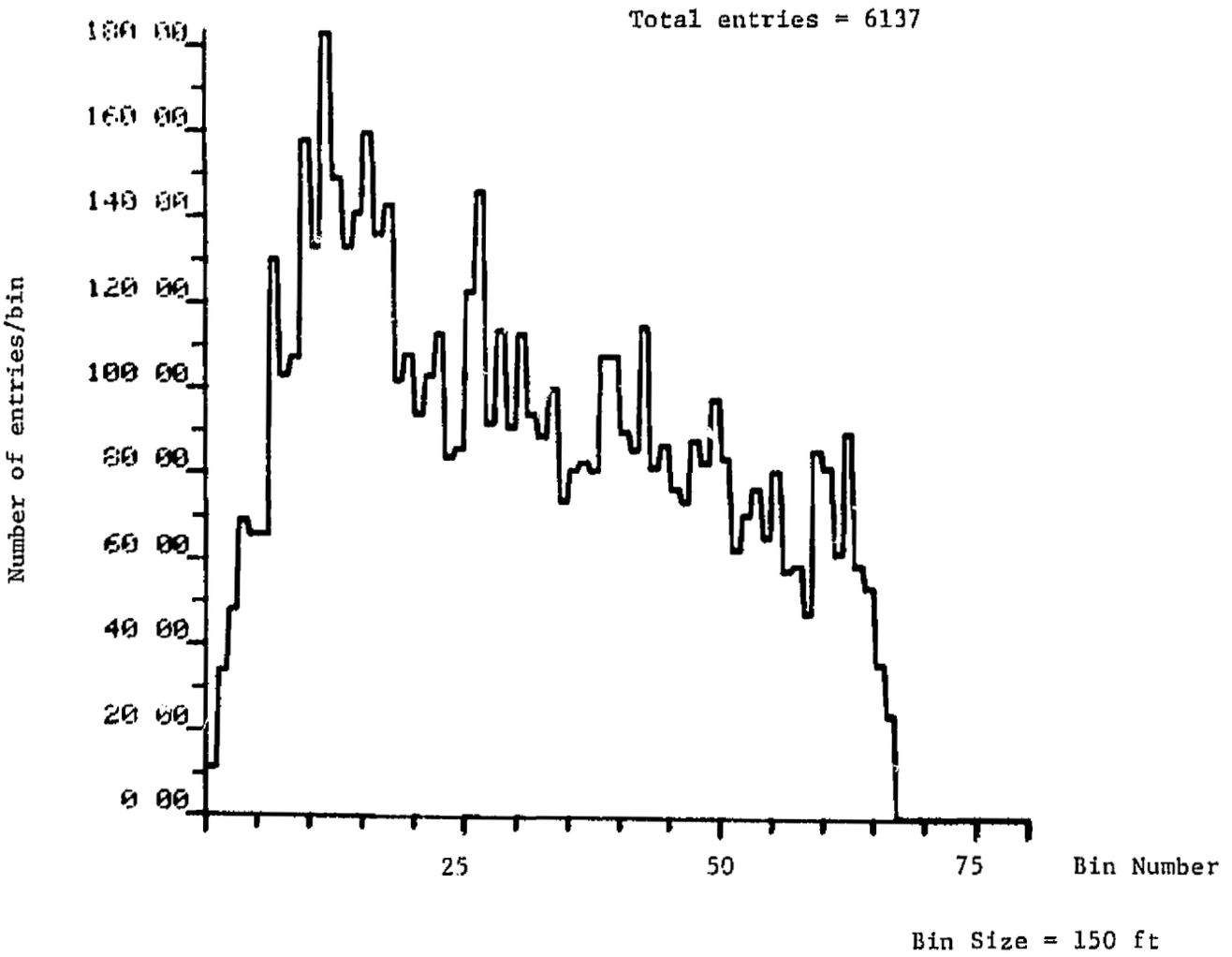

Figure 6-12. Distance Histogram for 100 Aircraft/Hour

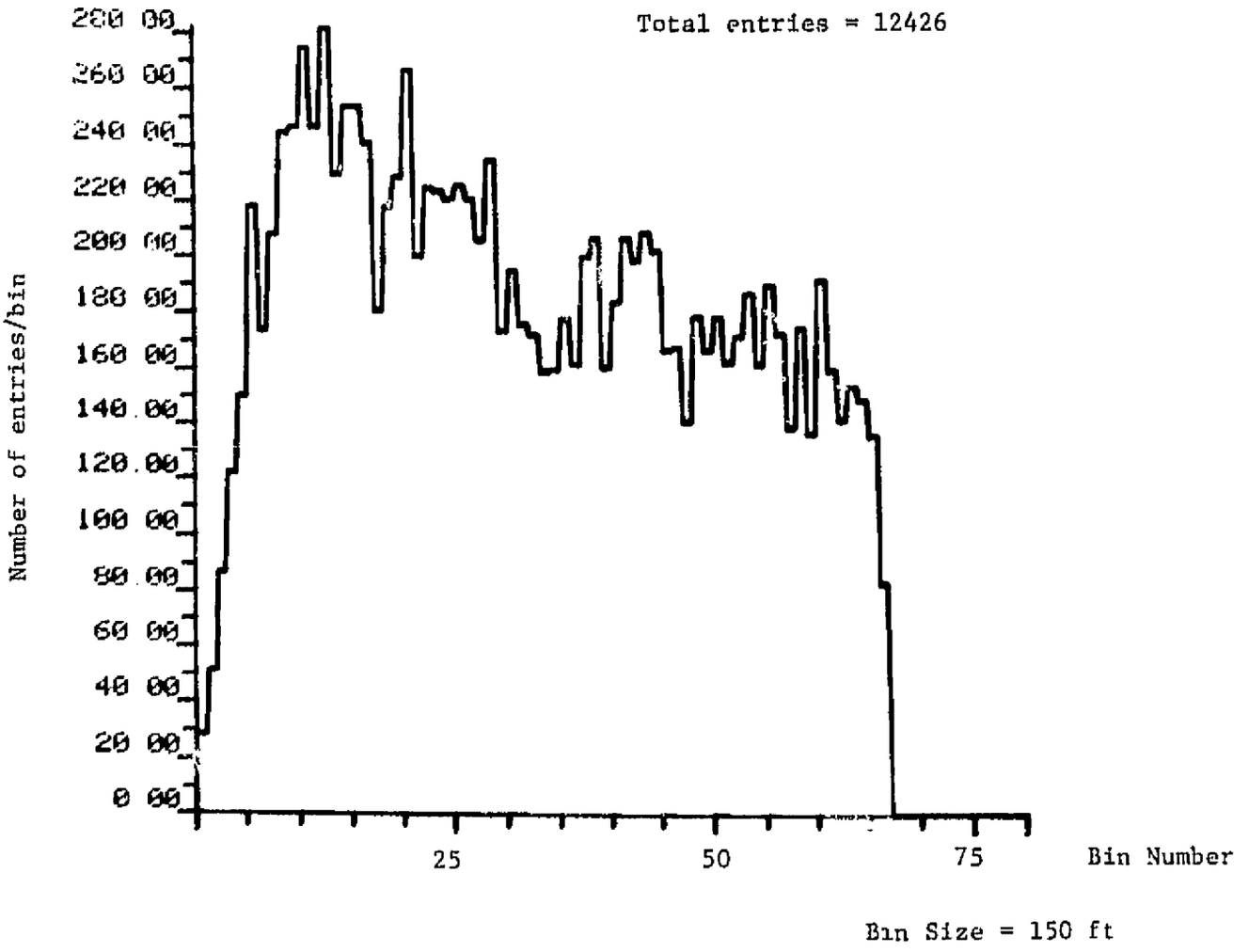

Figure 6-13. Distance Histograms for 200 Aircraft/Hour

A more meaningful assessment of the terminal area environment is what can be defined as "pilot workload." This is manifested as a histogram of the total time two aircraft spend at a separation distance less than some prespecified distance. This represents that distance at which a pilot would be concerned with the decision to make a see-and-avoid maneuver.

Figures 6-14 and 6-15 show histograms of encounter time length for an intensity parameter of 100 aircraft/hour and for minimum separation distances of 2000 feet and 1000 feet. Notice that the histograms appear exponential as would be expected from both the nature of the random variable and the density function assigned to inter-arrival times in the simulation. In going from a separation distance of 2000 feet to one of 1000 feet, the number of entries in the histogram decreased from 114 to 55. The histogram for 1000 ft is thus observed to be more erratic than the one for 2000 ft.

An alternate approach to representing "pilot workload" is to compute the cumulative time in an encounter normalized to the total time spent in the terminal area. Figures 6-16 and 6-17 show histograms demonstrating this type of data. Notice that as the separation distance parameter is decreased to 1000 feet, the prominance near bin 20 moves toward the origin. This is because, as the separation parameter is decreased, the number of aircraft which have the opportunity to spend a long time in an encounter is reduced (for a fixed number of aircraft) and more short encounters are produced (i.e. for zero feet separation parameter, there would be zero encounters while for infinite separation parameter, all aircraft would be in an encounter 100% of the time). Notice that for 2000 feet separation, 2% of the aircraft are in an encounter 100% of the time in the terminal area (see bin 51).

Table 6-2 shows a summary of the histogram data including means and standard deviations. Notice that as the intensity parameter varies for a given separation distance, the number of the entries for each histogram varies accordingly but that the mean and standard deviation do not vary appreciably. This is likely due to the fact that the same paths are generated for each case and suggests that 100 aircraft are sufficient to generate good sample means and standard deviations. Notice that as the separation distance parameter varies, the means and standard deviations vary accordingly.

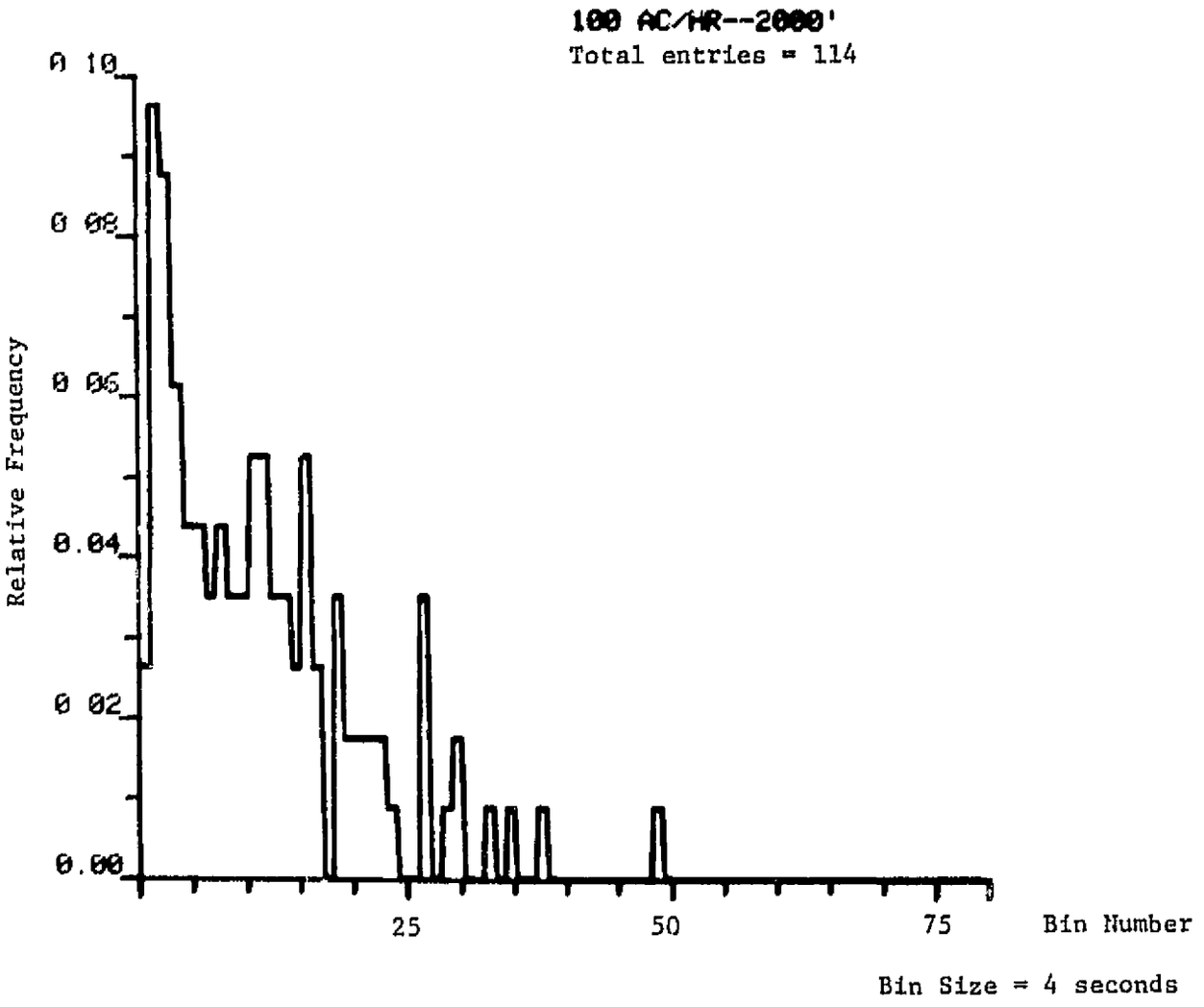

Figure 6-14. Encounter Length Histogram for 100 Aircraft/Hour and Minimum Separation Distance of 2000 ft.

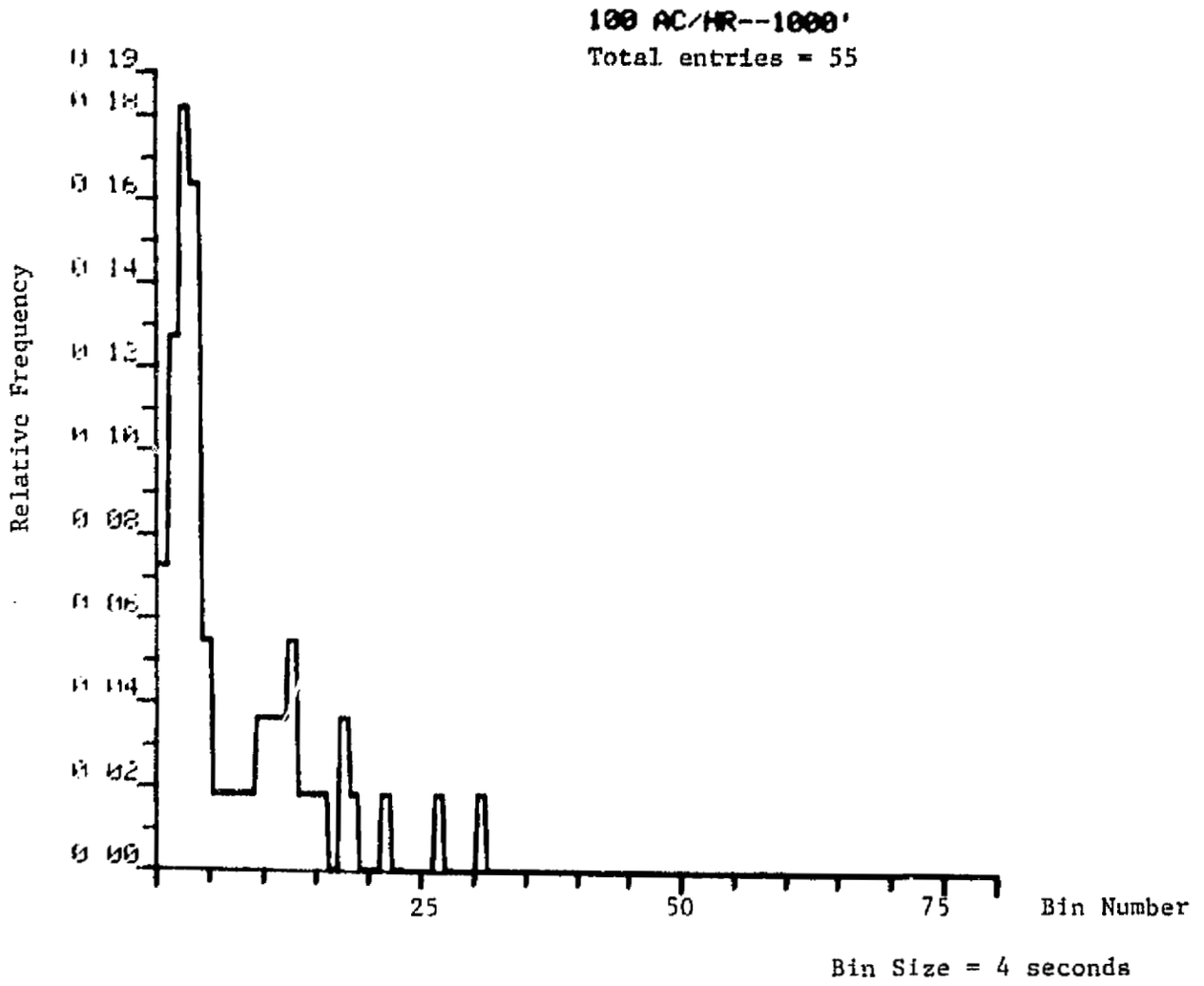

Figure 6-15. Encounter Length Histogram for 100 Aircraft/Hour and Minimum Separation Distance of 1000 ft.

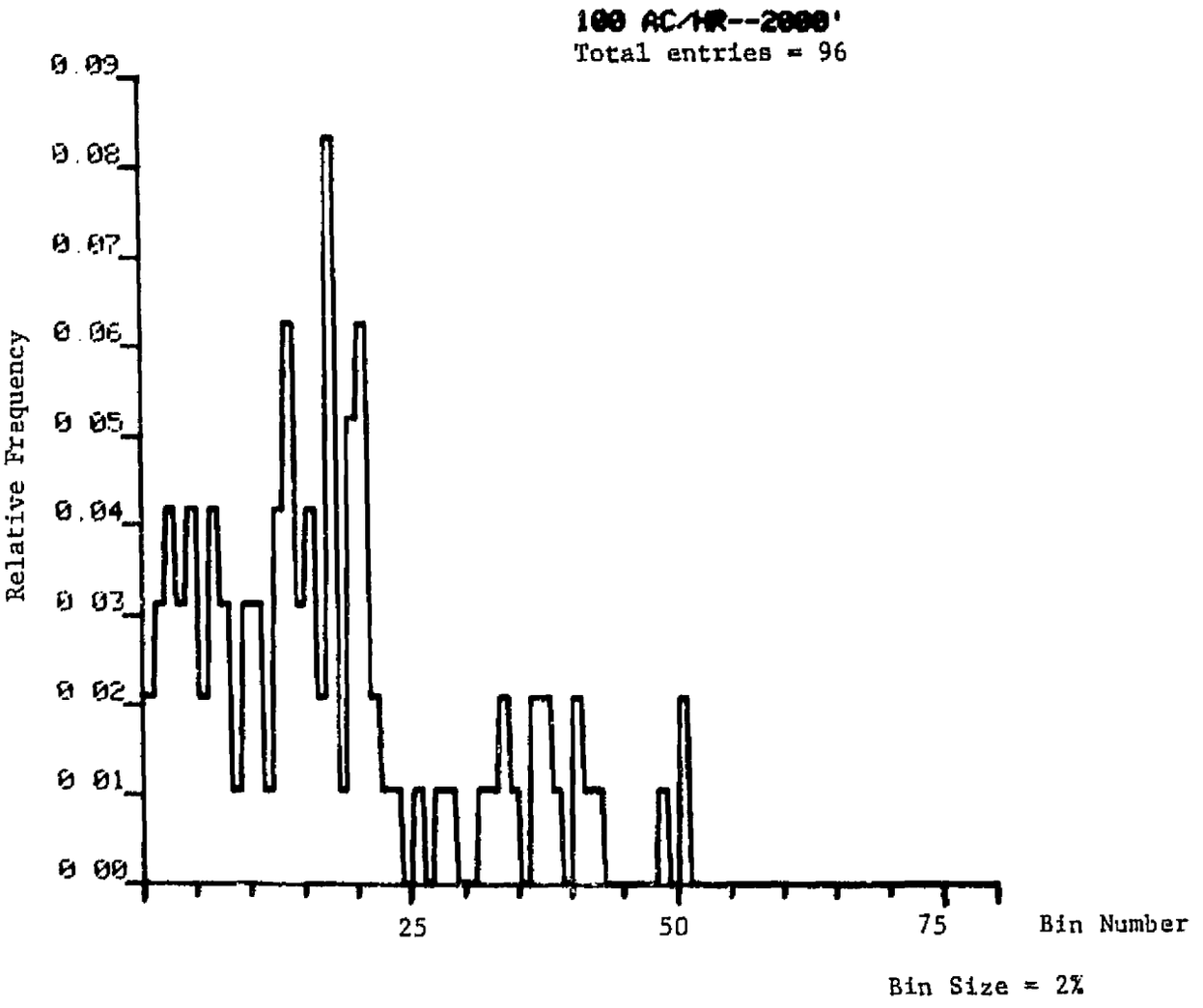

Figure 6-16. Histogram of Percentage of Time in an Encounter, 100 Aircraft/Hour and 2000 Feet Separation.

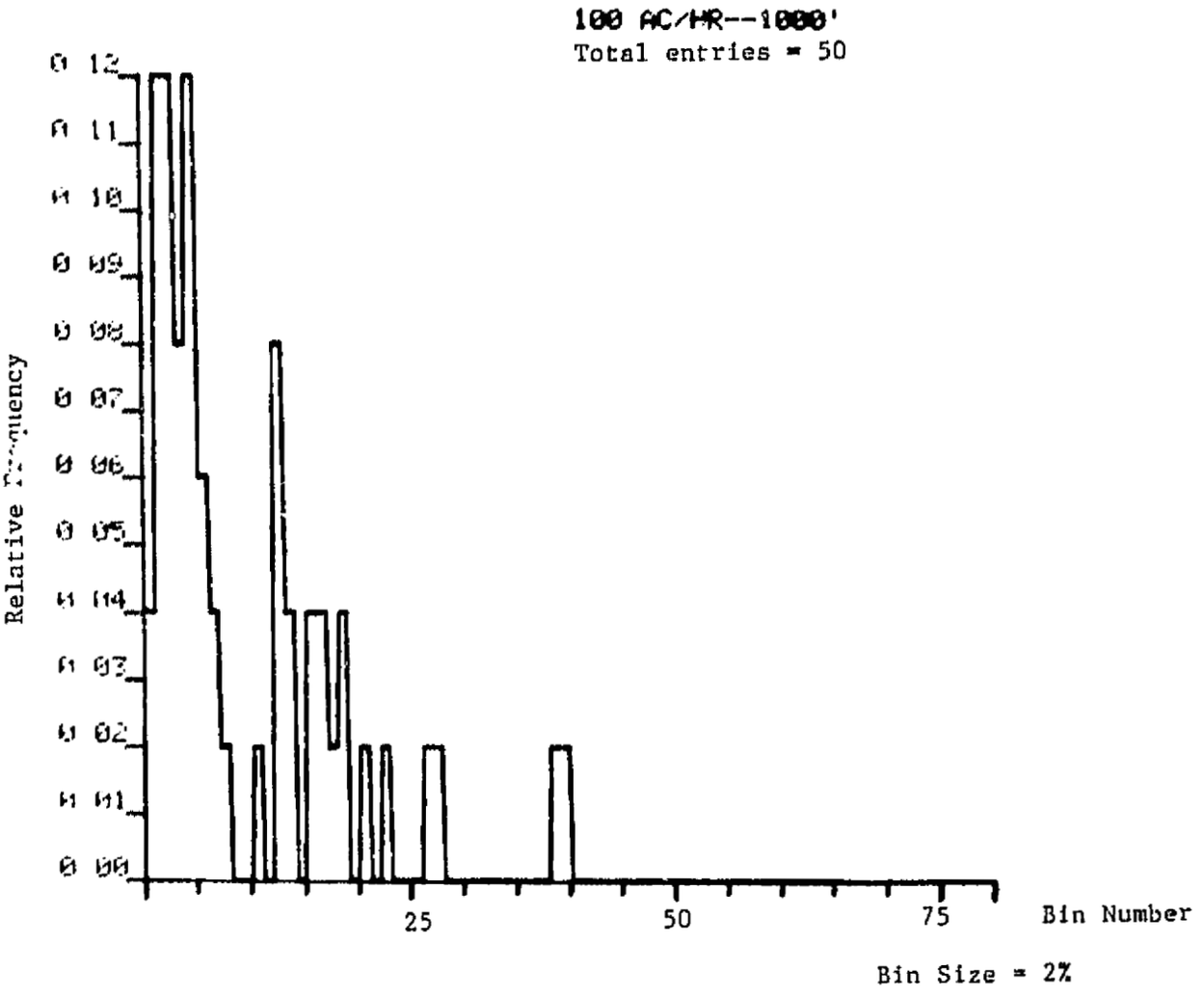

Figure 6-17. Histogram of Percentage of Time in an Encounter, 100 Aircraft/Hour and 1000 Feet Separation.

Table 6-2. Histogram Summary

Encounter Length Histograms
(Percentage of Aircraft having a Given Length of Time in an Encounter)

Aircraft/Hour =		50	100	200	
D_{MIN} = 1000 ft	TOTAL	24.0	55.0	104.0	(entries)
	MEAN	34.7	26.5	28.1	(seconds)
	STD DEV	26.2	27.1	28.6	(seconds)
D_{MIN} = 2000 ft	TOTAL	50.0	114.0	205.0	(entries)
	MEAN	47.4	43.7	45.4	(seconds)
	STD DEV	42.9	36.6	41.3	(seconds)

Percent Time in an Encounter Histograms
(Percentage of Aircraft having a Given Percent of Their Total Flight Time in the Terminal Area in an Encounter)

Aircraft/Hour =		50	100	200	
D_{MIN} = 1000 ft	TOTAL	20.0	50.0	94.0	(entries)
	MEAN	27.5	19.4	20.0	(percent)
	STD DEV	17.1	18.7	18.0	(percent)
D_{MIN} = 2000 ft	TOTAL	46.0	96.0	175.0	(entries)
	MEAN	34.1	34.8	35.1	(percent)
	STD DEV	28.1	24.4	27.0	(percent)

Another meaningful output available from the trajectory model is the number of independent times, "encounters," two aircraft are within a pre-specified distance. This is independent of the length of time spent in this situation and likely becomes the output most closely related to hazard probability. For example, if one incorporated distance, rate, relative heading, velocity, and binoculars, this output could be used in a Monte Carlo fashion to produce estimated probability of mid-air collision in the same sense that it is done theoretically in previous chapters.

To demonstrate the potential for using the simulation to examine hazard probabilities, the number of independent "encounters" was generated for minimum separation distances of 1000, 2000, and 3000 feet and for intensity parameters of 50, 100, and 200 aircraft per hour. The results are shown in Figure 6-18. Referring to Figure 4-1 and invoking the rationale that:

(1) ΔX be extended to the distance an aircraft travels from entering the airspace to touchdown,

(2) α corresponds to the minimum separation distance,

(3) the intensity parameter can be interpreted as a measure of average number of aircraft in the airspace, and

(4) the number of encounters (or for 100 aircraft, the average number per aircraft) can be interpreted as a measure of hazard probability.

One can observe that the simulation does indeed produce data in consonance with theoretical predictions.

Notice that the curves of Figure 6-18 tend to "flatten out" at high intensity parameters as opposed to the behavior observed with the large average number of aircraft in Figure 4-1. This is a direct result of the "saturation" mentioned previously as the intensity parameter is allowed to increase. In fact, for very large values the curves would peak, then diminish, becoming asymptotic to 100 encounters. That is, as the number of aircraft increases, a point is reached where a given aircraft is always in an encounter. Thus one obtains one and only one encounter per aircraft over 100 aircraft, producing 100 encounters independent of parameter value. This indicates the simulation is valid only over a practical range and is not useful in examining limiting conditions.

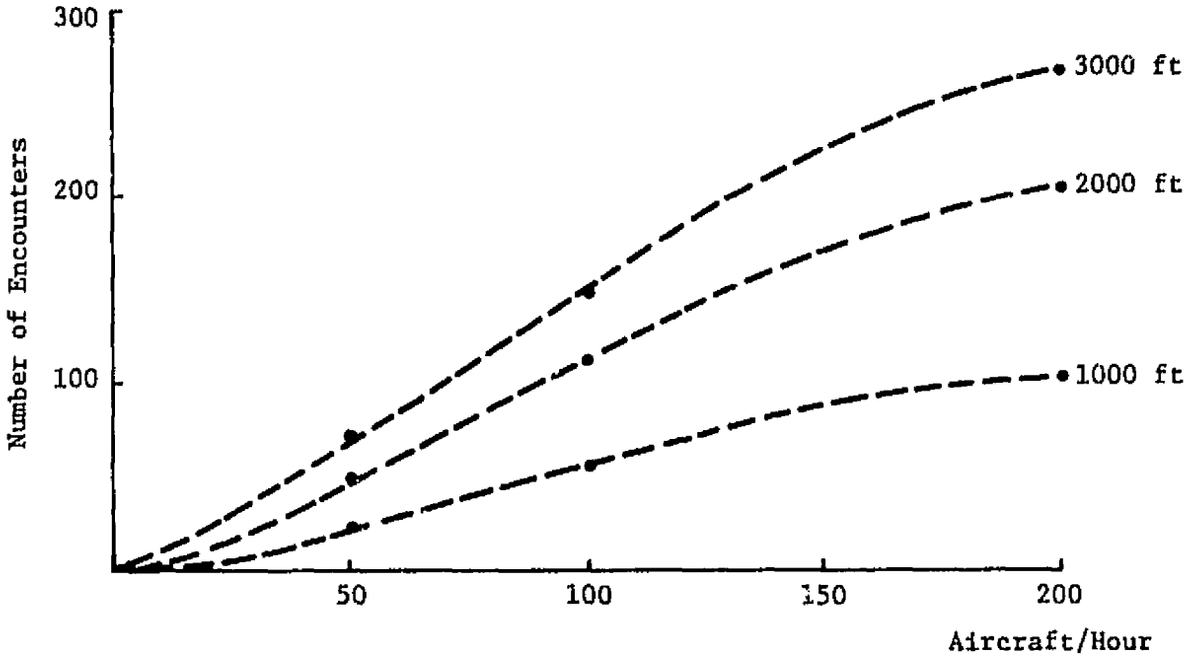

Figure 6-18. Number of Encounters vs Aircraft/Hour with Minimum Separation Distance as a Parameter.

CHAPTER 7

A NON-CLASSICAL MODEL FOR RANDOM AIRCRAFT TRAJECTORIES

The simulated trajectory model of Chapter 5 represents one reasonable approach to the simulation of random aircraft trajectories that enter a landing pattern under the Poisson regime. There are other models, such as the Gauss-Markov dynamical models popularized in the modern control literature, that one might consider. The application of such models to trajectory simulation and analysis is a well-developed, well-published topic.

In this section departure is made from the Gauss-Markov dynamical model to consider Poisson-driven dynamical systems. The purpose is merely to suggest that there are models other than Gauss-Markov models that deserve consideration. The actual choice of a suitable model must be based on careful statistical analysis of competing models and comparison with measured data.

7.1 Poisson-Driven Dynamical System

The construction of a Poisson-driven dynamical model for random aircraft trajectories proceeds as follows. The random telegraph wave (ref. 11)

$$\dot{T}(t) = (-1)^{N(t)} \tag{7-1}$$

with N(t) a Poisson counting process is defined as the control of the aircraft. This control is fixed at ± 1 between event times of the Poisson process as shown in Figure 7-1. The simplest of all Poisson-driven dynamical models for random trajectories is then obtained by letting y_t denote the cross-path deviation of a trajectory from the nominal landing pattern and modelling y_t as

$$y_t = T(t) \quad ; \quad T(t) = \int_0^t (-1)^{N(\sigma)}\, d\sigma \quad . \tag{7-2}$$

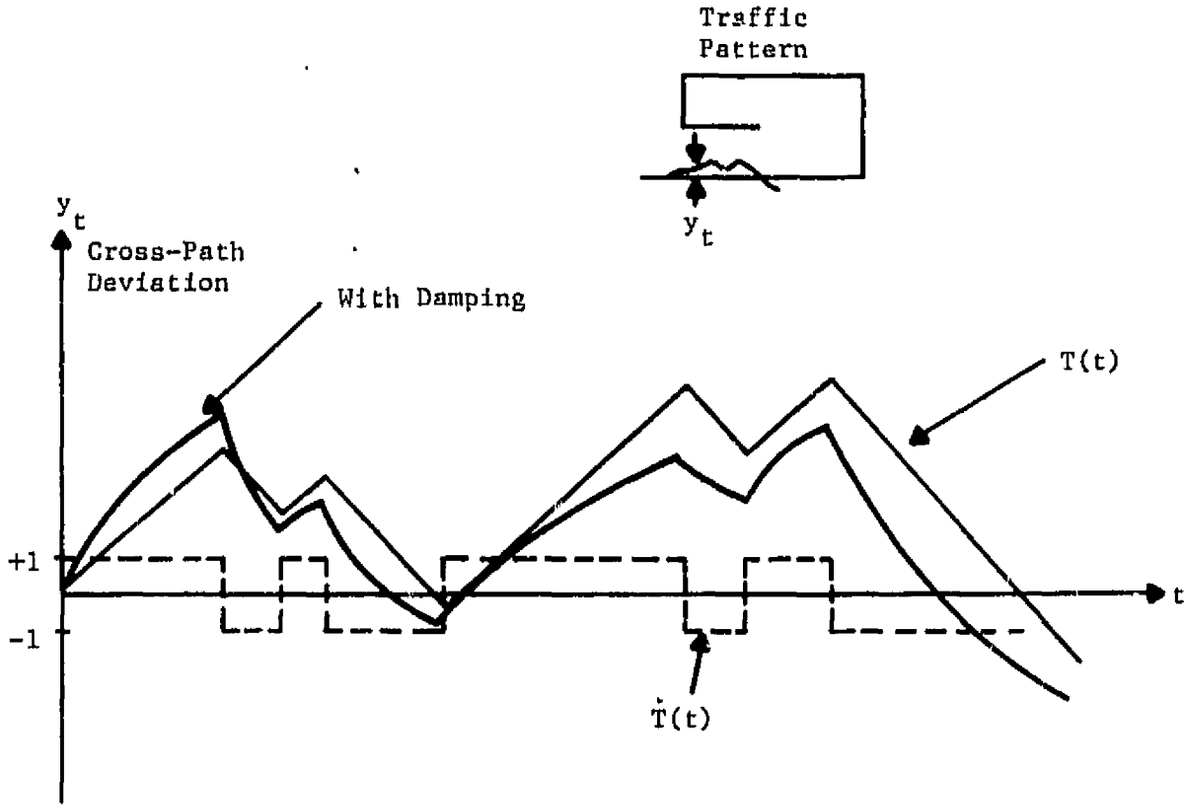

Figure 7-1. Typical Poisson Driven Trajectories.

Thus y_t is an integrated version of the random telegraph wave that represents fixed-velocity aircraft trajectories which deviate linearly from the nominal trajectory until they are corrected at a Poisson event time. A typical trajectory is illustrated in Figure 7-1. The process T(t) is often called a "random time" (ref. 11).

A refinement to eq. (7-1) is obtained by introducing a damping term β and writing y_t as

$$y_t = e^{-\beta(t-t_1)} y_{t_1} + \int_{t_1}^{t} e^{-\beta(t_1-\sigma)} (-1)^{N(\sigma)} \, d\sigma \, . \quad (7\text{-}3)$$

The corresponding random differential equation is

$$dy_t + \beta y_t \, dt = dT(t) \, . \quad (7\text{-}4)$$

A typical trajectory for this model is also illustrated in Figure 7-1. The model can, of course, be generalized further to account for inertial effects.

7.2 Density Evolution for Poisson-Driven Dynamical Systems

The statistical characterization for y_t is complete when the joint density function for $y_{t_1}, y_{t_2}, \ldots, y_{t_n}$ is known for all finite t-sets $(t_1, t_2, \ldots, t_n)$. In this section consider the determination of the partial differential equation that characterizes the first-order density function, denoted $f(\gamma;t)$, for y_t. In this derivation the increment dT(t) plays an important role.

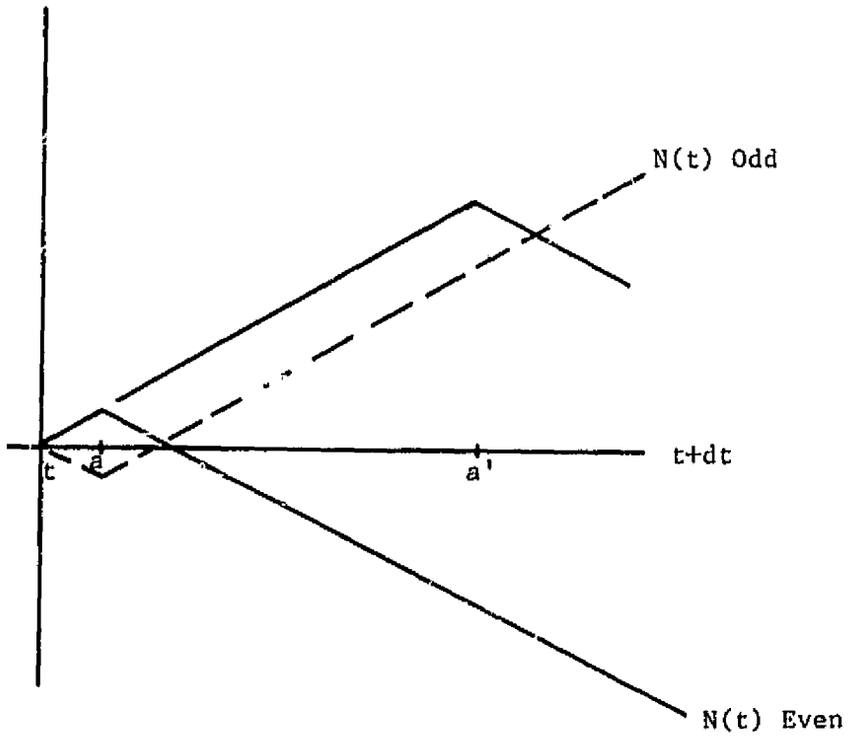

Figure 7-2. Typical Sample Functions of the Increment Process N(t).

Typical sample functions for $dT(t) = \int_t^{t+dt} \dot{T}(\sigma)\, d\sigma$ are illustrated in Figure 7-2 for various event times $t < a < t + dt$. The length of an increment is

$$dT(t) = \int_t^{t+dt} (-1)^{N(\sigma)}\, d\sigma = \int_0^{dt} (-1)^{N(t+u)}\, du$$

$$= -(dt - 2a)(-1)^{N(t)} \quad , \quad 0 \le a \le dt \quad . \tag{7-5}$$

Given that a Poisson event has occurred in the interval $[t, t + dt)$, the event time a is uniformly-distributed in $[t, t + dt)$. It can then be shown that the distribution function for $dT(t)$ is

$$F_{dT}(\gamma) = P[dT(t) \le \gamma]$$

$$= \begin{cases} 0 \ , & \gamma < -dt \\ [1 - \lambda dt]\, P_o + \frac{\lambda}{2}(\gamma + dt), & -dt \le \gamma < dt \\ 1 \ , & \gamma > dt \end{cases} \tag{7-6}$$

where P_o is the probability that $N(t)$ is odd and λ is the intensity parameter for $N(t)$. This distribution function, illustrated in Figure 7-3, has a jump of size $[1 - \lambda dt]\, P_o$ at $\gamma = -dt$ and a jump of size $[1 - \lambda dt][1 - P_o]$ at $\gamma = dt$. The result simply says the increment $dT(t)$ has length $-dt$ with probability $[1 - \lambda dt]\, P_o$, which is the probability that $N(t)$ is odd and no events occur in $[t, t + dt)$, and length dt with probability $[1 - \lambda dt][1 - P_o]$, which is the probability that $N(t)$ is even and no events occur in $[t, t + dt)$. The lengths $-dt < \lambda < dt$ are uniformly distributed with density $\lambda/2$. The mean and variance

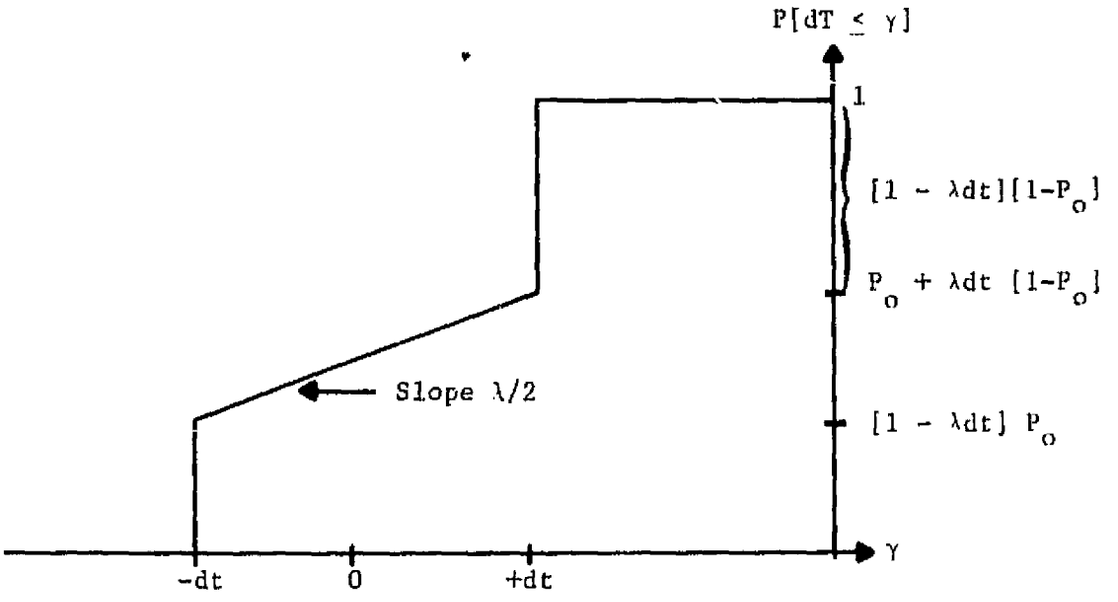

Figure 7-3. Distribution Function for the Increment Process dT(t).

of dT(t) are given by

$$E[dT(t)] = -dt[1 - \lambda dt]\, P_o + dt[1 - \lambda dt][1 - P_o]$$

$$= dt[P_e - P_o] + 0(dt) \qquad (7\text{-}7)$$

and

$$var[dT(t)] = 0(dt) \quad ,$$

where $P_e = 1 - P_o$ is the probability that N(t) is even and 0(dt) satisfies $\lim_{dt \to 0} 0(dt)/dt = 0$.

Considering the characteristic functional for y_t

$$\phi(\omega;t) = E\left\{e^{\,j\omega y_t}\right\}$$

where $E\{\cdot\}$ is the expected value operator, the partial differential equation describing the evolution of $f(\gamma;t)$ with time can be derived as in Appendix C. The resulting equation

$$\frac{\partial}{\partial t} f(\gamma;t) = \frac{\partial}{\partial \gamma} [e^{-2\lambda t} - \beta\gamma]\, f(\gamma;t) \qquad (7\text{-}8)$$

has boundary conditions

$$\lim_{t \to 0+} f(\gamma;t) = \delta(0) \qquad (7\text{-}9)$$

which ensures that all paths start at $y_o = 0$ and

$$f(\gamma{=}t;t) = f(\gamma = -t;t) + \lambda e^{-\lambda t} \qquad (7\text{-}10)$$

which insures that the probability mass for values of $-t < \gamma < t$ integrates to $1 - e^{-\lambda t}$, i.e.,

$$\int_{-t}^{t} f(\gamma;t)\, d\gamma = 1 - e^{-\lambda t} \quad . \tag{7-11}$$

The rest of the probability mass ($e^{-\lambda t}$) is atomic mass located at $\gamma=t$, representing the probability that no Poisson event occurs.

Equations (7-8) through (7-11) summarize the evolution of the probability density function for the cross-path deviation y_t in a Poisson-driven dynamical model for aircraft trajectories.

7.3 Extensions of the Poisson-Driven Dynamical Model

In order to apply this type of procedure to the analysis of the uncontrolled terminal area environment it would be necessary to increase dimensionality. Cross-path deviations could then be represented in a statistical description dependent fundamentally on a Poisson rate parameter. Validation can be accomplished through comparison of these descriptions with that obtained from the real data. Path structure definition will then be a prime factor in the time evolution of these path deviation density functions. Once path variations are characterized techniques such as those discussed in previous chapters can be used to evaluate hazard.

CHAPTER 8

SUMMARY AND RECOMMENDATIONS

This report describes results of a preliminary effort in a study designed to evaluate prescribed procedures used in the general aviation uncontrolled terminal airspace. Procedure evaluation is primarily from the standpoint of mid-air collision hazard in the "see-and-avoid" environment. A generalized expression for mid-air collision (MAC) probability is developed. This analysis indicates that traffic pattern design should minimize encounter rates and maximize visible avoidable encounters under the constraint of pilot visibility inherent in aircraft design.

Extensive data have been collected by NASA Wallops personnel in several uncontrolled environments subject to current prescribed procedure. Some results of analysis of these data have indicated that pilot adherence to present procedure does vary considerably. Indications are that this variation from procedure is based to some extent on individual attempts to maximize the ability to "see-and-avoid" within the terminal airspace. These data are to provide a basis for evaluating procedure in the uncontrolled environment.

Two basic approaches are described to the evaluation of procedure. One involves a deterministic model used to generate pseudo-random paths consistent with a given procedure. The ability to define these paths in a space-time coordinate system is demonstrated. Furthermore, a method of examining the mid-air collision hazard conditioned on a deterministic path structure is developed. An approach to the extension of this method to random paths is also discussed. A preliminary deterministic model is used to demonstrate how validation can be accomplished using real data analysis results. Terminal area density of aircraft for the approach phase is varied and a hazard measure is calculated to provide information relative to the evaluation of a path structure.

A second procedure developed involves the use of a statistical model. This is discussed in terms of a dynamical model which can generate path deviations in the form of a stochastic process generating function.

Expressions for the probability density function of these deviations are derived. This method can be used in conjunction with the developed procedures for hazard measures in a manner similar to that used with the deterministic model.

For the continuation of this effort, several recommendations are offered based primarily on results of studies thus far.

(1) NASA Wallops data should be made available in a format and organizational structure which would facilitate extensive additional analyses. As an example the major analysis done so far includes distributions of cross-path deviations at several geometric planes within the approach pattern. Since no time correlation is available it is of interest to do analysis of hazard probability with some assumed time structure. This analysis could be in the form of statistics such as encounter rates, duration of encounters, visibility of hazardous aircraft, etc.

(2) The available data can provide baseline evaluation of procedures to the extent that traffic volumes vary considerably and hazard evaluation can be made for a variety of procedures. In the current study time correlation of the data from individual aircraft has been assumed and is considered to be of definite benefit for a complete assessment of the uncontrolled airspace. Other information concerning aircraft simultaneously in the airspace can definitely complement the analysis, e.g., aircraft mode (landing, departure, etc.), and whether path deviations from procedure are pilot preference or are in fact the result of avoidance maneuvers. Therefore, consideration should be given to acquisition of additional data.

(3) The deterministic model should be extended to include the total terminal airspace so that a complete representation of current procedures is available. This procedure should be extended to evaluate various approach path structures. Consideration should be given to include in the model the decision algorithms necessary to include avoidance maneuvers based on the see-and-avoid concept. This can provide more realistic evaluation of procedure. Some information is available and more can be obtained concerning pilot workload, what portion of the time the pilot spends looking for other aircraft, and how he spends his look time. Ideas presented in this preliminary study indicate that path characteristics can definitely

enhance the see-and-avoid concept and should be influenced by this consideration. For example, most efficient use of the pilot's look time can be directly linked to the visibility of hazardous aircraft and the magnitude of the search region of potential hazardous aircraft. This is tied to the approach path structure and a measure of pilot adherence to the structure. It seems reasonable to expect that pilot adherence to procedure will be directly proportional to the value of the procedure from the standpoint of protection against potentially hazardous situations.

(4) The statistical modeling should be pursued further to provide a viable method for evaluating procedure from a hazard standpoint. Initially, this would involve extension of the analytical results to a multidimensional situation to more accurately represent the real environment in an uncontrolled airspace. This can provide a useful tool to evaluate any airspace environment with any conceivable pattern structure. Estimates of pilot adherence to prescribed procedure can be input in terms of statistical descriptions. In fact limits on adherence to proposed procedure could be a parameter used to qualify a hazard measure for any particular postulated and evaluated procedure.

Page intentionally left blank

APPENDICES

APPENDIX A

FLIGHT PATH GENERATION FOR SLOW AIRCRAFT

This appendix describes the algorithms used to generate aircraft tracks in the uncontrolled airport environment. Of twelve possible 30° entry sectors defined, only two sectors are included in the initial model and described here.

In this development of a geometric model for generating flight paths (tracks) for slow aircraft, several assumptions have been made concerning the aircraft and their path characteristics. These assumptions are made primarily to preserve simplicity in the model but are also based on examination of data. The assumptions are: (1) the runway is oriented in a north-south direction with the threshold (touch down point) at the south end, (2) the threshold is defined as the origin for a cartesian coordinate system with angles measured positively from the north-south line (runway centerline) in a clockwise direction, (3) aircraft tracks initiate at a point which is 3 statute miles (4.8 km) from the runway threshold, (4) all winds (if any) are from the north (0°), (5) all turns are smooth with a turn rate specified at the beginning of a run (up to 30° per position update), (6) all random variables are considered to be uniformly distributed, and (7) slow aircraft are those which have a terminal airspeed less than about 132 mph (195 fps) and an approach airspeed less than about 70 mph (103 fps)(these two speeds are used in the model).

A.1 Geometric Model for Sector 1

The Sector 1 is defined as that 30° arc between 0° and 30° of a 3-mile radius circle centered at touchdown. Angular measurement is positive-clockwise from the N-S line. Tracks originate with a uniform distribution between 0° and 30°. The algorithm functions as follows:

(1) Upon entering the sector an aircraft is assigned an entry point and an initial heading, θ, where

$$f(\theta) = .1 \quad ; \quad 235° \leq \theta \leq 245° \quad .$$

Note: $f(\cdot)$ indicates probability density function.

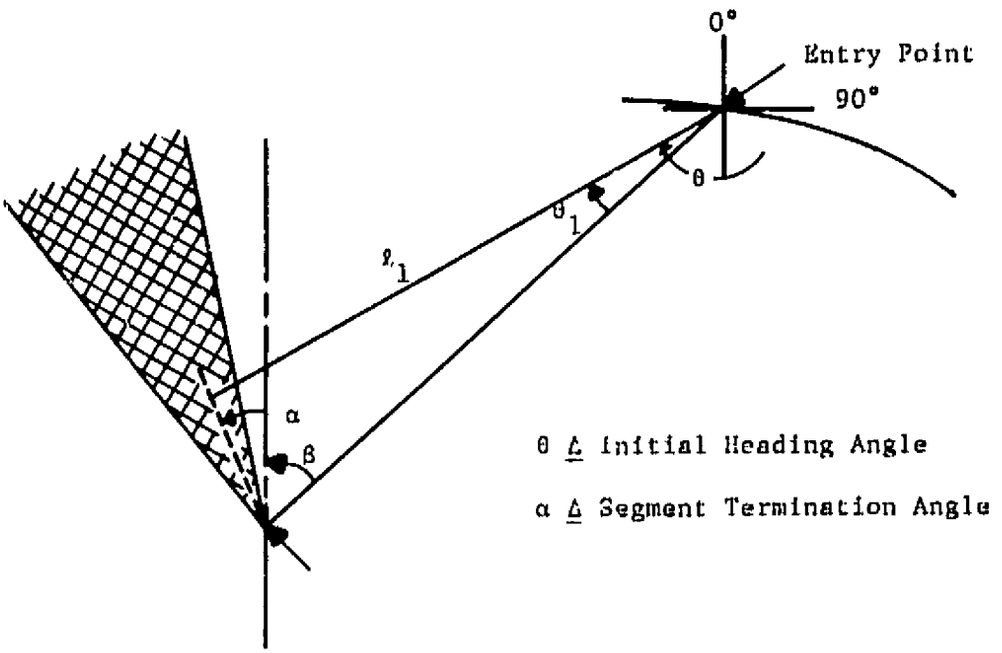

Figure A-1. Geometry Associated with Sector 1 Initial Entry Segment.

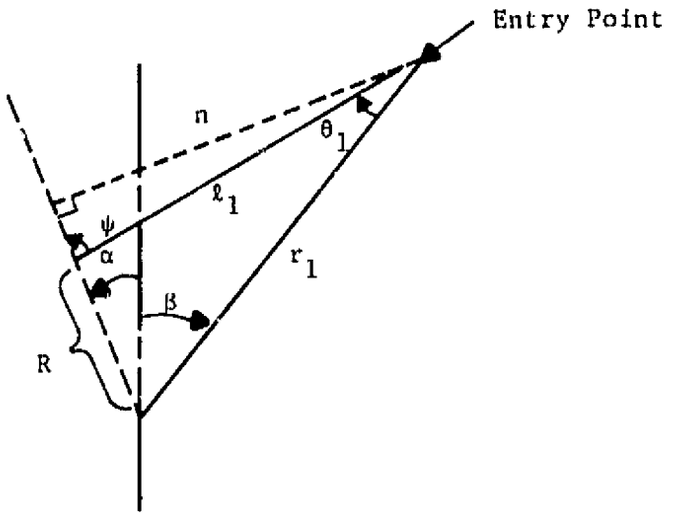

Figure A-2. Geometry of Segment Length Calculation for ℓ_1.

(2) The initial leg length, ℓ_1, is related to a randomly selected angle, α, which is measured counter-clockwise from the N-S line with vertex at touchdown. Then

$$f(\alpha) = .08333 \quad ; \quad -22^{\circ} \leq \alpha \leq -10^{\circ}$$

is used to select α which determines the end of the initial leg, ℓ_1, where a turn to the downwind leg is initiated. This geometry is illustrated in Figure A-1.

For any selected α the length ℓ_1 is calculated according to Figure A-2 as follows. Angle β is the actual sector angle at which the entry point is located. With initial heading θ, then

$$\theta_1 = \theta - (180^{\circ} + \beta) \quad .$$

The angle ψ

$$\psi = (\beta - \alpha + \theta_1) = (\theta - \alpha - 180^{\circ}) \quad .$$

Therefore the leg length

$$\ell_1 = \frac{n}{\cos\psi}$$

where

$$n = r_1 \sin(\beta-\alpha)$$

yielding

$$\ell_1 = \frac{r_1 \sin(\beta-\alpha)}{-\cos(\theta-\alpha)} \quad . \qquad \text{(A-1)}$$

Thus once α, β, and θ are generated the initial leg length ℓ_1 may be calculated from (A-1). The distance R given in Figure A-2 which is the distance from the terminus of ℓ_1 to touchdown is defined as the range of the aircraft.

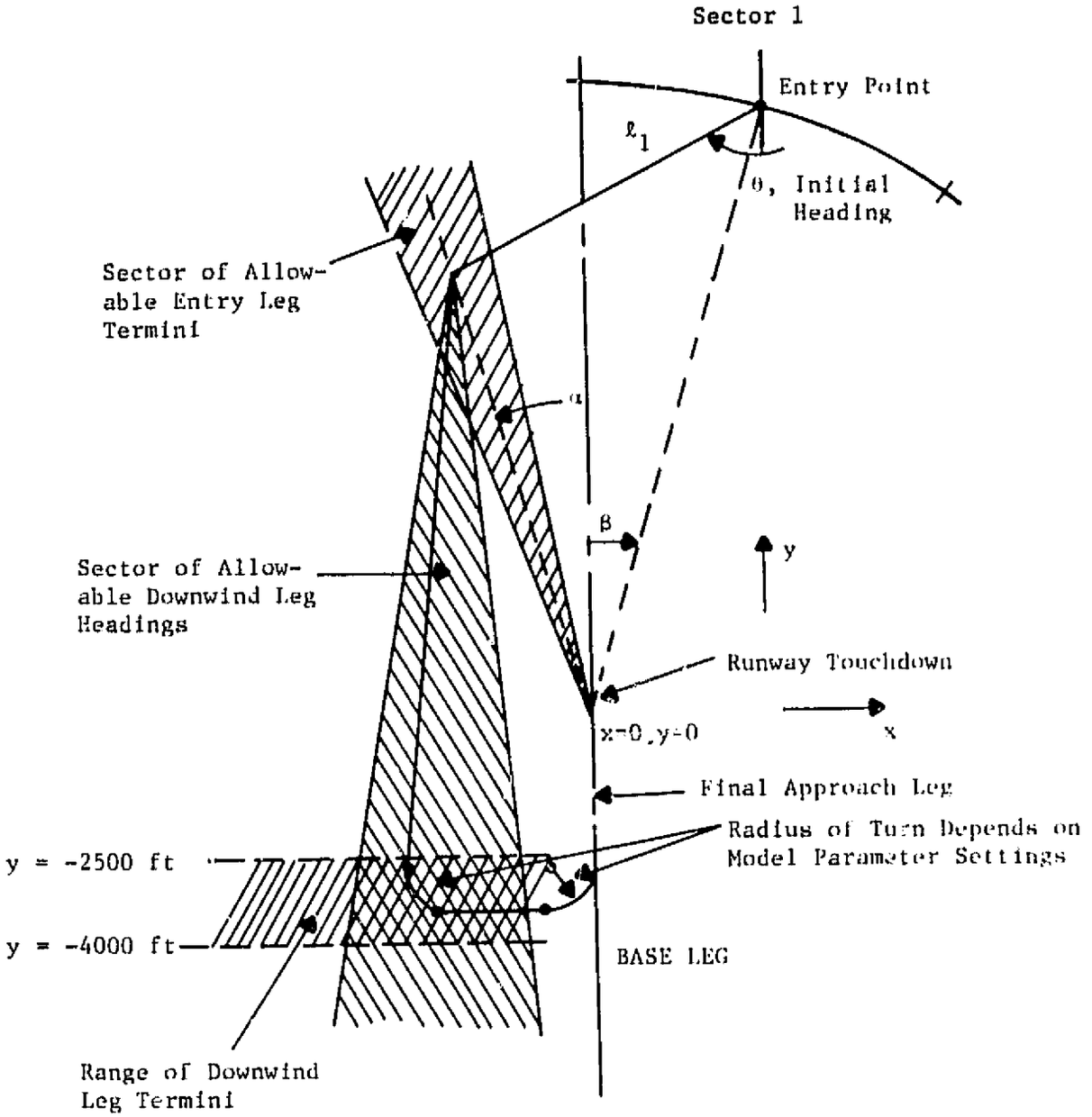

Figure A-3. Segments of Flight for Sector 1 Entries.

(3.) Upon completion of the initial leg a new heading HDGDW is determined as the downwind leg heading. A random value γ drawn according to

$$f(\gamma) = \frac{1}{27} \quad ; \quad -10^{\circ} \leq \gamma \leq 17^{\circ}$$

is used to form

$$HDGDW = 180^{\circ} + \gamma \quad .$$

(4.) The downwind heading is flown until y = DWN2 where DWN2 is selected from a uniformly distributed range of values - 2500 ft $\leq$ DWN2 $\leq$ - 4000 ft which terminates the downwind leg south of the runway.

(5.) Upon completion of the downwind leg the aircraft initiates a turn until a heading of 90° is reached. At this point the distance to the runway centerline is calculated and the difference between this distance and the radius of turn is the length of the base leg. The radius of turn is determined by the values of the rate of turn and the aircraft velocity. Rate of turn is dependent upon the initial parameter setting at the beginning of a run and the time between position updates.

(6.) Upon completion of the base leg a turn is initiated to bring the aircraft to a heading of 0° along final approach.

Figure A-3 illustrates the segments of flight for an entry into Sector 1. Figures A-4 and A-5 illustrate two typical computer generated Sector 1 entry tracks. Figure A-6 provides a flowchart of the Sector 1 entry algorithm.

A.2 Geometric Model for Sector 11

Sector 11 is defined as the 30-degree arc between 300° and 330° of a three-mile radius circle centered at runway touchdown. Angular measurements are clockwise from the N-S line (extended centerline of runway). Upon examination of the tracks from Sector 11 in the Wallops data base two basic types of tracks were apparent: (1) one type consisted of an initial entry leg which terminated close enough to the runway to permit direct entry into the downwind leg and (2) the other type consisted of an initial leg which ended too far from the runway to start a downwind so that a second leg inward

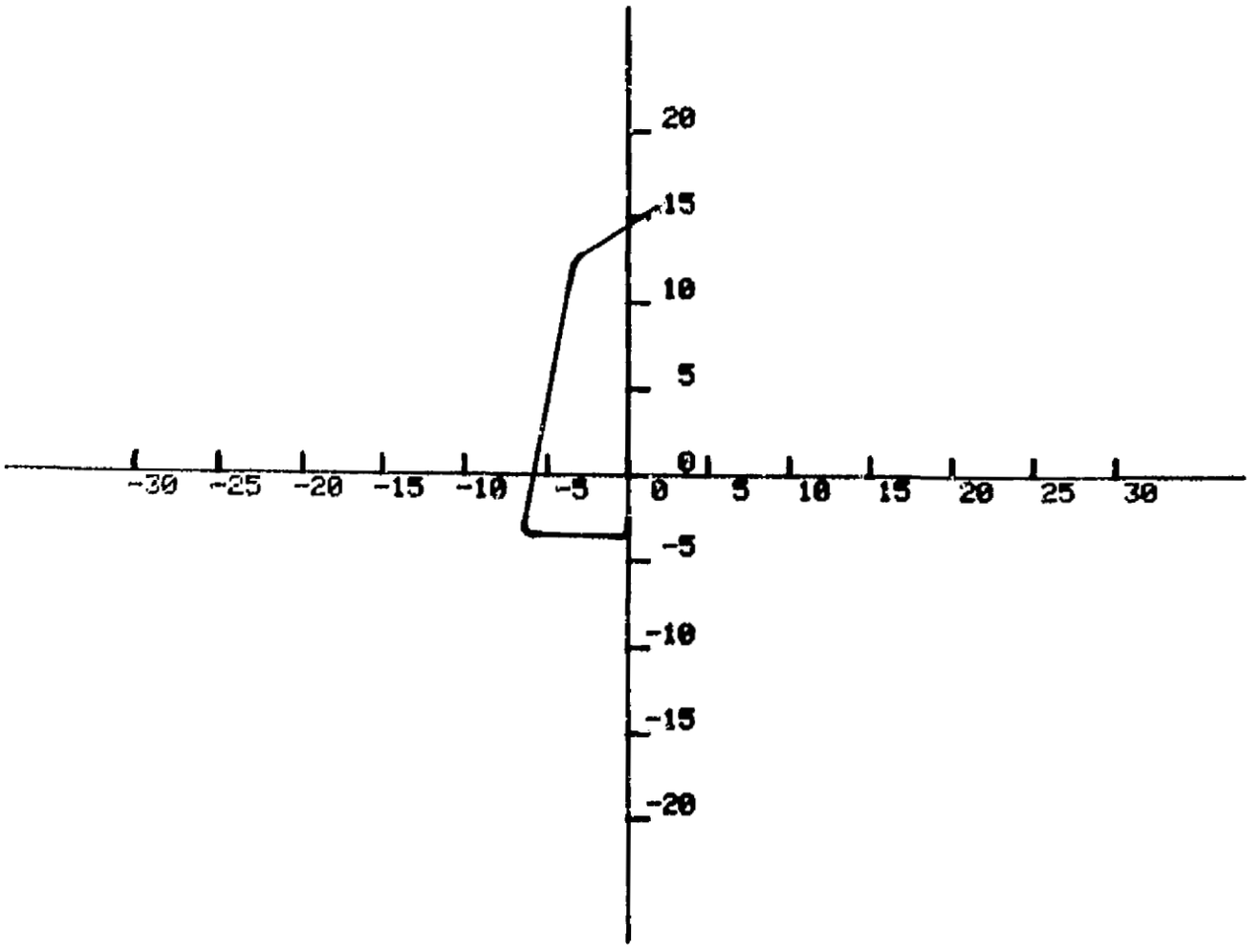

Computer Generated Track for Sector 1

Figure A-4. Example of Computer Generated Arrival Aircraft Track with Entry into Sector 1.

C-2

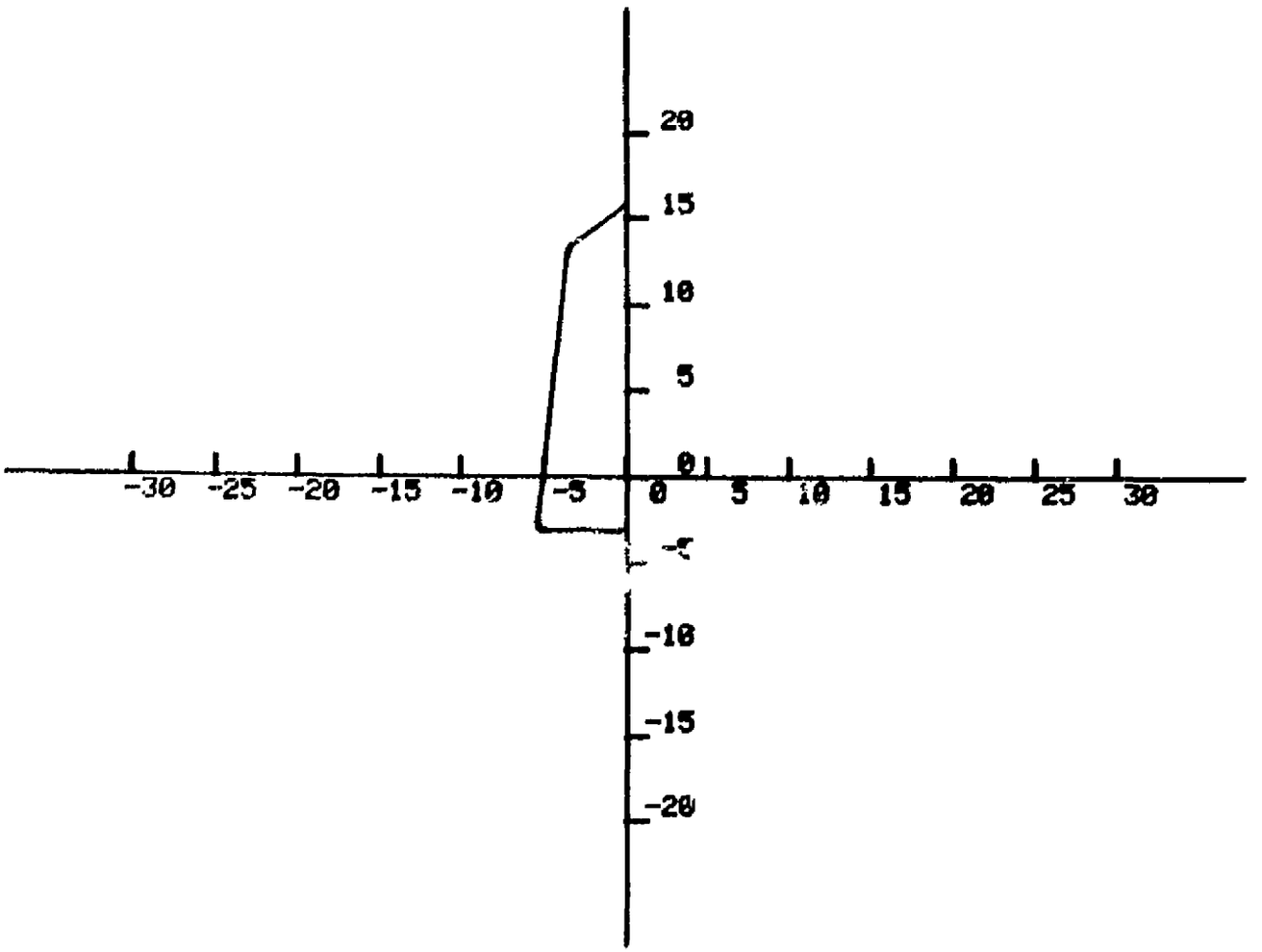

Computer Generated Track for Sector 1

Figure A-5. Example of Computer Generated Arrival Aircraft Track with Entry into Sector 1.

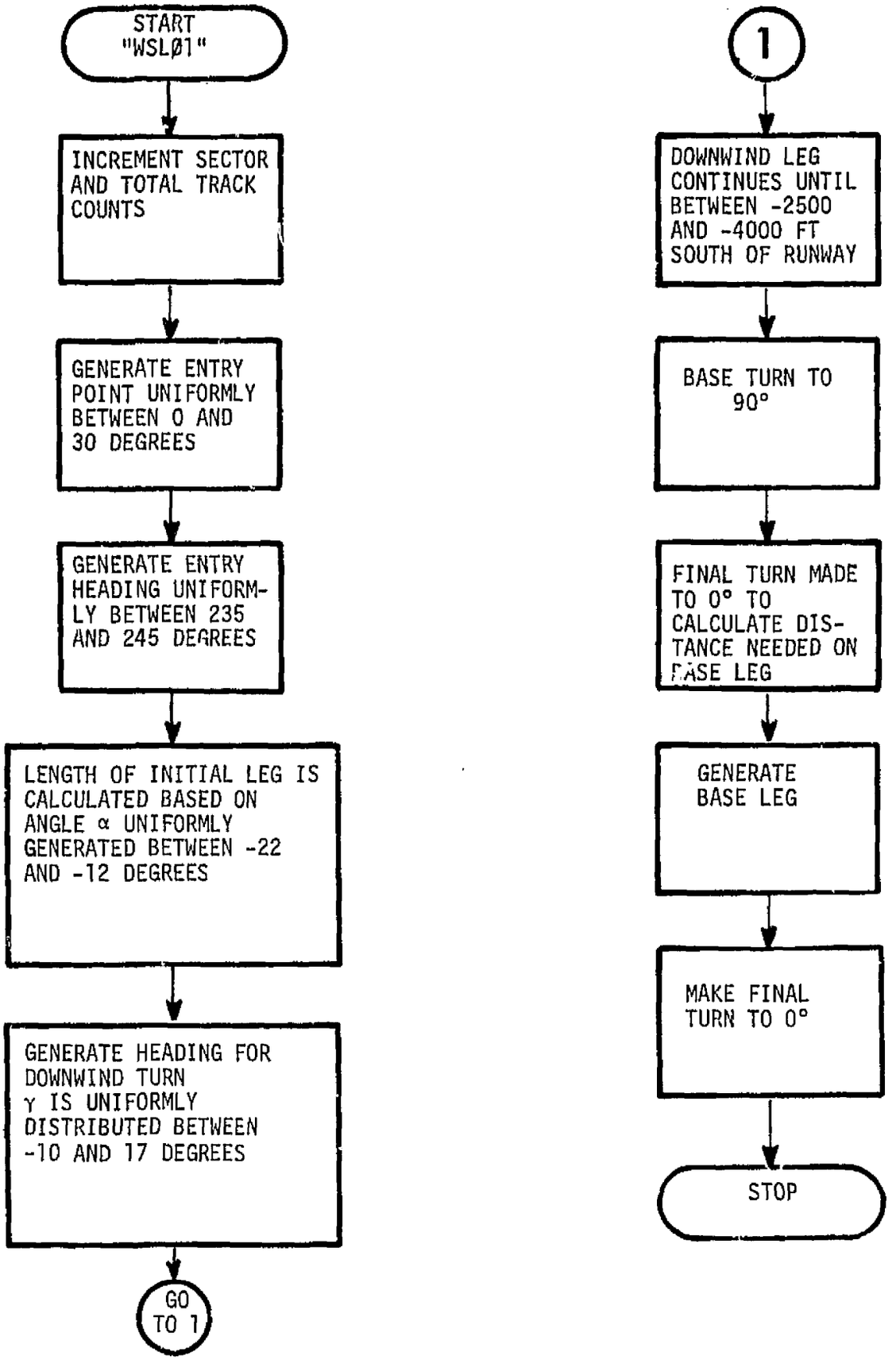

Fig. A-6. Program to generate track of slow aircraft arriving from Sector 1.

was necessary to get to the downwind leg. Examples from the actual data are shown in Figure A-7. A definition of these two types is shown in Figure A-8.

The simulation model provides for generation of these types of slow aircraft tracks entering Sector 11. The description of the algorithm is as follows:

(1.) Coordinates of entry (XAPT, YAPT) are selected at random assuming an equally likely distribution been 300° and 330° of the angle AANGL defined in Figure A-9. Thus

$$XAPT = - RADIUS * SIN (360 - AANGL)$$

$$YAPT = - RADIUS * COS (360 - AANGL) \quad .$$

(2.) The initial heading (HDGIN) is uniformly distributed between 118° and 180°. It is necessary to have the initial leg length depend on AANGL so that the length corresponding to AANGL = 330° will not cause the path to be too close to the runway centerline or overshoot it. The entering aircraft must always be able to enter a downwind leg. At AANGL = 330° the initial leg length is randomly chosen from an even distribution of lengths between 2500 and 5000 feet and at AANGL = 300° this range is between 5000 and 10000 feet. Each leg length limit varies linearly with AANGL as

$$LL \text{ (lower limit)} = 2500 + (330 - AANGL) * \frac{5000-2500}{330-300}$$

and

$$UL \text{ (upper limit)} = 5000 + (330 - AANGL) * \frac{10000-5000}{330-300}$$

and is illustrated in Figure A-10.

(3.) The coordinates at the end of the initial entry leg are calculated as

$$SBDWT = XAPT + DISIN * SIN(180-HDGIN)$$

$$YBDWT = YAPT - DISIN * COS(180-HDGIN)$$

as per Figure A-11.

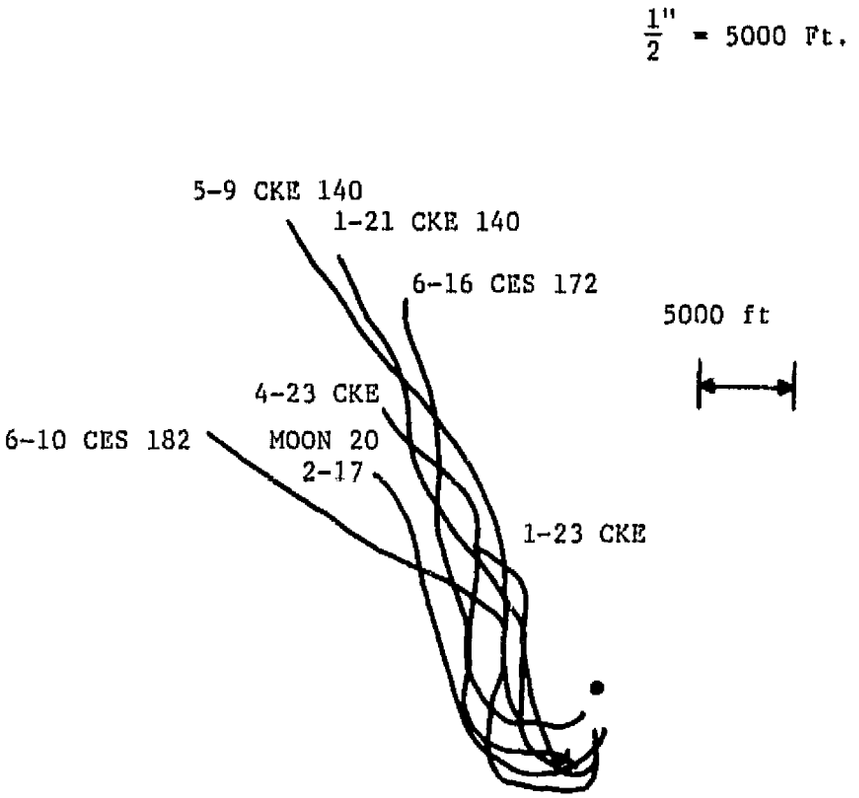

Figure A-7. Actual Tracks of Aircraft Arriving from Sector 11.

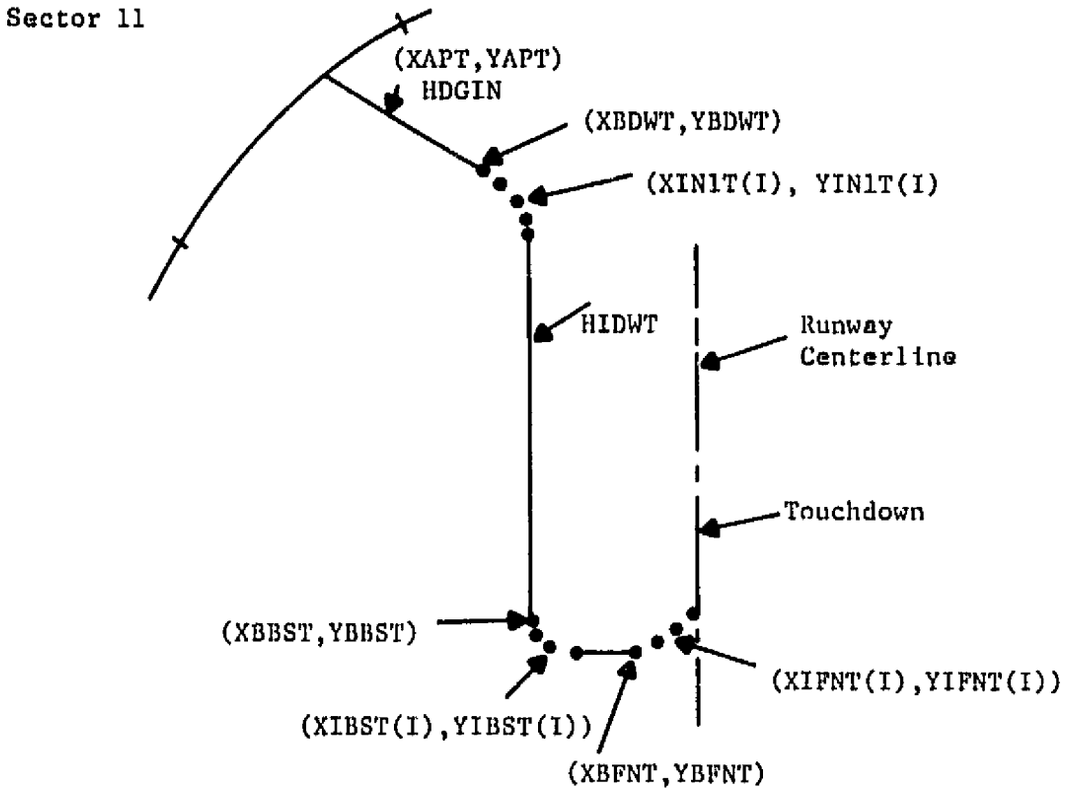

(a) TYPE I

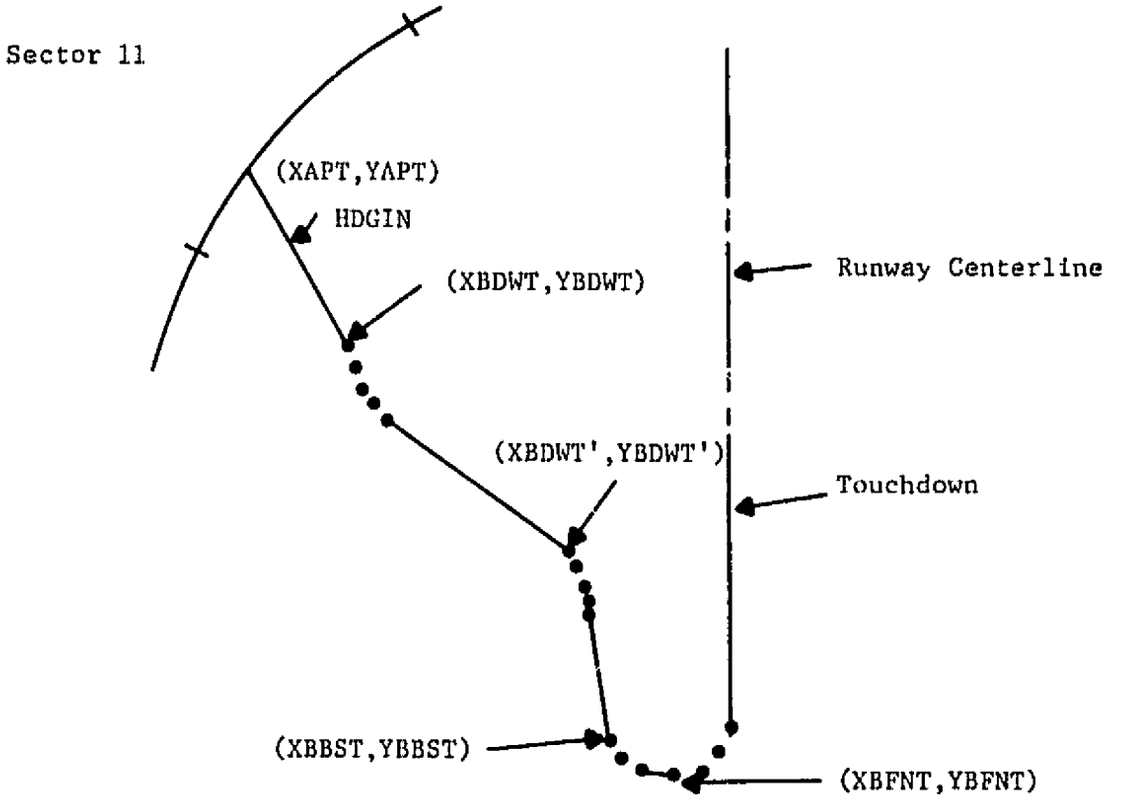

(b) TYPE II

Figure A-8. Two Types of Sector 11 Entry Approach Paths Modelled.

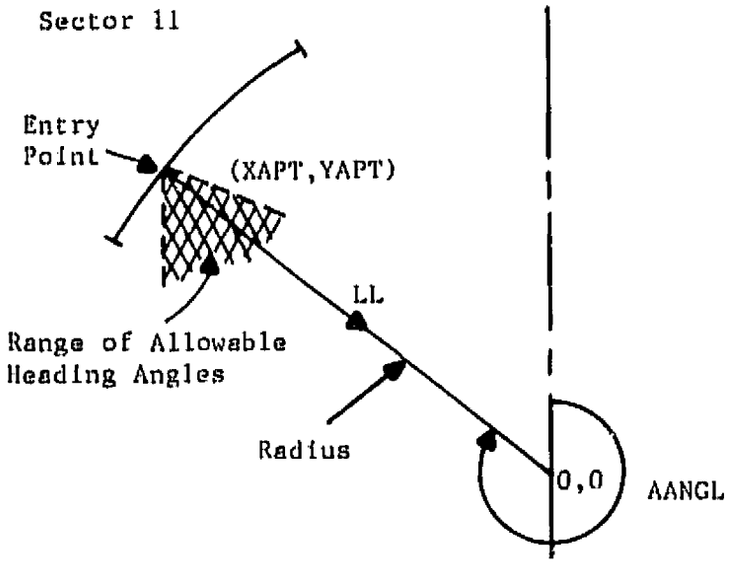

Figure A-9. Sector 11 Entry Point Geometry.

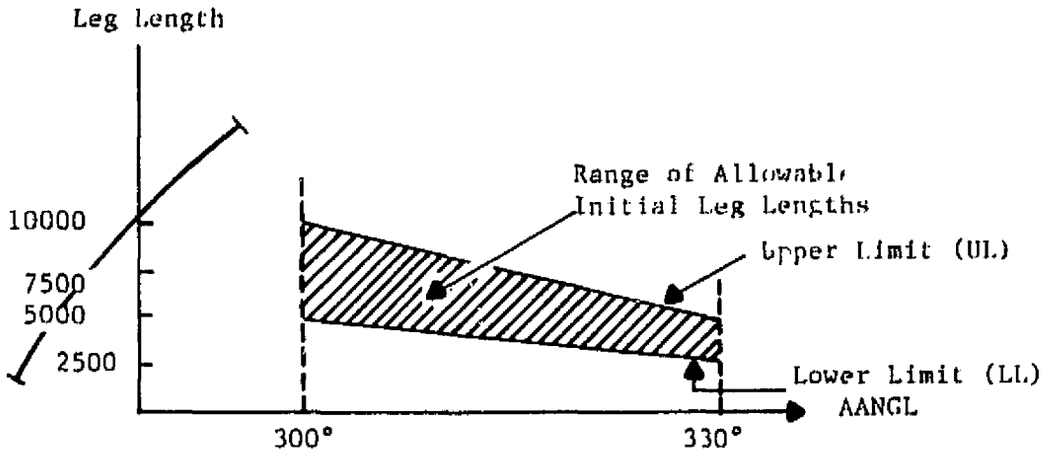

Figure A-10. Sector 11 Initial Leg Length Distribution vs AANGL (defined in Fig. A-9).

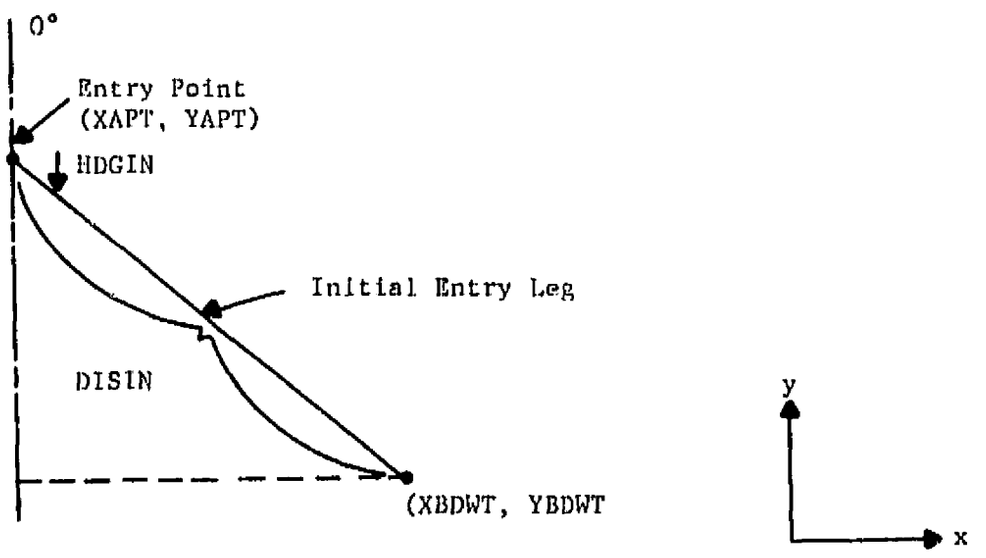

Figure A-11. Sector 11 Initial Entry Leg Terminus (XBDWT, YBDWT).

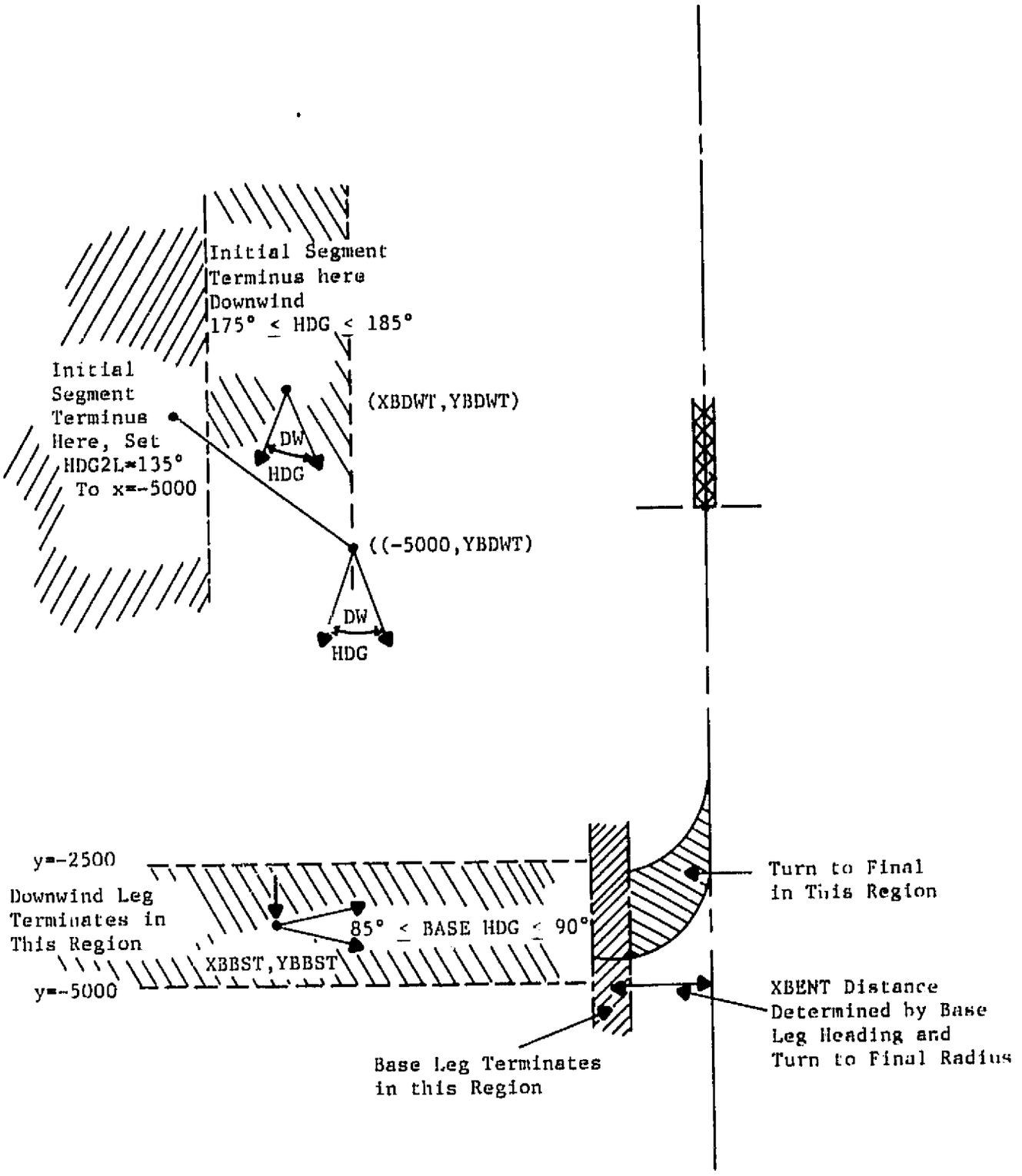

Figure A-12. Transition Regions for Sector 11 Entry.

(4.) If the aircraft is within 7500 ft of runway centerline, it is in a suitable position to proceed downwind. If not, it is made to proceed further inward on a heading of 135° (fixed) until it is within 5000 ft; then, it proceeds downwind. This latter situation occurs if lower AANGL values have higher HDGIN values (see Figure A-12).

(5.) Turns (if any) after initial leg are made at terminal velocity (VELHI). The TURNS subroutine accepts old and new headings, velocity, and coordinates at beginning of turn; it returns coordinates after turn.

When the initial leg terminates at a distance from the runway centerline greater than 7500 ft, a turn is made to get to a new heading of HDG2L = 135°. Downwind leg entry is delayed with new coordinates-before-downwind-turn calculated as XBDWT = - 5000 ft (see subparagraph 4 above) and YBDWT = YAFTT + (5000 + XAFFT) COTAN (180 - HDG2L). The program then continues with the following logic.

Once the termination of the initial entry leg is within 7500 ft of the runway centerline, a downwind heading is generated by sampling between 175° and 185° (see Figure A-12).

(6.) The downwind leg terminates between 2500 and 5000 ft below the threshold. XBBST, YBBST are coordinates of terminus of downwind leg where turn onto base leg begins (see Figure A-12).

(7.) A base heading is chosen between 085 and 095 from a uniform distribution (HBASE) (see Figure A-12).

(8.) The base leg length is determined from the point of termination of the downwind leg, the base leg heading (HBASE) and the distance required to make the turn to final. Figure A-13 illustrates the geometry involved in determining the distance XBENT and YBENT yielding the base leg distance

$$DIST = \{[XBENT - X(NN)]^2 + [YBENT - Y(NN)]^2\}^{1/2}$$

where X(NN), Y(NN) is the beginning of the base leg. From Figure A-13 XBENT and YBENT can be determined as follows.

$$X(NN) = XBBST + R + R \sin(90\text{-}HBASE)$$
$$Y(NN) = YBBST - [R - R \cos(90\text{-}HBASE)$$

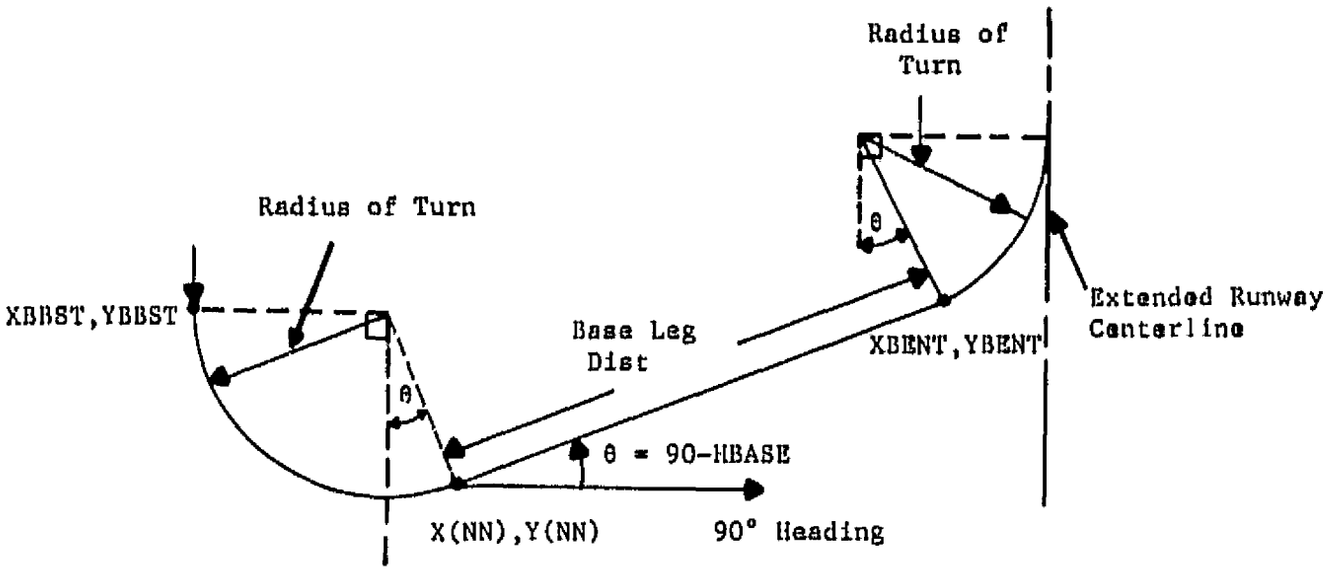

Figure A-13. Geometry for BASE LEG and FINAL APPROACH TURN for Sector 11 Entry.

$$XBENT = -[R - R \sin(90-HBASE)]$$
$$YBENT = Y(NN) + [XBENT - X(NN)] \tan(90-HBASE) \qquad (A-1)$$

where R is the turn radius and (90-HBASE) = θ as shown in Figure A-13. In the model these calculations are obtained using the subroutine TURNS. The downwind leg heading, the desired base leg heading, velocity and position (XBBST, YBBST) are input to yield [X(NN),Y(NN)]. Then using TURNS with the same input, except replacing desired base leg heading with the final approach heading, an output position [X(N),Y(N)] is used to find XBENT as

$$XBENT = X(NN) - X(N) \ .$$

Once XBENT is found, YBENT can be found using eq. (A-1).

(9.) The turn to the final approach heading (0°) is made at the same slower velocity at which the base leg is flown. Subroutine TURNS is again used.

Figures A-14, A-15 and A-16 provide plots of typical approach tracks generated by the computer algorithm.

Figure A-17 gives a flowchart of the algorithm.

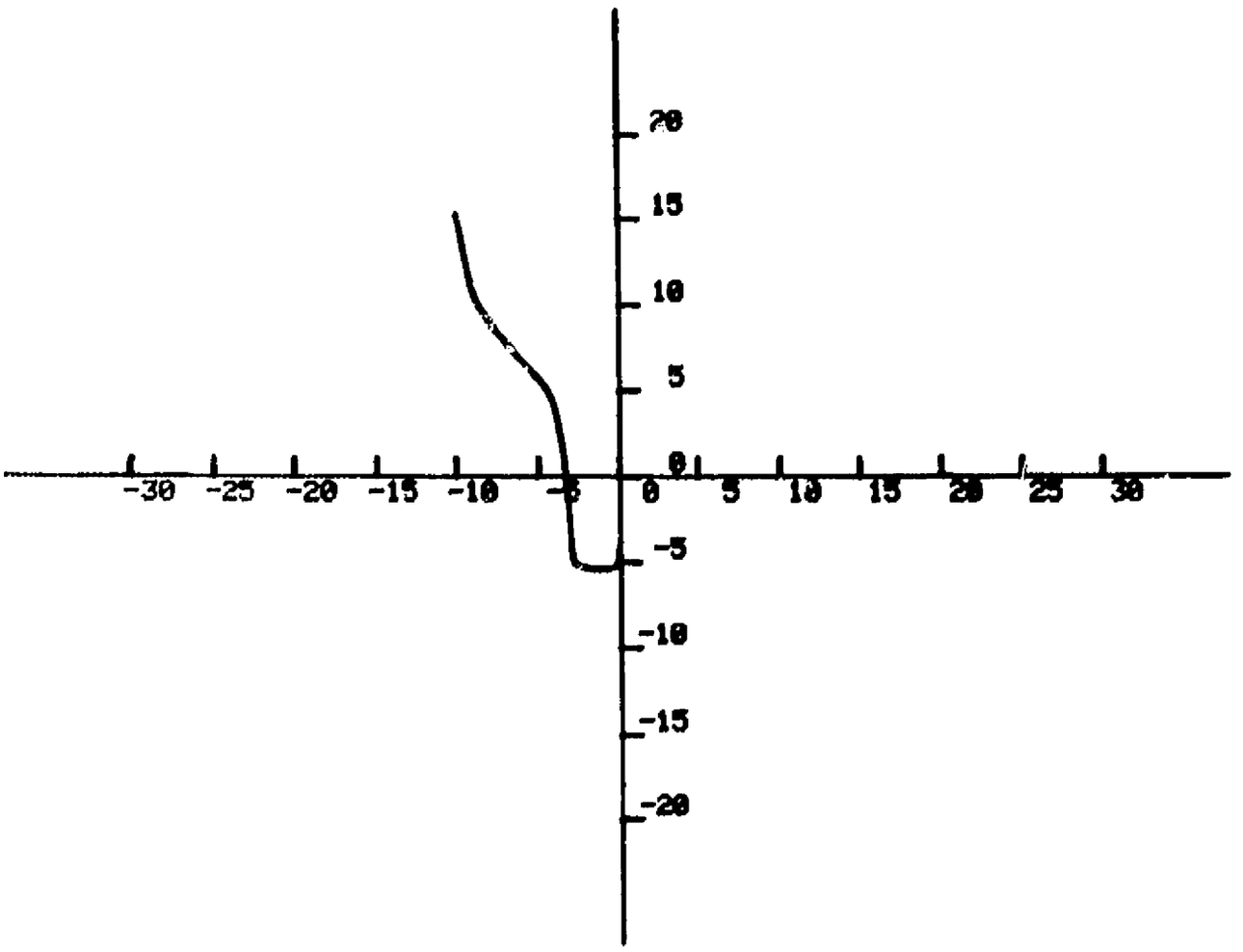

Figure A-14. Example of Computer Generated Arrival Aircraft Track with Entry into Sector 11.

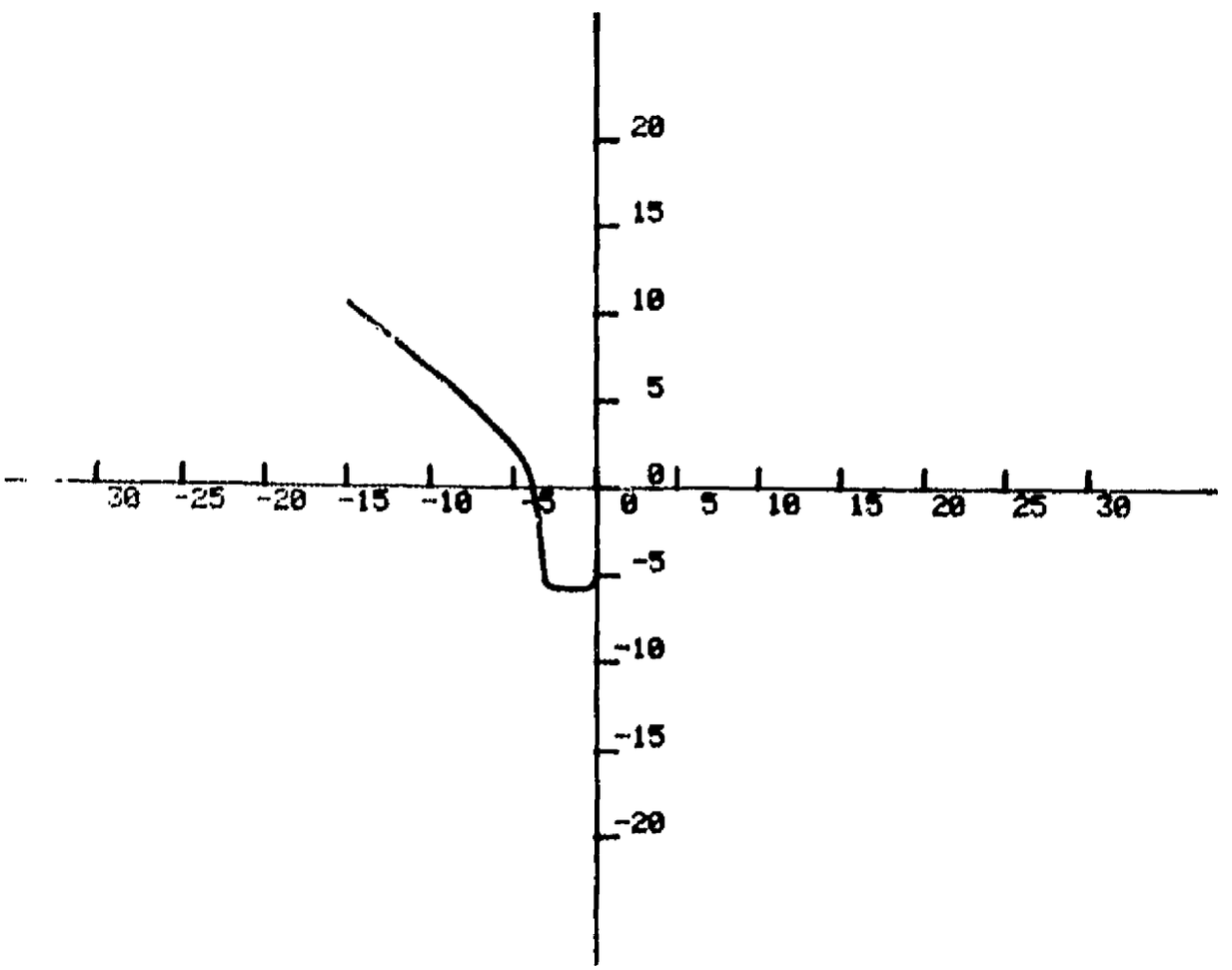

Figure A-15. Example of Computer Generated Aircraft Track with Entry Into Sector 11.

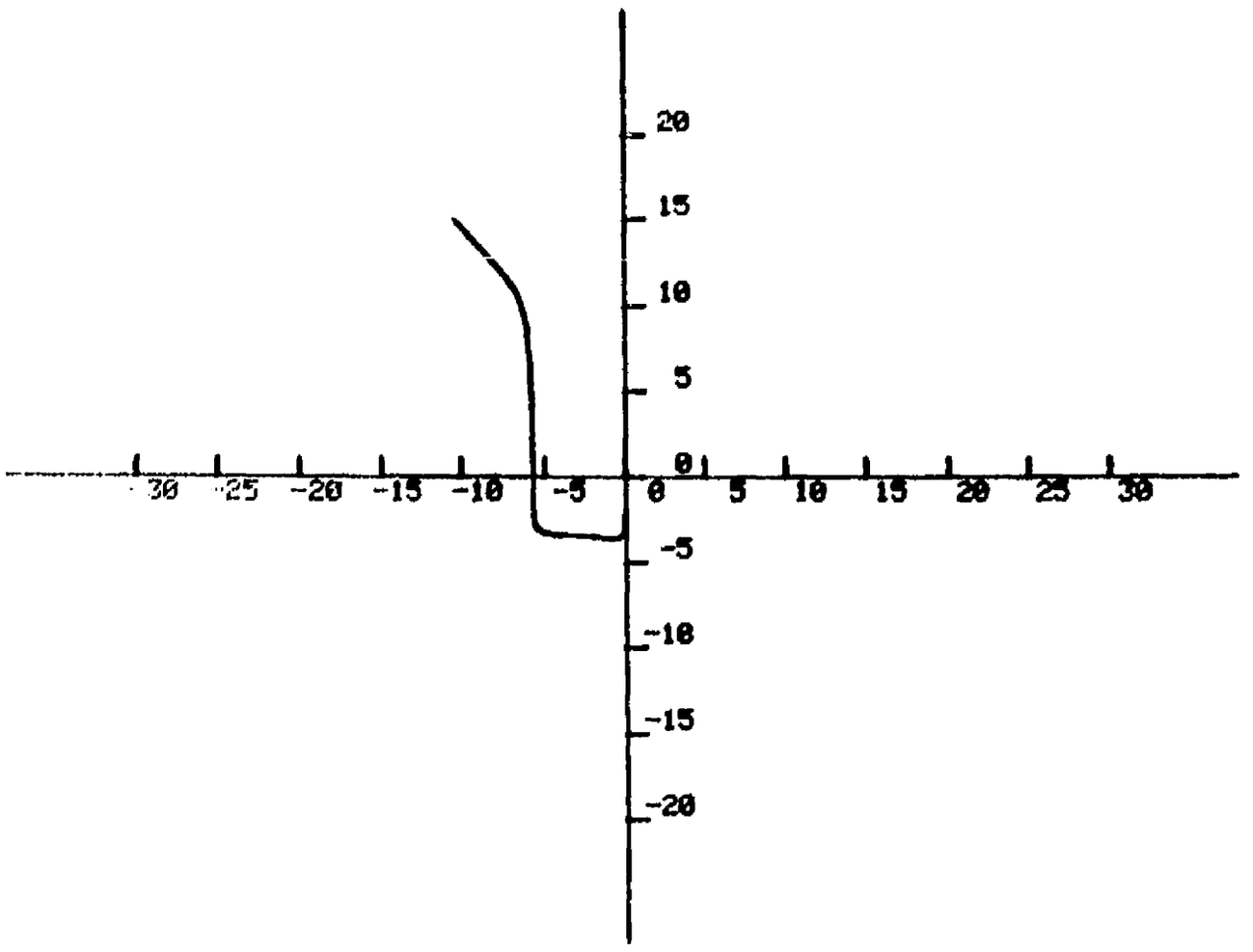

Figure A-16. Example of Computer Generated Aircraft Track with Entry Into Sector 11.

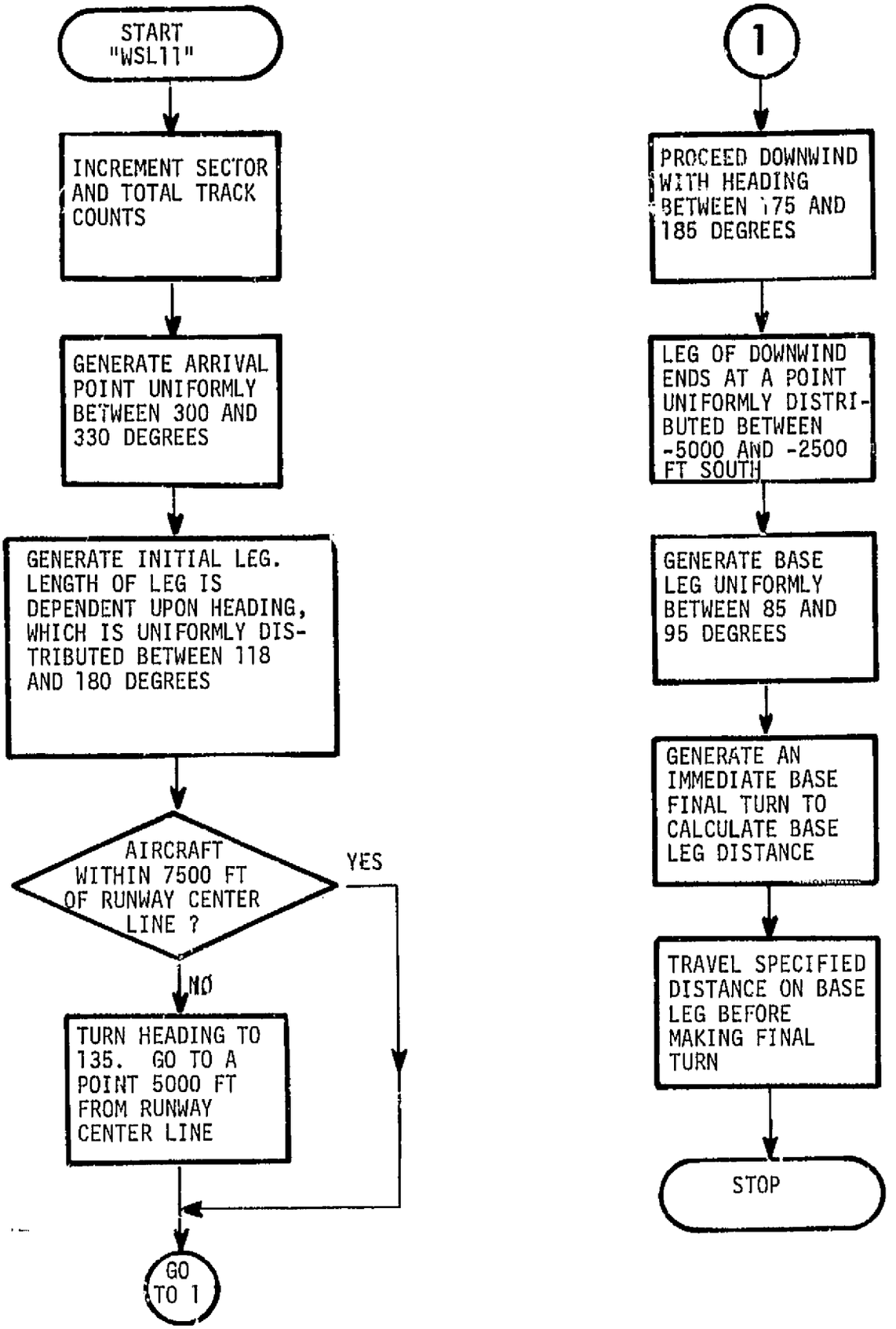

Fig. A-17. Program to generate track of slow aircraft arriving from Sector 11.

APPENDIX B

AIR TRAFFIC SIMULATOR

The air traffic simulator program to study the uncontrolled airport environment currently consists of five major programs as outlined in Figure B-1. A brief description of each program along with flowcharts in Figure B-3 follows.

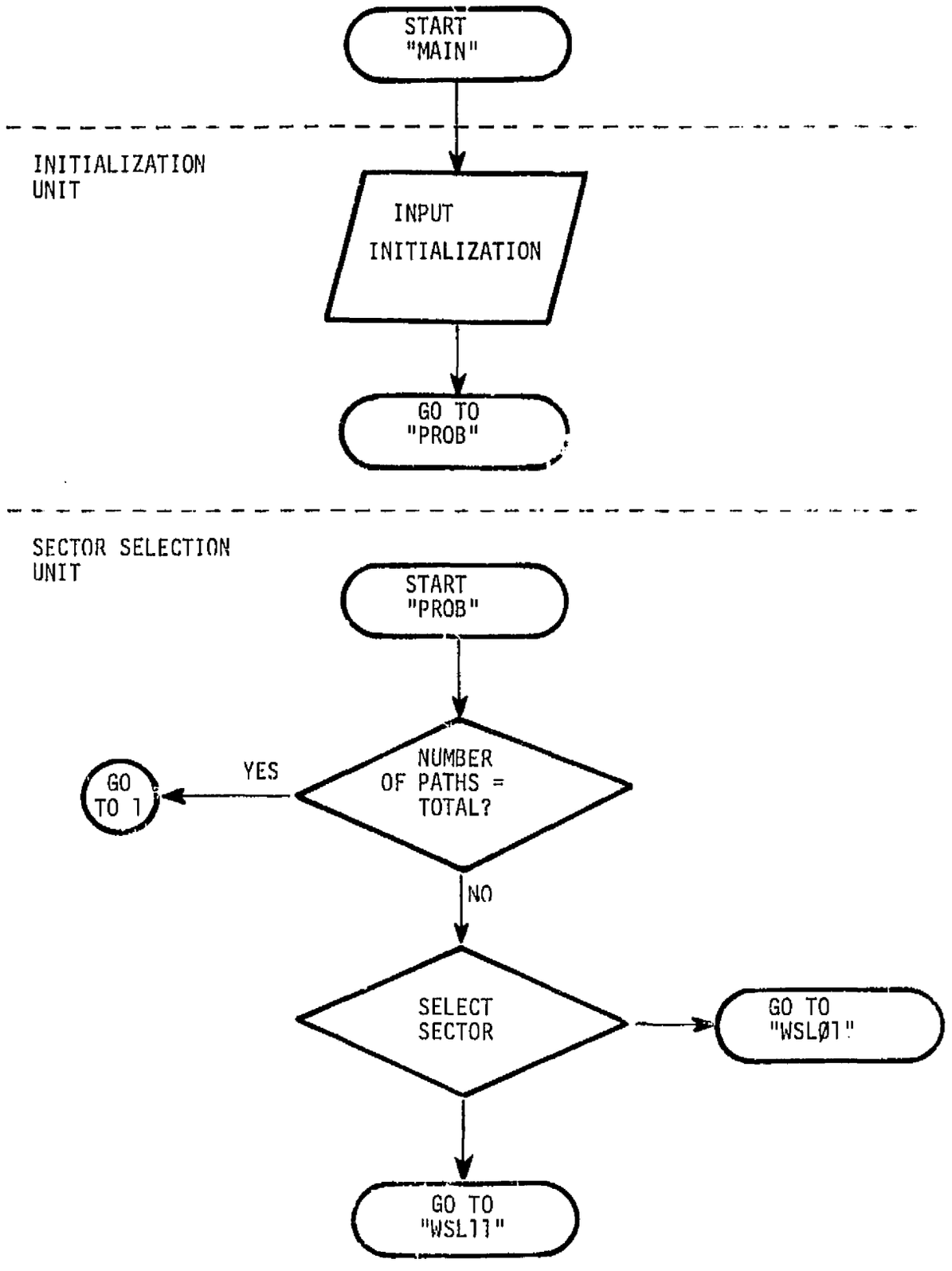

Fig. B-1. General flowchart of air traffic programs.

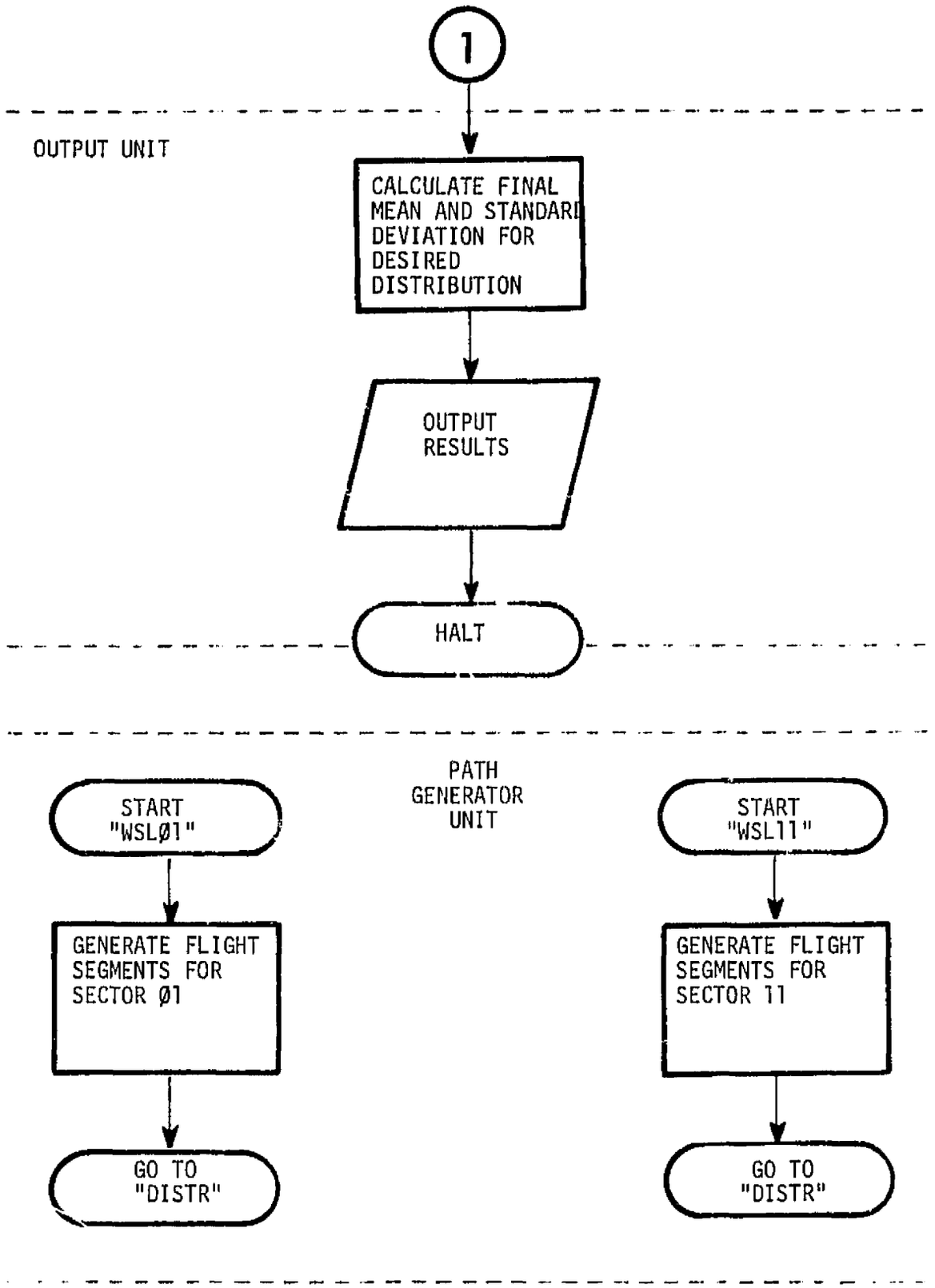

Fig. B-1. Continued.

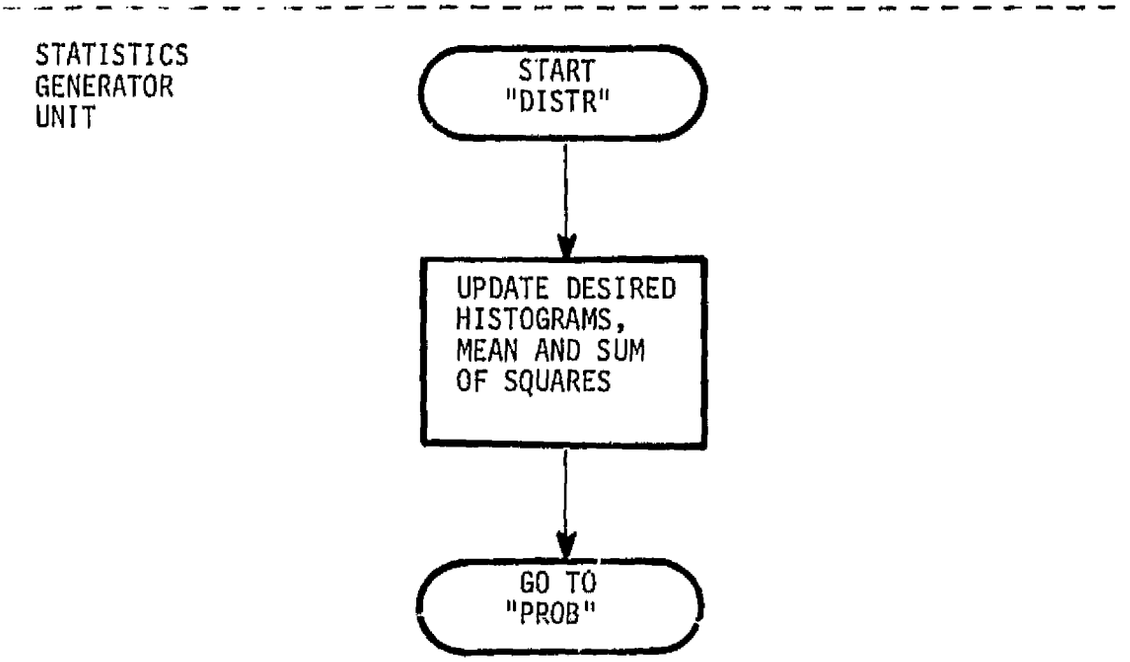

Fig. B-1. Concluded.

PROB is a program which incorporates two logical units: the Sector Selector and the Output Unit. The Sector Selector unit of PROB is executed if the number of paths generated has not exceeded the desired total. The function of this unit is to assign a value to the time parameter, TAU, and to select a sector based on a predetermined probability of selection.

TAU, the inter-arrival time between aircraft i-1 and aircraft i, is computed by the following equation

$$TAU = -\frac{1}{\lambda} \ln(x) \quad ,$$

where λ = number of arrivals/time period

and x = uniform random number.

The Output unit of PROB is executed after all paths are generated. It calculates the final mean and standard deviation for each desired distribution and prints the results along with the histograms.

DISTR incorporates the Statistics Unit. Execution of this program occurs after each flight path has been generated. Its function is to determine by interpolation where and when the aircraft crossed a given geometric plane. Figure B-2 illustrates this for a given set of points.

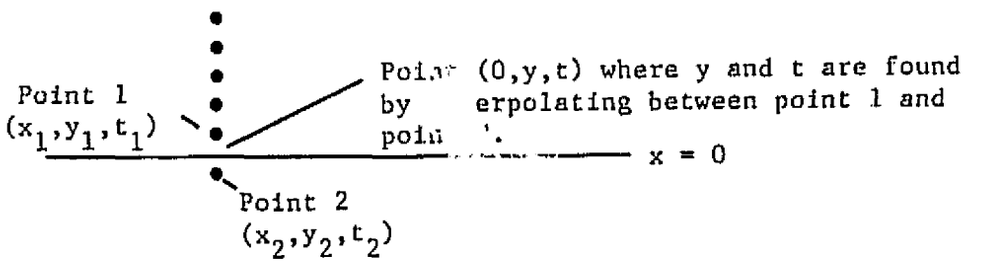

Figure B-2. Sequential Positions of Aircraft with Respect to Plane of Interest at x = 0.

If the flight path is the very first one to be generated then it is not included in the statistics but serves as a basis from which to obtain data for the next flight. Parameters TARG and IDSK are used to determine which statistics are to be maintained.

WSL01 is a Path Generator program (see Appendix A). It handles the aircraft entering Sector 1 (0 to 30 degrees of N-S line). Paths are generated in either straight line or curved segments. WSL01 determines the end points of each segment of the flight path. Intermediate points along the segment are obtained by calling subroutine FLY2.

WSL11 is a Path Generating program. It handles aircraft entering Sector 11 (300-330 degrees). Paths are generated in segments as in WSL01, and the subroutine FLY2 calculates intermediate points along the segment. A detailed description of the trajectory algorithms appears in Appendix A.

FLY2: This subroutine called from any Path Generating program calculates intermediate points along a segment. Provision is made for partial time intervals and for straight or curved segments.

The computer model has the following limitations:

1) It currently handles aircraft in only two of twelve sectors.
2) Aircraft altitude is not considered.
3) There are no provisions for aircraft flying by or taking off.

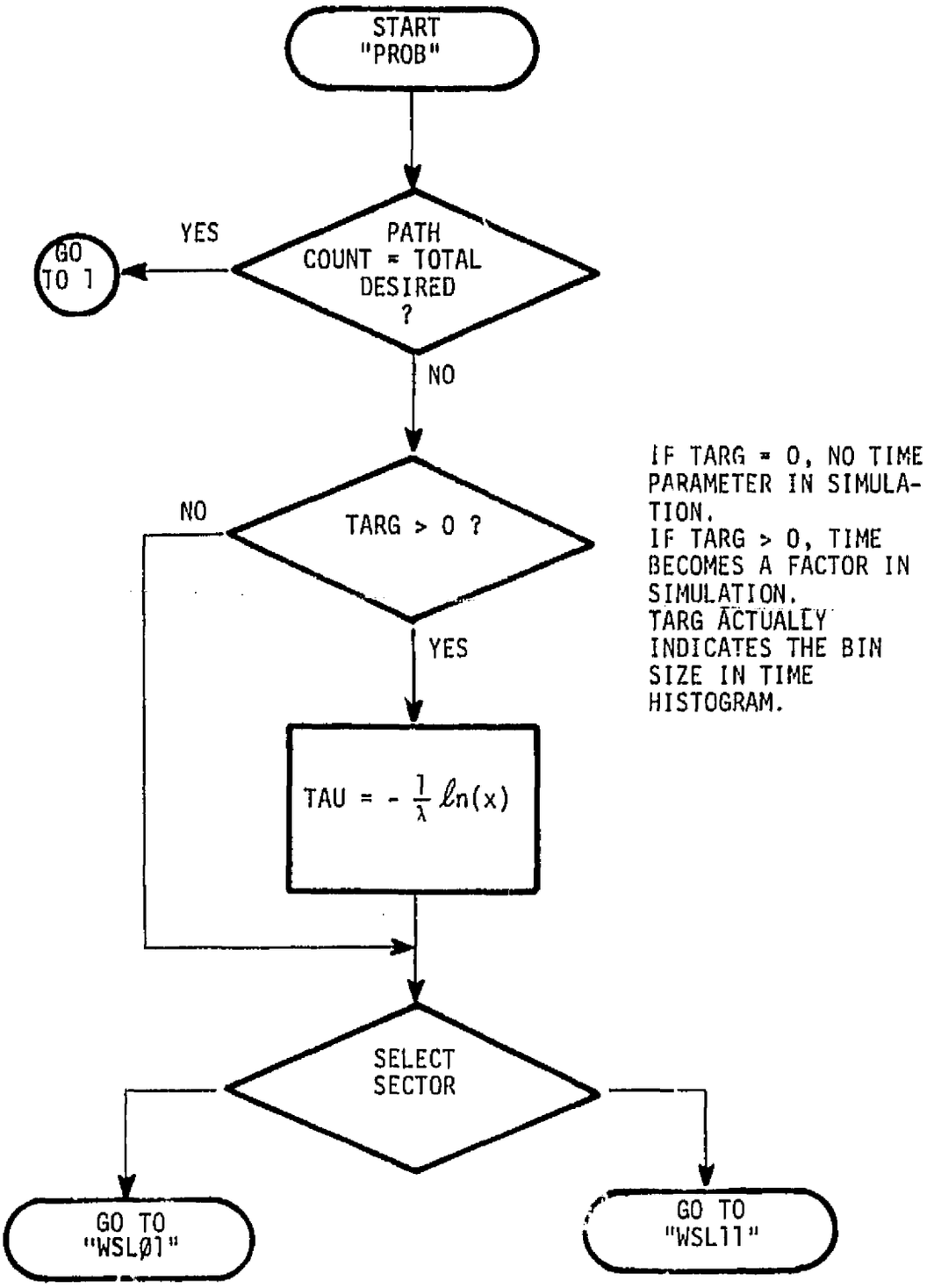

Fig. B-3. Individual flowcharts for air traffic programs.

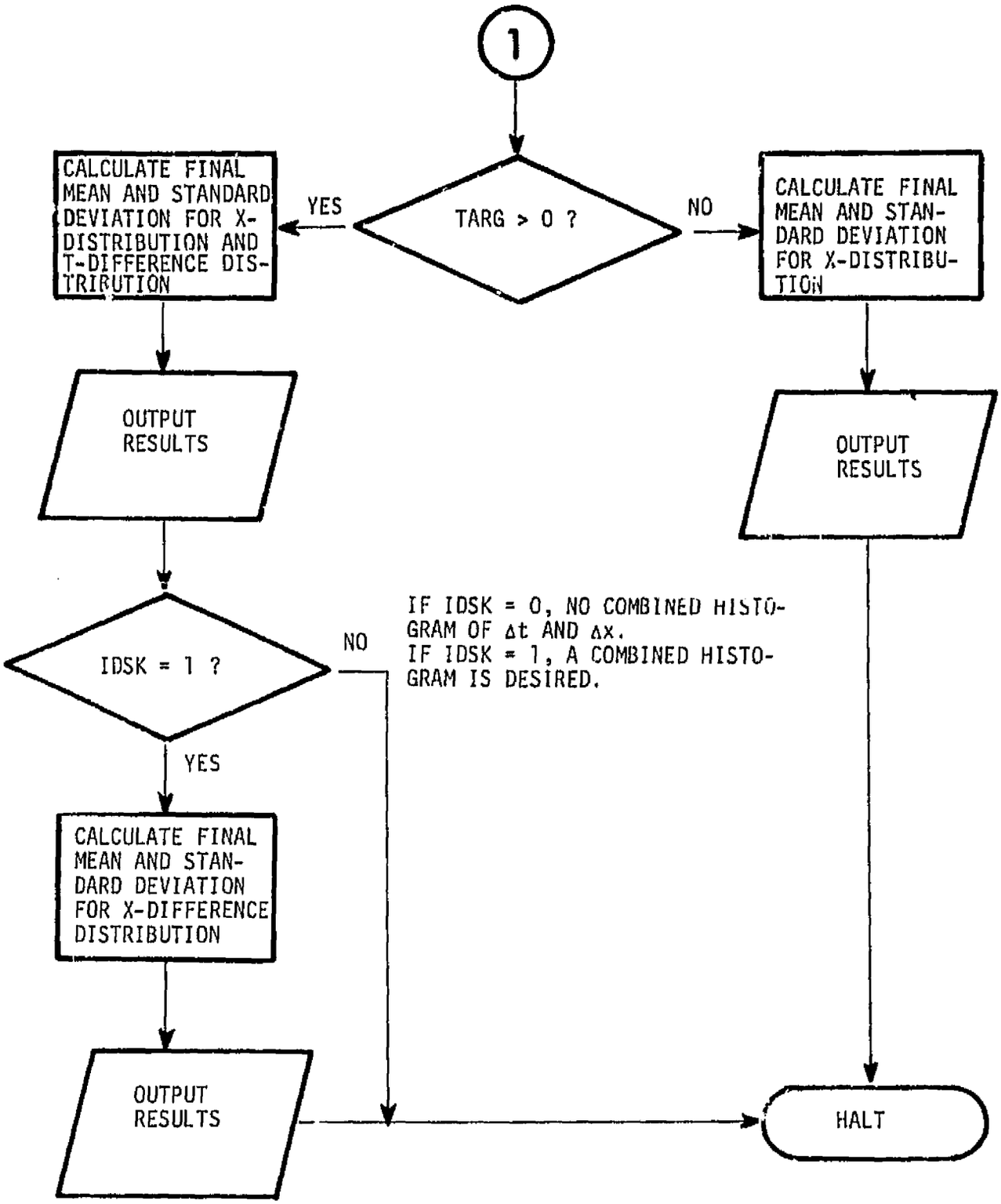

Fig. B-3. Continued.

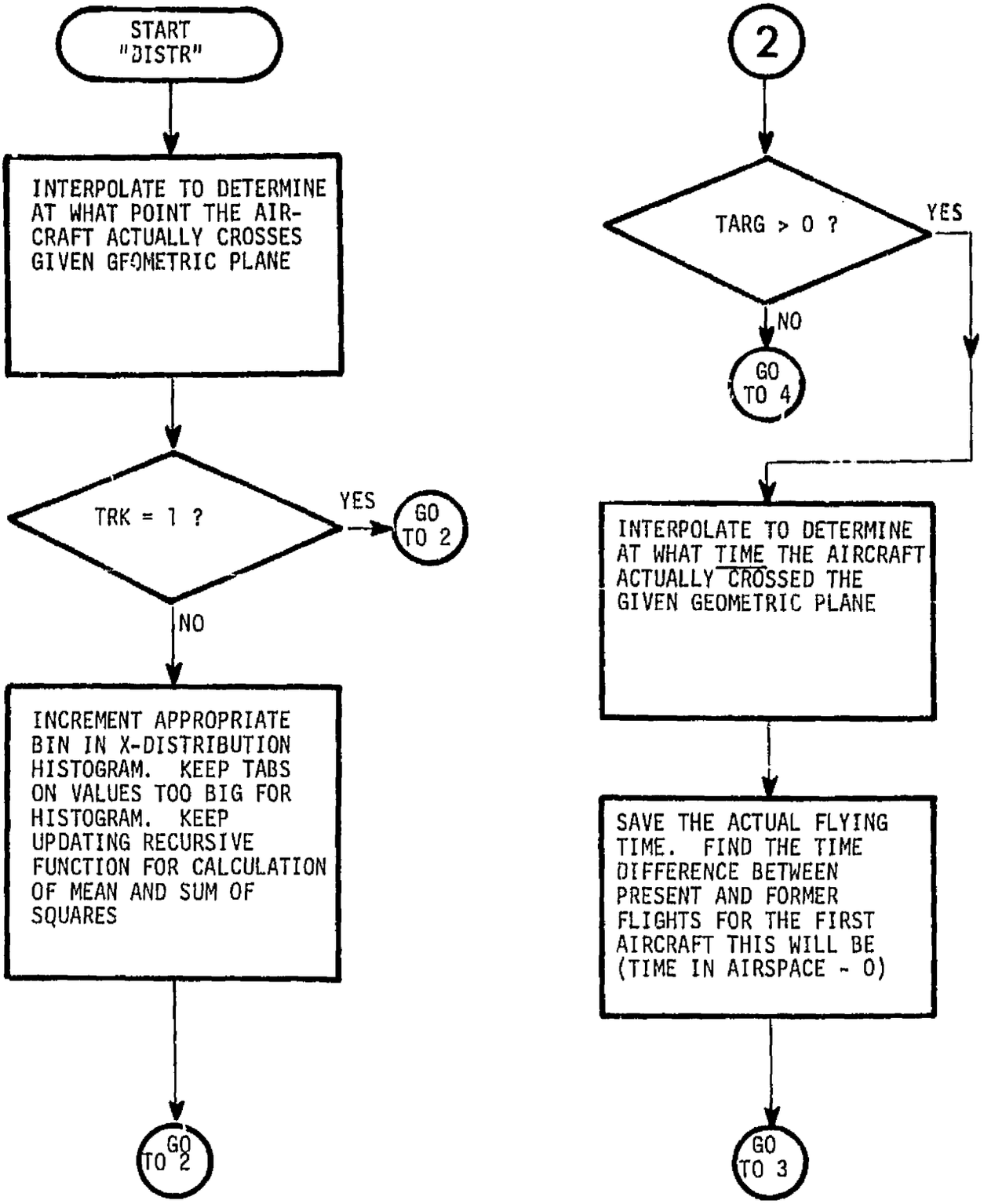

Fig. B-3. Continued.

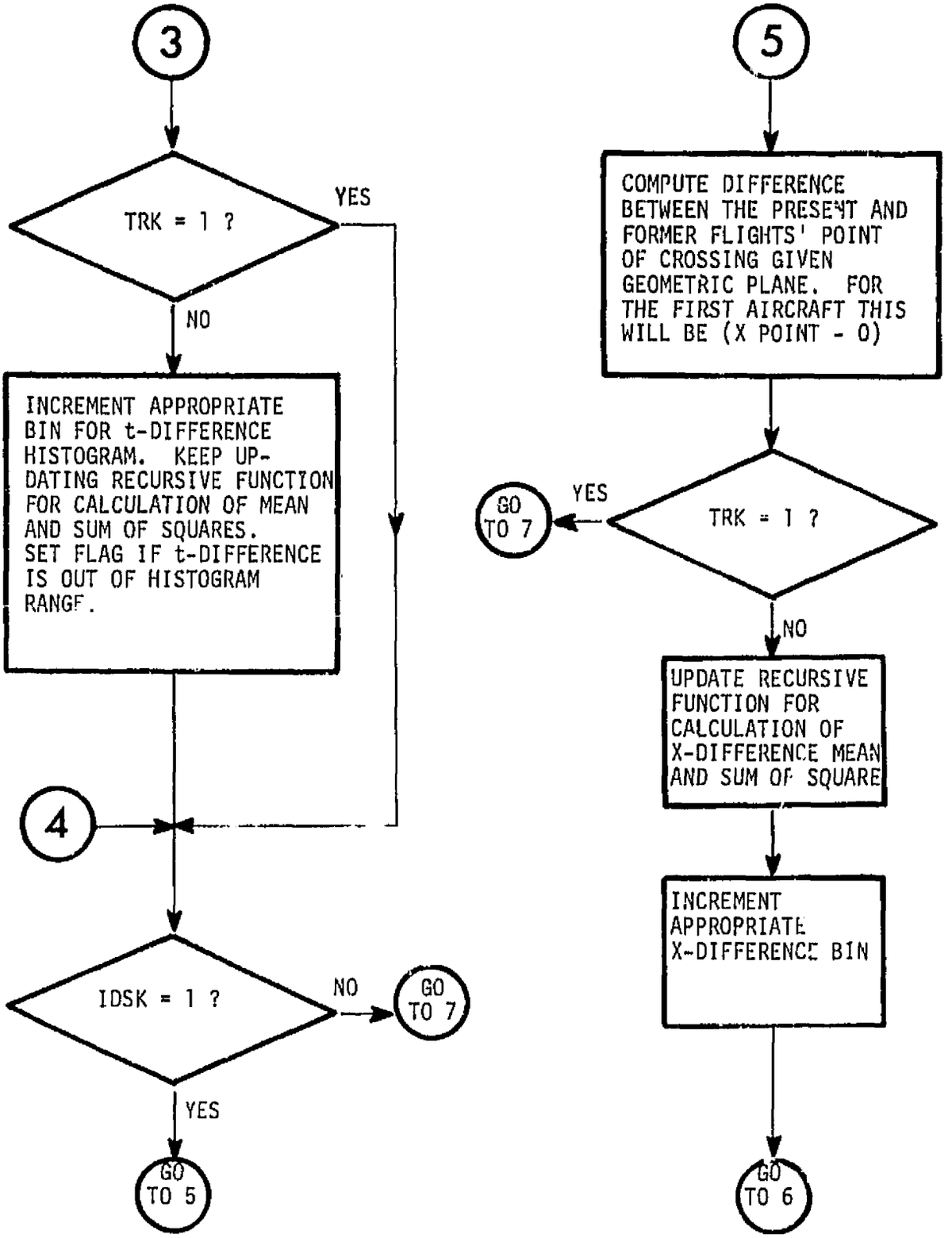

Fig. B-3. Continued.

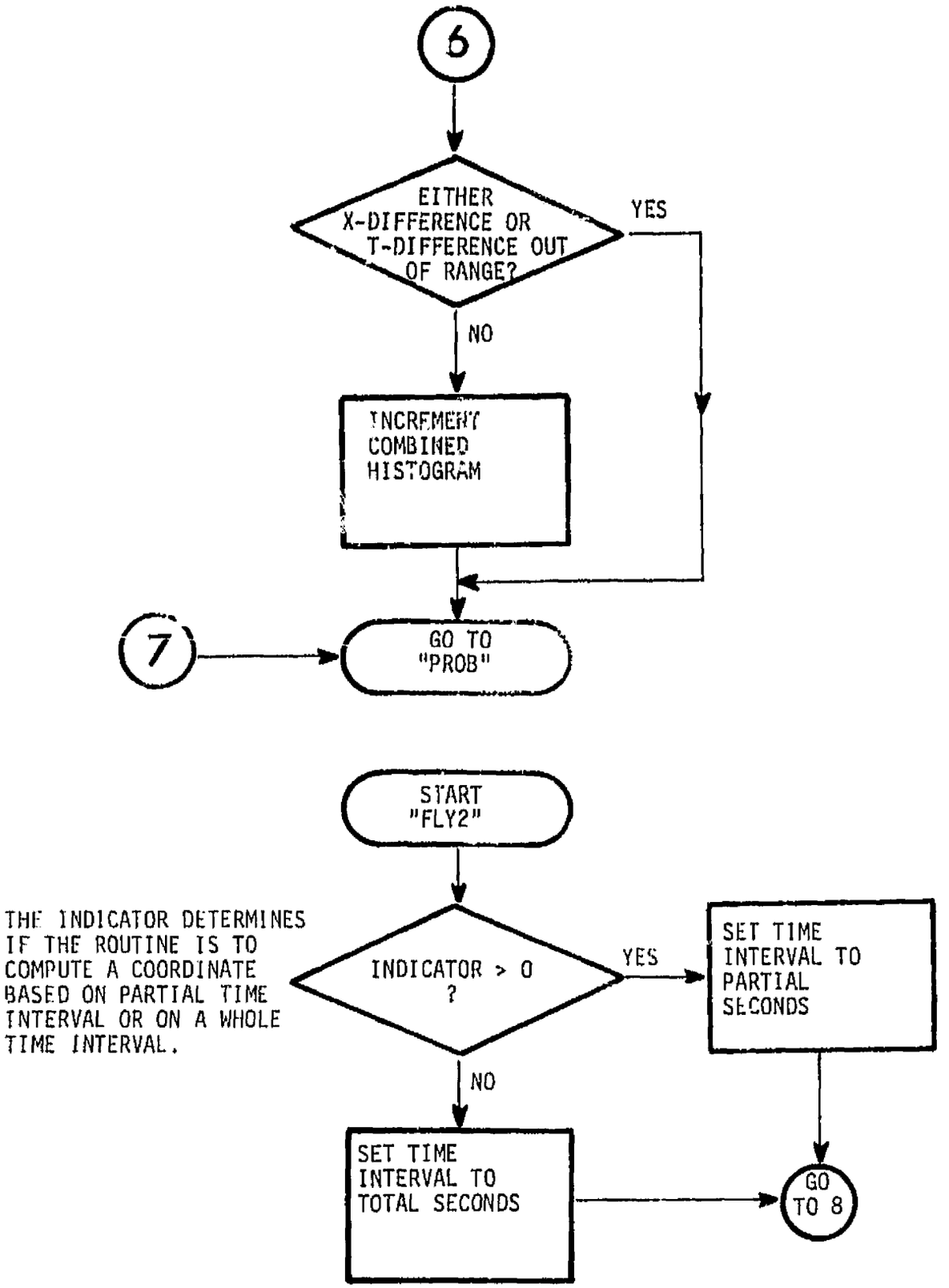

Fig. B-3. Continued.

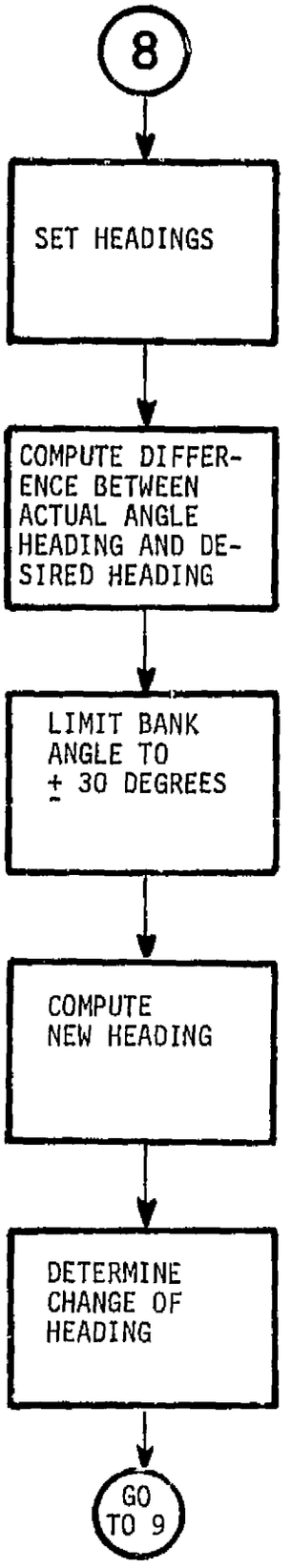

Fig. B-3. Continued.

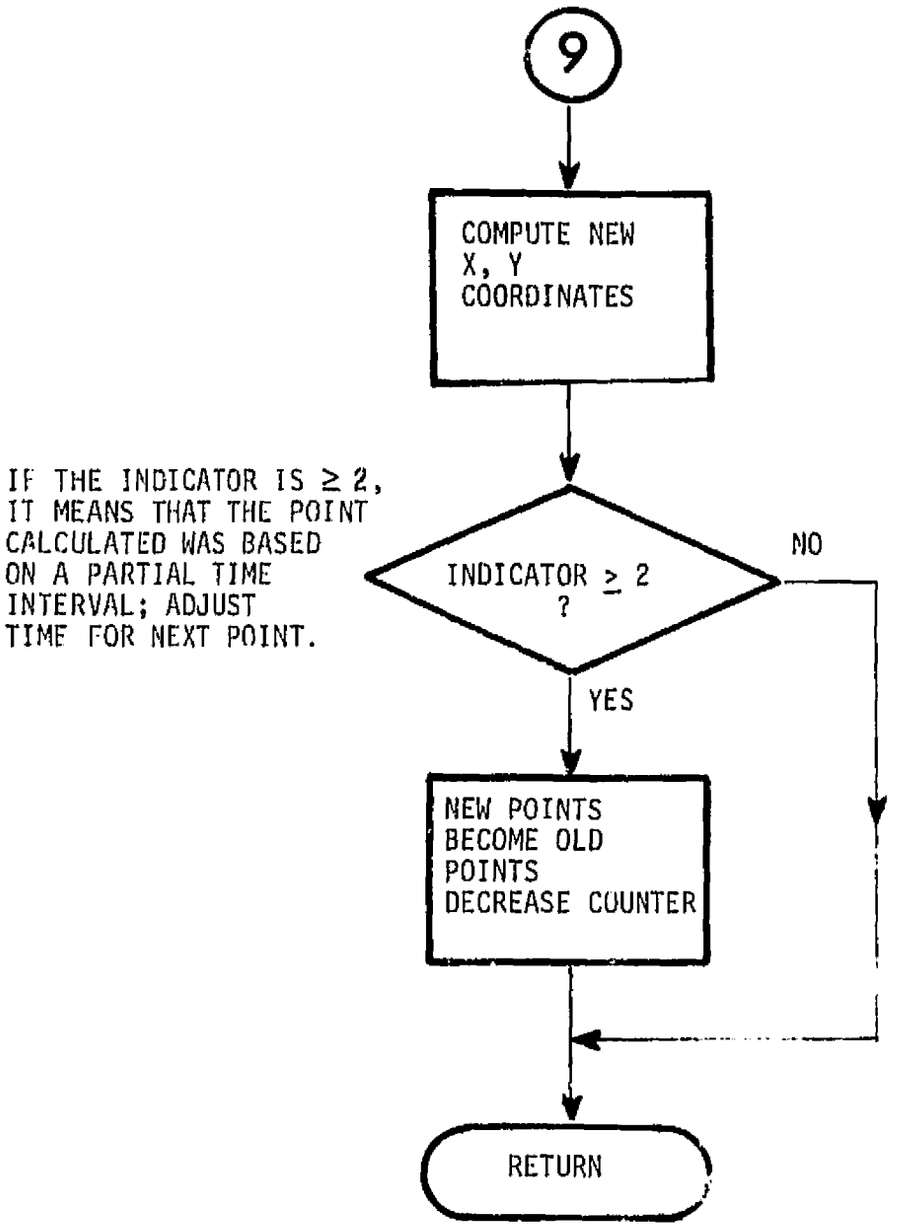

Fig. B-3. Concluded.

APPENDIX C

DIFFERENTIAL EQUATION FOR CROSS-PATH DEVIATIONS IN POISSON-DRIVEN DYNAMICAL SYSTEM

Consider the random differential equation describing cross-path deviation y_t at time t

$$d_{y_t} + \beta_{y_t}\, dt = dT(t) \tag{C-1}$$

where

$$y_t = e^{-\beta(t-t_1)}\, y_{t_1} + \int_{t_1}^{t} e^{-\beta(t_1-\sigma)}\, (-1)^{N(\sigma)}\, d\sigma$$

where β is a damping term. Here y_t is an integrated version of the random telegraph wave (ref. 11) described by

$$\dot{T}(t) = (-1)^{N(t)}$$

where N(t) is a Poisson counting process defined as a control (± 1) between event times of the Poisson process.

Let $f(\gamma;t)$ denote the first order density function for y_t. The increment dT(t) can be defined as

$$dT(t) = \int_{t}^{t+dt} (-1)^{N(\sigma)}\, d\sigma = \int_{0}^{dt} (-1)^{N(t+u)}\, du$$

$$= -(dt - 2a)(-1)^{N(t)} \quad , \quad 0 < a < dt$$

where a is an event time. Consider the characteristic functional for y_t

$$\phi(\omega;t) = E\{e^{j\omega y_t}\}$$

where $E\{\cdot\}$ is the expected value operator. This can be expressed as

$$\phi(\omega;t) = \int e^{j\omega\gamma} f(\gamma;t)\, d\gamma \quad .$$

The partial derivative with respect to t is

$$\frac{\partial\phi(\omega;t)}{\partial t} = \int d\gamma\, e^{j\omega\gamma} \frac{\partial}{\partial t} f(\gamma;t) \quad . \tag{C-2}$$

This result can also be obtained by examining

$$\frac{\partial\Phi(\omega;t)}{\partial t} = \lim_{\Delta t\to 0} (\Delta t)^{-1} \left\{ \Phi(\omega;t + \Delta t) - \Phi(\omega;t) \right\}$$

$$= \lim_{\Delta t\to 0} (\Delta t)^{-1} E\left[e^{j\omega y_t + \Delta y_t} - e^{j\omega y_t} \right]$$

$$= \lim_{\Delta t\to 0} (\Delta t)^{-1} E\left[e^{j\omega y_t} \left(e^{j\omega\Delta y_t} - 1 \right) \right] \quad .$$

The expectation can be written as a conditional expectation

$$\frac{\partial\Phi(\omega;t)}{\partial t} = E_{y_t} \left\{ e^{j\omega y_t} \lim_{\Delta t\to 0} (\Delta t)^{-1} E\left[(e^{j\omega\Delta y_t} - 1) \,\middle|\, y_t \right] \right\} \tag{C-3}$$

where E_{y_t} denotes expectation under the distribution of y_t. The latter expectation in eq. (C-3) can be written

$$E\left[\left(e^{j\omega\Delta y_t} - 1\right)\middle| y_t\right] = E\left[j\omega\Delta y_t - \frac{\omega^2}{2!}\Delta y_t^2 - j\frac{\omega^3}{3!}\Delta y_t^3 + \cdots\middle| y_t\right] \quad .$$

From the equation for dy_t given in eq. (C-1),

$$E\left[\left(e^{j\omega\Delta y_t} - 1\right)\middle| y_t\right] = j\omega\left[-\beta y_t + P_e - P_o\right]\Delta t + O(\Delta t)\right] \quad .$$

Therefore

$$\frac{\partial\Phi(\omega;t)}{\partial t} = E_{y_t}\left\{e^{j\omega y_t}\; j\omega[P_e - P_o - \beta y_t]\right\} \quad .$$

A final simplification follows by observing that the expected value of the random telegraph wave satisfies

$$E[\dot{T}(t)] = P_e - P_o \quad .$$

It is easily shown that (ref. 12)

$$E[\dot{T}(t)] = e^{-2\lambda t} \quad .$$

Thus we can write

$$\frac{\partial\Phi(\omega;t)}{\partial t} = E_{y_t}\left\{e^{j\omega y_t}\; j\omega\,[e^{-2\lambda t} - \beta y_t\right\}$$

$$= \int d\gamma e^{j\omega\gamma}\; j\omega\,[e^{-2\lambda t} - \beta\gamma]\, f(\gamma;t) \quad . \qquad \text{(C-4)}$$

Equating eqs. (C-2) and (C-4), yields

$$\int d\gamma e^{j\omega\gamma} \frac{\partial}{\partial t} f(\gamma;t) = \int d\gamma e^{j\omega\gamma} j\omega[e^{-2\lambda t} - \beta\gamma] f(\gamma;t)$$

or, integrating the right-hand-side by parts

$$\frac{\partial}{\partial t} f(\gamma;t) = \frac{\partial}{\partial \gamma} [e^{-2\lambda t} - \beta\gamma] f(\gamma;t) \quad . \tag{C-5}$$

This partial differential equation describes the evolution of $f(\gamma;t)$ with time.

REFERENCES

1. Terminal Air Traffic Control Handbook w/Changes. Department of Transportation, FAA 7110.8C, 1973.

2. Parker, L. C.: General Aviation Air Traffic Pattern Safety Analysis. Symposium of The System Safety Society, Denver, Colorado, 1973.

3. Parker, L. C.: General Aviation Air Traffic Pattern Study. NASA TM-X-6955, NASA Wallops Station, Wallops Island. Va., July 1973 (same as reference 2).

4. Joel, Steele, Filliben, Hare: Approach to Evaluating the Effects of VFR Towers on Flow and Safety. NBS Technical Report. Washington, D.C., April 1971.

5. Marks, B. L.: Air Traffic Control Separation Standards and Collision Risk. RAE Technical Note No. Math 91, February 1963. AD 407 312.

6. Reich, P. G.: A Theory of Safe Separation Standards For Air Traffic Control. RAE Technical Report No. 64041, November, 1964. NTIS N65-20667.

7. Research Triangle Institute: Investigation of the Performance Characteristics of a Doppler Radar Technique for Aircraft Collision Hazard Warning--Phase III. NASA CR-2020, March 1972.

8. Britt, C. L., Jr.: An Evaluation of Aircraft Collision Hazard Warning Radar Techniques in the Terminal Area. Technical Report, Research Triangle Institute, Engineering Division. December 17, 1969.

9. Britt, C. L., Jr.; Baxa, E. G., Jr.; Poole, W. K.: Develop and Exercise an Analytical Model of the Air Traffic System. Proposal No. E-71-19, Research Triangle Institute, Engineering Division, January 1971,

10. Parzen, E.: Modern Probability Theory and Its Applications. J. Wiley & Sons, New York, 1964.

11. Kac, M.: Probability and Related Topics in Physical Sciences. Interscience, New York, 1959.

12. Papoulis, A.: Probability, Random Variables, and Stochastic Processes, McGraw-Hill, 1965.